Fatigue Behaviour of Hot Mix Asphalt for New Zealand Pavement Design

---

By Anthony P. Stubbs

Department of Civil and Natural Resources Engineering
University of Canterbury

A thesis submitted in partial fulfillment
of the requirements for the
Degree of Master of Engineering

2011

ABSTRACT

Asphalt's fatigue and modulus characteristics play an important role in pavement design. Ultimately they govern the required thickness of asphalt to structurally support heavy vehicles. The thickness of the asphalt layer is a major contributor to the cost of construction. In New Zealand, the design of structural asphalt layers has been a problem for some time and gives rise to two areas of concern. First, the present fatigue failure criterion, the Shell fatigue transfer function, which has been adopted from overseas, not only underestimates the fatigue life of the country's asphalts, but does not accurately characterise the fatigue behaviour of our local asphalt mixes. Consequently, asphalt thicknesses are overdesigned. Second, asphalt's fatigue behaviour is influenced by numerous factors and therefore can be difficult to characterise. The primary objective of this thesis is to develop fatigue and modulus models, by carrying out fatigue and modulus tests, to characterise the behaviour of two typical New Zealand structural asphalts. Both resilient and stiffness moduli tests were performed at a range of temperatures and loading rates developing moduli master curves, which predict the asphalt's modulus for any pavement temperature and vehicle speed. A general full factorial experiment was carried out utilising the four-point flexural beam fatigue test. Tests were carried out at different strain levels, temperatures, and loading rates. An analysis of variance showed that the impacts of strain amplitude, temperature, binder type, the interaction of strain amplitude and temperature, and the interaction of strain amplitude and binder type have a significant effect on fatigue behaviour. The developed models, which account for temperature effects give the pavement engineer the ability to undergo a more accurate assessment of fatigue damage than at present for different climatic temperatures demonstrated by using an incremental damage analysis approach. The research shows that with such characterisation for the given pavement's design life, thinner and less expensive roads can be constructed in New Zealand.

ACKNOWLEDGMENTS

I would like to thank all those have supported and advised me throughout this research.

To Mofreh Saleh, thank you for your encouragement, support, and expert advice. Your passion for pavement engineering and challenging the Shell fatigue transfer function has been inspiring. I am further appreciative for your support and encouragement for me to present at national and international conferences. Thank you.

Without the technical expertise help from John Kooloos this research would not be possible. I am also grateful for his friendship in the journey of this thesis.

Thanks go to Kenneth Kuhn for his assistance with the preparation of this manuscript.

To Downer, in particular to David Hutchison, Janet Jackson, Howard Jeffery-Wright, and Simeon Hall, thank you for your interest in the research and for the donation of materials to carry out the research.

I am grateful to Nir Kumar KC for his assistance in the laboratory.

Thanks to the Department of Geological Sciences, in particular Cathy Higgins, for providing me access to the Rock Mechanics room, which allowed me to prepare testing specimens.

I am indebted to Val Melhop from the Learning Skills Centre, for her support to improve my writing abilities and style, which has greatly assisted with this research.

Without my friends this thesis would have been a very long slog so thanks indeed for all the good times. Finally, to my family, thank you for your love and support.

TABLE OF CONTENTS

LIST OF FIGURES

LIST OF TABLES

LIST OF PUBLICATIONS AND PRESENTATIONS

Conference Proceedings (Peer Reviewed)

Stubbs, A., Saleh, M., Kuhn, K., Hutchison, D., and Hall, S. (2011) Investigation factors affecting hot mix asphalt fatigue behaviour using factorial analysis, *Proc. 5th International Conference Bituminous Mixtures and Pavements*, Thessaloniki, Greece.

Stubbs, A., Saleh, M., Kuhn, K., Hutchison, D., and Hall, S. (2011) Developing a resilient modulus master curve for New Zealand Asphalt, *Proc. 7th International Conference on Road and Airfield Pavement Technology*, August 2011, Bangkok, Thailand.

Stubbs, A., Saleh, M., and Jeffery-Wright, H. (2010) Investigation of the viscoelastic and fatigue behaviour of hot mix asphalt, *Proc. of the 24th Australian Road Research Board Conference, Melbourne*, Australia.

Stubbs, A., Saleh, M., and Jeffery-Wright, H. (2010) Investigation into the validation of the Shell fatigue transfer function, *IPENZ Transportation Conference*, Christchurch, NZ.

Oral Presentations (Peer Reviewed)

Stubbs, A. (2011) Can we build our motorways more cheaply? NZTA/NZIHT 12th Annual Conference – Building & Maintaining Highways for the Future, New Plymouth, NZ

Stubbs, A. (2010) Investigation into the validation of the Shell fatigue transfer function, *REAAA NZ Chapter*, Christchurch NZ.

1

GENERAL INTRODUCTION

The first step in civilisation is to make roads,
The second to make more roads,
And the third to make more roads still.
— Old saying

1.1 CONTEXT

Roads play a vital role in the economic growth of a country and the day-to-day lives of its citizens, but they are very expensive to build. The road network is designed to provide both an appropriate level of serviceability while maintaining suitable safety requirements and structural support for any given traffic demand. Over the past four decades New Zealand has seen an increase in traffic loadings, volumes and speeds, leading to greater pressure on the network (New Zealand Transport Agency, 2009). Continuing to support this demand remains central to sustaining economic growth and the well-being of the population.

Constructing the most economical road without compromising its structural integrity throughout its design life is the objective of the pavement engineer. New Zealand's motorway network has generally been constructed of structural asphalt (typically of asphalt thicknesses greater than 80mm). Structural asphalt has been chosen due to the relatively large volume of heavy vehicles that carry the country's freight. Over time, the sheer volume of heavy traffic and adverse weather conditions causes the pavement to deteriorate and ultimately fail.

For heavy loads, pavements need to be supported structurally. In doing so, pavement engineers follow the AUSTROADS Pavement Design: A Guide to the Structural Design of Pavements (2008a), hereinafter referred to as the AUSTROADS, and the New Zealand Supplement to the AUSTROADS (2007). The guidelines determine the appropriate thickness of pavement layers according to particular traffic loads, volumes, and speeds; construction materials; meteorological climatic conditions; and failure criteria for the expected design period of the road. For a flexible pavement system, the pavement design procedure is based on a multi-layered structural analysis comprising: asphalt, unbound granular material, cemented materials, and the subgrade. These structural layers are designed to prevent two modes of failure, the fatigue of bound materials and the permanent deformation of the subgrade.

To calculate the fatigue damage of structural asphalts, AUSTROADS have adopted the Shell fatigue transfer function (FTF), also known as the Shell fatigue performance criterion. The Shell FTF was developed by investigating asphalt mixes from overseas, not New Zealand's asphalt (Shell International Petroleum Company Ltd., 1978; Van Dijk., 1975). Consequently, the Shell FTF does not characterise the behaviour of local materials in New Zealand. Within the New Zealand and Australian roading industry there is uncertainty with regard to the validity of the Shell FTF for predicting the asphalt fatigue life of the country's structural asphalts. Furthermore, field evidence suggests that the Shell FTF is overly conservative. Two thirds of the Wellington and Auckland motorway network was constructed with structural asphalt having been designed using the earlier guideline, the State Highway Pavement and Rehabilitation Design Manual, in which the thickness of asphalt is 30 per cent less than the Shell FTF. They are performing well past their design lives with minimal structural maintenance required (Transit New Zealand, 2007). The status quo is not acceptable; therefore, there is a need

to characterise accurately the fatigue behaviour of New Zealand's structural asphalts in order to design the country's roads more economically.

1.2 STATEMENT OF THE PROBLEM

Three problems that are inherent in the AUSTROADS mechanistic empirical pavement design (MEPD) guidelines for fatigue cracking are addressed in this thesis. They are briefly outlined below and are all central to improving the fatigue characterisation of New Zealand's asphalts. The first, second, and third problems are addressed in Chapter 4, Chapter 5, and Chapter 6 respectively.

1.2.1 Problem 1: Modulus Characterisation

Asphalt's modulus is a material property, and is an important variable in pavement design. In the New Zealand and Australian pavement design guidelines, the asphalt modulus is determined by measuring the resilient modulus with the indirect tensile test at a single temperature (25°C) and loading rate (40 ms rise time). Yet roads are subjected to a variety of climatic conditions, and modulus properties are dependent on temperature, loading rate, and other factors.

There is also a lack of available data to characterise the performance of asphalt's modulus over a range of different climatic conditions for typical New Zealand asphalts. The goal of Problem 1 is to characterise asphalt's modulus for different conditions, enabling this to be integrated with the AUSTROADS MEPD to better understand the fatigue behaviour of asphalt given that the modulus also affects fatigue.

1.2.2 Problem 2: Characterising Asphalt Fatigue Behaviour

Asphalt's fatigue performance is influenced by a number of different factors (i.e. strain, temperature, frequency, and modulus), making the fatigue life of asphalt difficult to characterise accurately. Traditionally, laboratory fatigue models are evaluated at a fixed testing temperature and a fixed testing frequency. However, because this approach examines the effect of strain at a single temperature and a single frequency, it fails to consider the impacts of interaction between factors affecting the fatigue life and the

effect of temperatures and frequency that may exist. Given this effect of a range of contributing variables on fatigue behaviour, it would be helpful to understand the global effect of these variables and their interactions.

1.2.3 Problem 3: Incremental Damage Analysis

In the AUSTROADS MEPD, the design of pavement layers is based on one seasonal temperature, the Weighted Mean Annual Pavement Temperature (WMAPT). Nonetheless, seasonal variations greatly affect both asphalt modulus and fatigue characteristics because they are largely temperature dependent. Without temperature dependent models for both moduli and fatigue behaviour, it is impossible to perform incremental damage analyses at a range of temperatures.

1.3 OBJECTIVES

The principal goal of the thesis is to develop a set of new generation modulus and fatigue models that will enable an incremental damage analysis and address the different factors affecting fatigue behaviour.

While this thesis has multiple goals, they are all central to better understanding New Zealand's asphalt fatigue behaviour. The specific research objectives are to:

(i) Develop a modulus master curve for the different types of asphalt mixes. A modulus master curve can predict the laboratory modulus for any loading frequency and pavement temperature. This modulus master curve is needed so further thesis objectives can be achieved.

(ii) Quantitatively determine the effect of factors and their interaction on asphalt's fatigue behaviour. Given the breadth of factors affecting fatigue, this research project will thus focus on what are believed to be some of the primary factors:

- Strain amplitude applied to the asphalt layer

- Pavement temperature
- Load frequency
- Binder types: 60/70 and 80/100 classified by penetration grade.

(iii) Ascertain the fatigue characteristics of the two common asphalt mixes, whilst developing a set of asphalt fatigue models that accounts for different statistically significant factors affecting fatigue behaviour.

(iv) Integrate the modulus master curve and the set of fatigue models into an incremental damage analysis thus facilitating the incremental damage for different seasons to be accessed during the pavement's performance period.

(v) Develop the incremental design analysis framework so it can be implemented into the AUSTROADS design procedure.

1.4 THESIS ORGANISATION

Seven chapters are presented in this thesis. Chapter 1 introduces the thesis as a whole, describing the research problem of asphalt fatigue cracking in New Zealand. Chapter 2 provides a historical background to asphalt fatigue in New Zealand, including the adoption of the Shell FTF. Chapter 3 describes in detail the materials and specimen preparation undertaken in the laboratory to measure the fatigue life and the modulus of the structural asphalts used in this study. Chapter 4 characterises the asphalt's modulus. The AUSTROADS procedure to determine the asphalt stiffness modulus is also explained in a brief literature review. Chapter 5 is the main focus of this research, and investigates the factors influencing the fatigue behaviour of structural asphalts, and develops fatigue models that mark the behaviour of the asphalt for the variables affecting its fatigue life. Chapter 6 integrates Chapter 4 and Chapter 5 by examining the fatigue damage due to seasonal variations throughout the pavement's design life, and

presents a framework for the analysis. Background information of incremental pavement design and analysis procedure is also explained. Finally, Chapter 7 discusses results, offers conclusions, and points out areas where further research is warranted. The significance of the research and adaption of the work to the roading industry is also addressed.

2

ASPHALT FATIGUE IN NEW ZEALAND: HISTORICAL BACKGROUND

New Zealand's Main roads are coming under increasing strain because of a combination of greater levels of traffic and heavier vehicles. A new method of constructing such roads needs to be found – one that is probably unique to New Zealand – so that as sections of highway are resurfaced they can successfully withstand these new demands (at a cost that makes sense in the New Zealand environment) — Damon Collins, Trade me Jobs (2011) — See Appendix A.

Structural asphalt roads are a long-lasting pavement construction alternative that can endure very heavy traffic loads. They are uncommon in New Zealand because they are seen to be prohibitively expensive. A principal reason for this cost is because these types of roads are built too thick. As will be discussed later, field and laboratory evidence suggest that New Zealand structural asphalt roads are over designed. As a result, when these types

of pavement construction options are compared with other designs in an economic evaluation, structural asphalt is simply discounted. Thus cheaper alternatives are built. The use of the Shell fatigue transfer function (FTF) is central to the overdesign of asphalt roads.

Specifically, this historical background chapter relates to the Shell FTF and asphalt fatigue cracking. In the first section, the Shell FTF is introduced, along with its issues surrounding asphalt pavement design in a New Zealand context. Reasons for adopting this FTF are explained, and its derivation is also presented. The final section defines the asphalt fatigue cracking phenomenon; gives background information on laboratory fatigue cracking characterisation and explains the differences between laboratory and field conditions for fatigue cracking.

2.1 SHELL FATIGUE TRANSFER FUNCTION

In the construction of highways, structural asphalt layers are designed to withstand fatigue cracking. Fatigue cracking is mainly caused by the repetitive horizontal tensile strain developed in the asphalt from heavy traffic loads. To predict asphalt fatigue cracking, the AUSTROADS (2008a) and New Zealand supplement to the AUSTROADS (2007) have adopted the Shell FTF.

Asphalt thicknesses are governed by this fatigue cracking criterion, and are based on particular traffic loads, climatic conditions, and the expected lifespan of the pavement. The Shell FTF is defined as Equation 2–1

$$N_f = RF\left[\frac{6918(0.856 \times V_b + 1.08)}{S_{mix}^{0.36} \times \mu\varepsilon}\right]^5 \qquad \textbf{2–1}$$

where:

N_f = allowable number of loading repetitions until fatigue cracking failure
RF = reliability factor
V_b = percentage by volume of bitumen in the asphalt mix (%)
S_{mix} = asphalt stiffness (flexural) modulus (MPa)
$\mu\varepsilon$ = tensile strain at the bottom of the asphalt layer (microstrain)

The reliability factor is another interesting quantity which has its own inherent problems. Reliability factors are “transfer functions that relate a mean laboratory fatigue life (Shell

1978) to the in-service fatigue life predicted using this Part at a desired project reliability." AUSTROADS (2008a). They account for two components. First, a shift factor that relates the mean laboratory fatigue life to the mean field fatigue life, which takes into account the differences between laboratory and field conditions. Second, the reliability factor takes into account the variability from construction, environment, and traffic loading AUSTROADS (2008a).

2.1.1 Derivation

The derivation of the Shell FTF is based on the fatigue data from Van Dijk and Visser (1977). Their work was carried out on 13 asphalt mixtures (wearing and base course mixes) with conventional binders. Table 2.1 presents some of their mix properties; further information can be found in the Shell Pavement Design Manual (Claessen, Edwards, Sommer, & Ugé, 1977; Shell International Petroleum Company Ltd., 1978). Appendix 3 of the Shell Pavement Design Manual (1978) gives the full derivation of the Shell FTF, which is reproduced below.

Table 2.1 Composition of asphalt mixes used in the development of the Shell life prediction model (Claessen, et al., 1977).

Mix Type	Binder Grade	Binder Volume (%)	Air Voids (%)	Voids in mineral aggregate VMA (%)
Asphalt Concrete State of California	40/50	14.2	1.7	15.9
Dense Asphaltic Concrete	40/50	11.4	1.9	13.3
Gravel Bitumen French	40/50	9.3	9.3	18.6
Dense Bitumen Macadam	40/60	11	3.6	14.6
Rolled Asphalt Base Course Mix	40/60	14.1	2.2	16.3
Bitumen Sand Base Course	45/60	8.9	20.3	29.2
Gravel Sand Asphalt, Dutch (Stroe)	45/60	11	11	22
Rich Sand Sheet	45/60	19.3	7.8	27.1
Gravel; Sand Asphalt Dutch (Muiden)	50/60	13.3	6.6	19.9
Dense Bitumen Macadam	80/100	11	3.4	14.4
Lean Bitumen Macadam	80/100	4.9	33.2	38.1
Lean Sand Asphalt	80/100	10.5	8.4	18.9
Asphalt Base Course Mix German (Struttgart)	B80	9.3	2.6	11.9

These mixes were typical of asphalts for the various countries including France, Netherlands, America, England and Germany. They are not New Zealand asphalts. It is obvious from the data in the table the large variations of the asphalt mix properties. For example, air voids range from 1.7–33.2 per cent. In New Zealand, target air voids for structural asphalts are between 3–5 per cent (New Zealand Transport Agency (NZTA), 2010).

In addition, the Shell FTF was developed from a number of laboratory conditions. Fatigue tests were carried out using a sinusoidal loading shape in both two-point or three-point bending modes, with test temperatures ranging from -10–50°C, and a test frequency from 10–50 Hz (Van Dijk & Visser, 1977). A haversine loading pulse, however, is generally acknowledged to represent the in-service conditions.

Two approximations were used in the derivation of the Shell FTF. The first approximation is that the exponent in the fatigue life, which can be represented as $N_f = k \times \varepsilon_{fat}{}^{-n}$, is assumed to equal five (that is n=5) for all of the 13 asphalt mixes. For different testing temperatures the slopes ranged from 2.02–7.5 and normally varied between 4–6 (Van Dijk & Visser, 1977).

The second approximation assumes that the slopes of the $\log \varepsilon_t$ versus $\log S_{mix}$ are all equal to -0.36, for a fixed number of loading cycles thus Equation 2–2

$$\log \varepsilon_t = -0.36 \log S_{mix} + \text{Constant} \qquad \textbf{2–2}$$

where:

ε_t = tensile strain (mm/mm)
S_{mix} = asphalt mix modulus (N/m^2, not MPa)

Fatigue measurements are also used to determine the value of this constant. The fatigue strain for failure at a million cycles, $(\varepsilon_{Fat})_{N=10^6}$, for a mix stiffness modulus of 5000 MPa was found to increase with increasing percentage of bitumen (by volume), V_b, in accordance with Equation 2–3. The influences of other variables on asphalt fatigue were not noted.

$$(\varepsilon_{Fat})_{N=10^6} = (17.4 \times V_b + 22) \times 10^{-6} \qquad \textbf{2–3}$$

where:

ε_t = tensile strain (mm/mm)
V_b = percentage of volume of bitumen in the asphalt mix (%)

Joining Equation 2–2 and Equation 2–3 becomes Equation 2–4.

$$(\varepsilon_{Fat})_{N=10^6} = (17.4 \times V_b + 22) \times 10^{-6} \times \left(\frac{S_{mix}}{5000}\right)^{-0.36} \quad \textbf{2–4}$$

From the first assumption with n=5, $N_f = k \, x \, \varepsilon_{fat}{}^{-5}$ can alternatively be expressed as Equation 2–5.

$$\varepsilon_{Fat} = (\varepsilon_{Fat})_{N=10^6} \times \left(\frac{N_{fat}}{10^6}\right)^{-0.2} \quad \textbf{2–5}$$

Finally, combining Equation 2–4 and Equation 2–5 gives Equation 2–6.

$$\varepsilon_{Fat} = (0.856 \times V_b + 1.08) \times S_{mix}{}^{-0.36} \times N_{fat}{}^{-0.2} \quad \textbf{2–6}$$

2.1.2 Adoption into AUSTROADS

Before AUSTROADS was established in 1989 its former governing body was known as the National Association of Australian State Road Authorities (NAASRA) (AUSTROADS, 2011). The Shell FTF was first adopted in 1987 in the NAASRA as the asphalt FTF (or performance criterion).

Back then, the Shell FTF was recognised as Equation 2–7, not Equation 2–1. The differences between the former AUSTROADS Shell FTF, Equation 2–7 is that the reliability factor is absent from this original adopted function. Until 2004, the reliability factor was not introduced into the AUSTROADS Pavement Design: A Guide to the Structural Design of Roads Pavements.

$$N_f = \left[\frac{6918(0.856 \times V_b + 1.08)}{S_{mix}^{0.36} \times \mu\varepsilon}\right]^5 \quad \textbf{2–7}$$

where:

N_f = allowable number of loading repetitions until fatigue cracking failure
V_b = percentage by volume of bitumen in the asphalt mix (%)
S_{mix} = asphalt stiffness (flexural) modulus (MPa)
με = tensile strain at the bottom of the asphalt layer (microstrain)

At the time of adopting the Shell FTF in 1987, the working group of the NAASRA wanted to adopt a fatigue life relationship for asphalt that had the following attributes (AUSTROADS, 2008b):

- Controlled strain testing as this would be applicable to thin asphalt courses
- Allowance for crack propagation
- Allowance for some cracking during field fatigue life
- Appropriate for mixes with stiffness between 500–20,000 MPa.

Although the Shell FTF is said to make allowances for some cracking in the wheel path, it is not clear what percentages of cracking that the Shell FTF was designed or calibrated for. Determining the amount of cracking in the wheel path is important as this will help establish when the pavement needs to be rehabilitated.

According to Anderson (1982), who undertook a comprehensive review of the international literature on these fatigue life relationships for asphalt, found that the Shell FTF "was the most versatile in terms of mix properties, temperatures, and loading time." (AUSTROADS, 2008b). Thus it was decided to adopt the Shell FTF for the asphalt fatigue performance criterion.

In an attempt to save time and money, the NAASRA commissioned Anderson (1982) to undertake a study to search for an appropriate FTF for asphalt rather than perform their own research effort. Interestingly, back in New Zealand in 1989, it was stated in the State Highway Pavement Design and Rehabilitation Manual that "[t]he bridging of the gap between laboratory data and in-situ behaviour is one of the most urgent research problems in this field at the time of writing" (National Roads Board, 1989). The gap still remains in the New Zealand roading industry.

Investigating research into the performance of the pavements in New Zealand is thus required. Details on such a research effort will be discussed in Chapter 7.

Nevertheless, field validation of the adopted Shell FTF was requested, and thus an accelerated field study was carried out. A full-depth asphalt field trial using the Accelerated Loading Facility (ALF) in Melbourne was carried out and completed between November 1989 and March 1991 (Jameson, Sharp, & Vertessy, 1992). They found the Shell laboratory fatigue relationship, referred to as the Shell FTF in this thesis, predicts the fatigue life when about 50 per cent of the area trafficked was severely fatigue cracked. In their study, they "recommend that the Shell relationship continue to be used for pavement design." (Jameson, et al., 1992). However, within their report they also state:

> *In recommending the use of this relationship in Australia, it was assumed that it included factors to take account of the translation of laboratory fatigue life to field fatigue life. Recent discussion with Shell personnel, however, have suggested that this equation does not include these factors and that Shell (Gerritsen and Koole 1987) recommends that the fatigue life calculated using this equation be multiplied by a factor of 10-20 when field fatigue life is to be determined. — Jameson et al. (1992).*

Although, their final verdict was to recommend the Shell FTF for *Australia*, their calibration was done under accelerated loading conditions. In practice, loading cycles are intermittent, not continuous. Intermittent loading is much less damaging, and due to vehicle wandering the strains at the bottom of the asphalt are varied. Unfortunately, the work hasn't provided a conclusive answer as this is a tricky problem.

To compensate for these differences and to correct for field fatigue, Shell published a compound factor based on seven years' of experience with the Shell Pavement Design Manual (Gerritsen & Koole, 1987). These correction factors are related to both the depth of the asphalt and Weighted Mean Annual Pavement Temperature (WMAPT), and are presented in **Table 2.2**.

Table 2.2 Correct factors for the combination of intermittent loading, lateral distributions of wheel loads and temperature gradients in the asphalt layer (Reproduced from (Gerritsen & Koole, 1987)

Thickness of asphalt layer	WMAPT (°C)	Mix Code			
		S1[1] – F1	S2[2]– F1[3]	S1 – F2[4]	S2– F2
h1<100 mm	4	15	15	10	5
	12	20	20	15	10
	20	20	20	15	10
	28	25	25	20	10
100 mm < h1 < 200 mm	4	15	15	10	5
	12	15	15	10	10
	20	15	15	15	10
	28	15	15	15	10
h1>200 mm	4	10	10	10	5
	12	10	10	10	5
	20	10	10	10	5
	28	10	10	10	5

Within New Zealand, Saunders (1982) stated that to relate the laboratory fatigue result of Shell Chart M-3 to the field fatigue a shift of 10 was needed; allowing for intermittent loading, temperature gradients, and traffic wandering. The Chart M-3 is for a fatigue characteristic of a F1[3]. Boon (1979) recommended local mixes (Mix 20 and Mix 40) to be a mix code of S1-F1-100, where the binder penetration grade is 100.

Despite the acknowledgement from AUSTROADS that the Shell FTF is for fatigue failure in the laboratory and not in the field (AUSTROADS, 2004), no field shift factors have to date been accepted, other than the reliability factor. Yet, before the reliability factor was introduced, Jameson (1999) proposed that Equation 2–7 be multiplied by a shift factor of five as given by Equation 2–8.This change was recommended because Jameson's review of existing information on the relationship between asphalt fatigue observed in the field (mainly from accelerated loading trails) and performance predicted using the Shell FTF (AUSTROADS, 2004). However, the 2004 Reference Group for the AUSTROADS

1 S1 Dense base course mix types with average aggregate, bitumen, and voids content by volume (Shell
2 S2 Open graded mixes with high voids contents and low bitumen contents, or dense mixes with relatively low aggregate contents and high bitumen contents (Shell 1987).

3 F1 Many base course mixes with moderate bitumen and voids content (Shell 1987).

4 F2 Many base course mixes with relatively higher voids content (Shell 1987).

dismissed this shift factor of five and introduced a reliability factor because of concerns that this factor or resulted in significant reduction in thickness of "thick" (i.e. greater than 150 mm) asphalts. Remarkably, adopting a project reliability of 97.5 per cent (i.e. for an average annual daily traffic greater than 2000 or for a freeway) yields a "shift factor" of 0.67 to the Shell FTF, making the Shell FTF even more conservative than previous. This seems excessive.

$$N_f = 5\left[\frac{6918(0.856 \times V_b + 1.08)}{S_{mix}^{0.36} \times \mu\varepsilon}\right]^5 \qquad \textbf{2–8}$$

where:

N_f = allowable number of loading repetitions until fatigue cracking failure
V_b = percentage by volume of bitumen in the asphalt mix (%)
S_{mix} = asphalt stiffness (flexural) modulus (MPa)
$\mu\varepsilon$ = tensile strain at the bottom of the asphalt layer (microstrain)

Though the Shell FTF has been calibrated in Melbourne, Australia, consideration by the New Zealand roading industry must be made as to whether the Shell FTF should be calibrated for New Zealand conditions.

A further issue with the adoption of the Shell FTF is the inclusion of 6918^5 in the current Shell FTF as this is not present in the original laboratory derived Shell fatigue life model, Equation 2–6. It appears that is value has not been explained, although it is acknowledged by the author that Equation 2–6's stiffness modulus is measured in N/m^2 and not MPa.

The next section addresses the ability of the Shell FTF to predict New Zealand asphalt pavements.

2.1.3 Inherent Issues with the Shell FTF

Uncertainty of the validity of the Shell FTF in the New Zealand and Australian context exists. Practitioners have stated that the Shell FTF appears to be overly-conservative (Pidwerbesky, 2010; Stubbs, 2010; Transit New Zealand, 2005). To date, no literature within New Zealand supports the validation of the Shell FTF for the country's asphalt mixtures. Literature, however, advocates that the Shell FTF is inappropriate for a New Zealand context.

Since asphalt thicknesses using the earlier State Highway Pavement and Rehabilitation Design Manual (National Roads Board, 1989) were based on the Shell pavement design manual (Shell International Petroleum Company Ltd., 1978), these thicknesses were built 30 per cent thinner than those required by the current AUSTROADS (2008) Shell FTF. Yet, two thirds of the Wellington and Auckland motorway network were constructed with structural asphalt having been designed using this earlier guideline and are still performing *well* past their design lives (Transit New Zealand, 2007). Surely then, the application of the Shell FTF for New Zealand conditions needs revisiting.

Even back in 1982 it was noted that "[a] strong case would be made for research effort to establish design charts and formulae for New Zealand conditions and materials" (Saunders, 1982). Today, New Zealand's roading industry, however, still continues to request characterisation of asphalt's modulus and fatigue behaviour (Gribble & Patrick, 2008). This research aims to address this issue.

Although, the AUSTROADS amongst others rightly state that any laboratory fatigue model needs to be calibrated for field conditions, practitioners appear to have lost sight that so too does the Shell FTF. No references to date provide such information. Typically, when engineers face such issues, good engineering judgement is required. Yet, if designers continue to use the Shell FTF without calibration for New Zealand conditions this is simply poor engineering.

Calibration or extensive fatigue testing has not been carried out in New Zealand before because: (1) the majority of our highways historically, have had low traffic volumes that did not warrant structural asphalt in the first instance; and (2) the large number of resources and time required to complete such a project is costly. Researchers might have to wait 25 plus years until the pavement fails in field conditions. However, sooner or later this work has to be done and the sooner the better in order to achieve a robust MEPD method that represents New Zealand materials and field conditions. If the industry does not start [testing] now the time lost only compounds the problem.

In 1971 a test section of an asphalt wearing course was built on 60 meters of the Christchurch Northern Motorway. Field strains were measured by Patterson (1972) to compare the effect of traffic compaction from 0 and 8 months on both flexible and rigid

pavements foundation. It is unfortunate that this test site is no longer monitored as this could have provided an answer to field calibration in New Zealand.

Laboratory fatigue testing carried out at the University of Canterbury also demonstrated that the Shell FTF is overly conservative. Stubbs et al. (2010) showed that the Shell FTF underestimates the laboratory fatigue life of a typical New Zealand roading hot mix asphalt (HMA) – mix type AC14 60/70 (aggregate maximum nominal size is 14 mm and binder penetration grade is 60/70) by an average of 5.5 times (range 3.1–8.9). Their laboratory model when used as a FTF resulted in a potential cost saving of $90,000 per lane kilometre. If a field calibrated model is used, even greater savings could be made. Saleh (2010) further confirmed, using a methodology for the calibration and validation of the Shell FTF using experimental laboratory data, that the calibration factor was in the order of 5.7 for the AC14 60/70 HMA. Haora (2011) showed another typical New Zealand roading HMA, AC10 80/100 had an even greater laboratory fatigue life than the Shell FTF. The AC10 80/100 (aggregate maximum nominal size is 10 mm and binder grade is 80/100 by penetration grade, with design air voids of 4%, endures a fatigue life on average by 9.3 times (range 5.9–14.6) greater than the prediction from the Shell FTF. **Figure 2.1** illustrates the strain level versus fatigue life behaviour of these two studies and compares the measured fatigue life data with the prediction of the Shell FTF.

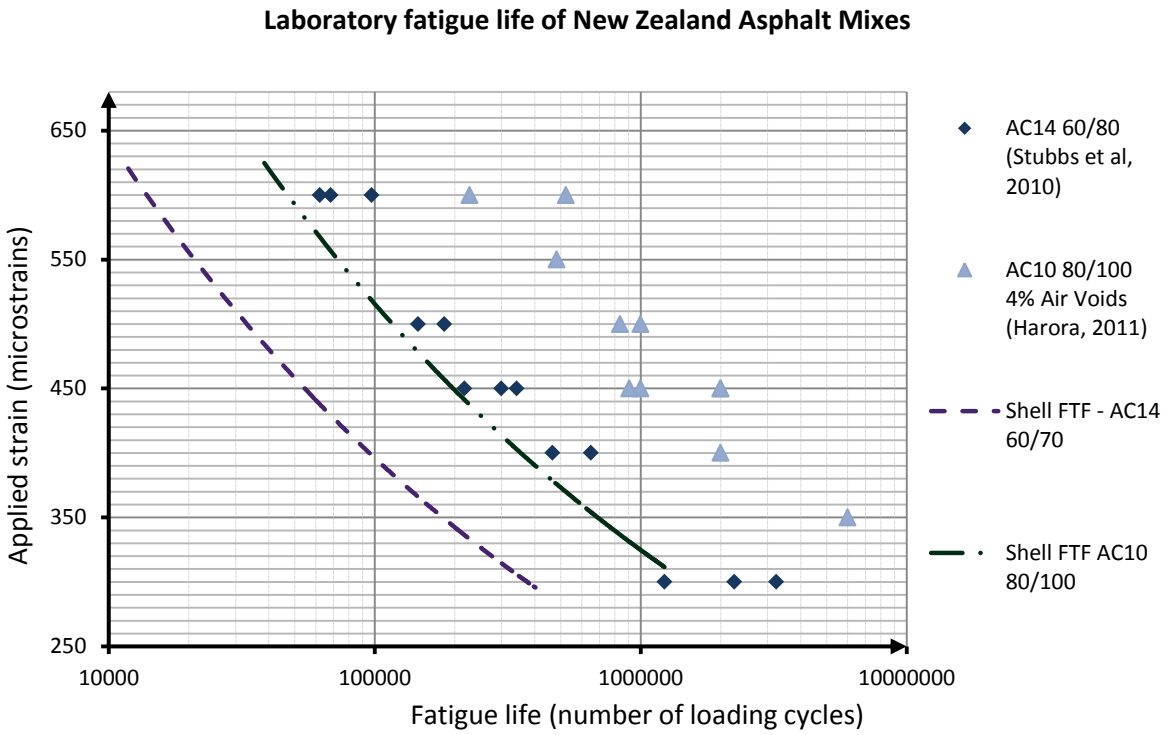

Figure 2.1 A fatigue life prediction comparison of the Shell FTF for two types of New Zealand hot mix asphalts: AC14 60/70 (Stubbs et al., 2010) and AC10 80/100 (Haora, 2011).

In New Zealand, Pidwerbesky states by personal communications that to account for the over-conservatism in predicting asphalt's thicknesses by the Shell FTF, a reasonable approach is to multiply the reliability factor by a value of 5 (Transit New Zealand, 2005). Moreover, the New Zealand Supplement to the AUSTROADS (Transit New Zealand, 2005) further states that they agree with Pidwerbesky. However, this statement was later taken out of the current New Zealand Supplement to the AUSTROADS (Transit New Zealand, 2007), probably because this statement was based on anecdotal evidence and was not validated by research.

One of the reasons why the New Zealand roading industry over design asphalt pavements based on the Shell FTF is that the NZTA is not prepared to accept the level of risk if these pavements were to fail early. Subsequently, this could result in major repair costs to these roads, causing service disruption and delays to traffic, particular on very heavy trafficked roads. This would lead to slowing down the supply of freight delivery. The current overestimation of the design to cover the risk of failure is equally unacceptable.

A further inherent discrepancy with the development of the Shell FTF is how layer thicknesses of asphalt affect fatigue. It is understood that the importance of dimensions of testing specimens on the fatigue behaviour of asphalt was not taken into consideration in the Shell Pavement Design Manual, including the Shell FTF Jacobs (1995) Asphalt beam dimensions in the preparation of the Shell FTF, for the three-point loading scheme, were 230 x 30 x 40 mm (Van Dijk & Visser, 1977).

2.2 ASPHALT FATIGUE CRACKING

2.2.1 Asphalt Fatigue Cracking Phenomenon

The primary distress mechanism in asphalt pavements is fatigue cracking. In flexible pavement, fatigue is induced by repeated heavy axle loads as in **Figure 2.2** (a), causing the pavement layer to flex as in **Figure 2.2** (b). The cracking itself is caused by the repetition of horizontal tensile stresses and strains that are developed by the repeated action of cyclic loading and unloading. Damage occurs when the cumulative number of loading cycles exceeds the fatigue life capacity. Load related fatigue cracks are first visible by longitudinal cracks in the wheel path as in **Figure 2.2** (c). Over time, these longitudinal cracks develop into 'block' cracks, shown in **Figure 2.2** (d). Because of their pattern, block cracks are also referred to as alligator or crocodile cracks.

Once the asphalt has reached a "defined" level of cracking, it is said to have reached its fatigue life. There is, however, debate within the industry as to what percentage of cracking within the wheel path is deemed failure. Nonetheless, it is generally accepted that the pavement is to be rehabilitated once the condition of the pavement structure has reached a level of serviceability that is no longer tolerable for the roading agency. In this country, the roading agency is the New Zealand Transport Agency (NZTA). Wealthy countries will generally tolerate lower percentages of cracking than poorer ones. Lower serviceability, in this case means greater percentage of fatigue cracking, and increased road user costs.

The root of classical fatigue cracking is acknowledged to be caused by the tensile strain at the bottom of the asphalt layer. Here the cracks propagate towards to surface. This type of fatigue crack is known as "bottom-up" cracking. Fatigue cracks can also occur as "top-

down" and are initiated at the surface. One of the main aims in the MEPD is to limit the maximum horizontal tensile strain at the bottom of the asphalt layer as this is proportional to the rate of fatigue cracking. The tensile strain at the bottom of the asphalt layer can be reduced by either increasing the asphalt layer thickness or increasing the asphalt's modulus. In regard to this design philosophy a balance between cost and risk needs to be well thought out.

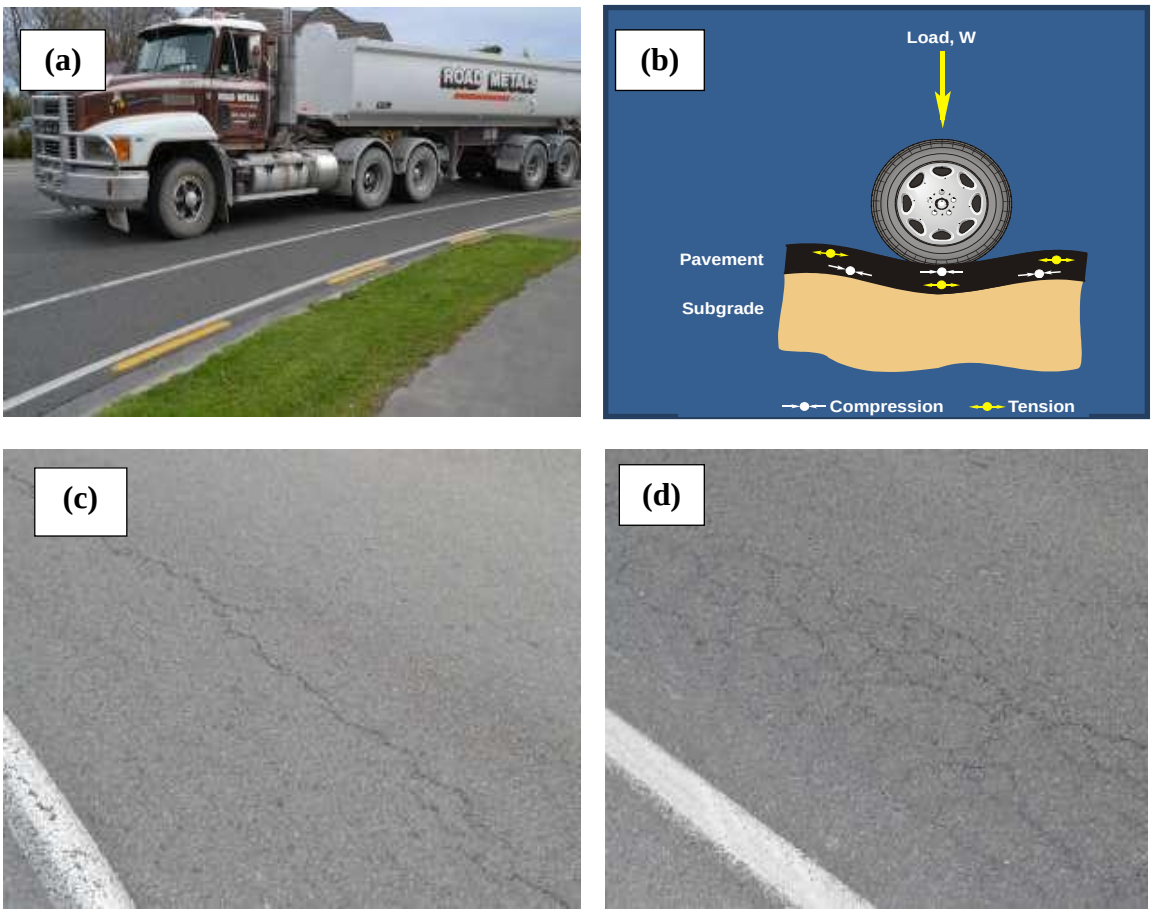

Figure 2.2 Development stages of fatigue cracking: induced by repetitive heavy axle loads (a) causing the pavement to flex (b) (courtesy of Pidwerbesky, 2009); progressing into longitudinal fatigue cracks (c), and finally disintegrating into "block" like cracks (d)

From a maintenance perspective, top-down are easy to repair because a crack sealant can be used to seal the surface as in **Figure 2.3**. Bottom up fatigue cracks, in contrast, aren't as easier to repair and are more expensive. With many of New Zealand's heavy traffic roads being of major significance, NZTA cannot afford the cost from delays with repairs on these major routes.

Figure 2.3 Top-down cracks are sealed with a crack sealant on a structural asphalt motorway (courtesy of Hudson, 2006)

Load induced fatigue cracking is not only dependent on the number of heavy axles that causes the pavement to crack, but environmental effects also influence its behaviour. That is, the effect of binder ageing on fatigue cracking. Ageing increases the stiffness of the mixture, thus changing the fatigue characteristics of the mix over time. This effect of ageing on fatigue is not well quantified. Good binder selection is thus required in the design process to avoid cracking failure of ageing in the pavement's design life. Further research investigating the effect of aged binder on fatigue in the laboratory would be a good start. A pressure ageing vessel can be used to simulate 7–10 years of ageing in the field.

2.2.2 Laboratory Characteristics

Fatigue cracking in the laboratory is influenced by a number of variables. Both fatigue and stiffness testing are dependent on the type of test method, loading mode and conditions, and failure criterion. Notably, there are several different testing methods used to measure

the fatigue life of asphalt that aim to replicate the pavement response (or state of stresses) in field conditions. These different testing set-ups include: bending testing (two, three and four-point loading schemes), indirect tensile testing, and direct tensile testing as in **Figure 2.4**. Each loading set-up creates different states of stresses.

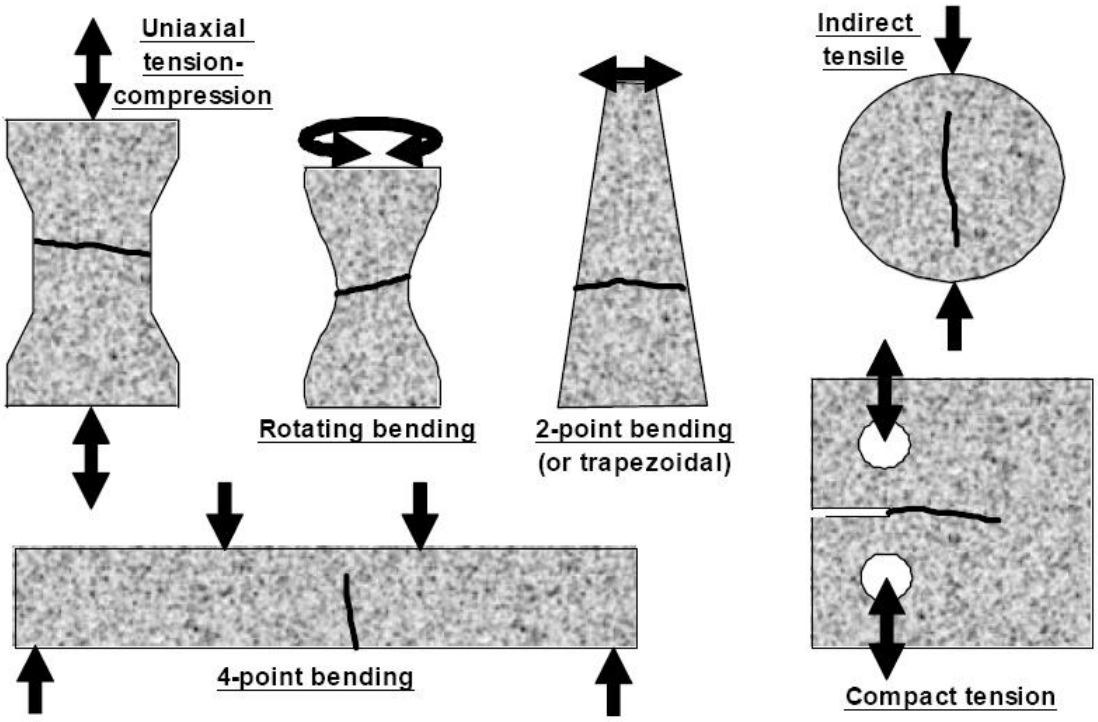

Figure 2.4 Various loading set-ups and different induced states of stresses (courtesy of Thom, 2006)

Flexural fatigue testing is the preferred Australian procedure as it is said to reproduce the actual behaviour of an asphalt layer under wheel loading more closely than any another method (AUSTROADS, 2008a). However, in the field, the asphalt is "subjected to complex three-dimensional stressing" (Pell & Copper, 1975), and tri-axial loading best replicates these stresses. On the other hand, two-point loading is advantageous as it does not provide a stress concentration at the point of loading, due to the specimen's trapezoid shape. Four-point loading is recommended over three-point loading because there is a constant bending moment in the middle third of the specimen; furthermore, "any weak spot due to non-uniform materials will show up in the test result" (Huang, 2004). Since, asphalt is already a non-homogeneous material, this type of testing produces more consistent results.

Among these various loading set-ups are also two types of loading modes: controlled strain and controlled stress. Controlled strain testing is defined by maintaining a constant deformation during cyclic loading throughout the test; hence, controlled strain is also known as controlled displacement testing. In this test, the load is decreasing over time to keep a constant deformation. As the number of cycles increase, the stiffness (or flexural) modulus of the sample beam decreases, and thus the material softens. Since there is no clear failure, failure is often defined when the stiffness modulus is reduced to 50 per cent of its original value (Baburamani, 1999).

In contrast to controlled strain testing, controlled stress testing is achieved by maintaining a constant loading stress throughout the test. It is therefore referred to as controlled force testing. In this case, the deformation increases during the test as a result of cracking; hence, failure is defined when the specimen fractures.

Within the literature, controlled strain testing is said to be more applicable for relatively "thin" asphalt pavements (less than 100 mm thick) (Baburamani, 1999), on the other hand, controlled stress testing is more relevant for "thick" pavements. Huang (2004), however, states that controlled strain is more suitable to thicknesses less than 2 inches (51 mm); and controlled stress is more suited for thicknesses greater than 6 inches (152 mm). Nonetheless, it is generally agreed that controlled strain testing is best for thin pavements because, the level of strain at the bottom of the asphalt layer is more sensitive to the stiffness's and thicknesses of the underlying pavement layers. In addition, Pellinen et al. (2004) notes softer and more flexible mixes perform best for thin pavements as they provide superior performance. As mentioned before, the Shell FTF was developed from controlled strain testing, and this was one of the reasons why it was adopted in the AUSTROADS guidelines.

2.2.3 Lab and Field Differences

Differences exist between measured fatigue in the laboratory and the field. Baburamani (1999) stated that these discrepancies between the field and the laboratory are due to differences in the loading set-ups; establishing realistic loading times and rest periods between traffic loading; the surrounding temperature during the pavement service life; and the level of compaction of the asphalt.

In addition, in the laboratory, the same *level* of load is applied in the same position – in every load cycle; the surrounding temperature is constant; the loading rate is constant; and the asphalt beam is simply supported. Conversely, in the field, traffic loads are variable and dependent on the axle configuration. These loads "wander", and thus are not always loaded in the same line; the air temperature is continuously changing; the traffic loading rate is dependent on the vehicle speed, which is varied continually; and asphalt layer is fully supported from the underlying layers.

Together, these differences make laboratory fatigue tests more stringent and severe than field conditions. Indeed Austroads (2008) state "the actual number of load applications producing cracking in the field may be many times the number obtained by laboratory testing." Because laboratory conditions are known to be more conservative than field conditions, a field shift factor (FSF) is commonly applied to laboratory fatigue models to estimate field fatigue, as given by Equation 2–9.

$$N_{f(field)} = FSF \times N_{f(lab)} \quad \textbf{2–9}$$

where:

$N_{f(lab)}$ = fatigue life as predicted in laboratory conditions
$N_{f(field)}$ = allowable number of loading cycles until field fatigue failure
FSF = field shift factor

The FSF value depends on the level of cracking that is to be tolerated by the given transport agency (i.e. 10% cracking or 50% cracking). The literature found shift factors can vary from 10 to 20 (Baburamani, 1999) and 40 to 100 (Adhikari, Shen, & You, 2009). For polymer modified sections field shift factor of 4.2 has been used (National Cooperative Highway Research, 2010). Pierce and Mahoney (1996) have noted for Washington State pavements FSF values are between 4 and 10. Generally, for thicker pavements and decreasing strain levels lower shift factors are used. In the Asphalt Institute model, the FSF is given by Equation 2–10.

$$FSF = 18.4 \times 10^{M} \quad \textbf{2–10}$$

where: $M = 4.84 \times (VFB - 0.69)$ and $VFB = (V_b/(V_b + V_b))$.

It is not clear from the available literature what percentage of fatigue cracking in the wheel path the Shell FTF was calibrated for.

Summary

A review of the design of structural asphalt pavements using the Shell FTF has been provided. The literature demonstrates that the Shell FTF is outdated and that the status quo is not acceptable for the design of structural asphalt pavements in New Zealand. The chapter has given the derivation of the Shell FTF and discussed its adoption into the AUSTROADS design guidelines along with its inherent issues. The complications of understanding the asphalt fatigue cracking phenomenon have also been addressed, illustrating its complexity. The chapter additionally defines the fatigue cracking mechanism and describes the various ways to characterise asphalt fatigue in a laboratory environment. Differences between laboratory fatigue and field fatigue have also been outlined. Having argued the issues with asphalt fatigue for New Zealand, the goal of the next chapter is to explain the material properties and specimen preparation needed to improve the status quo.

3

PREPARATION OF MATERIALS AND SPECIMENS

A pavement engineer's objective is to design a consistent roading material that survives its design life. The aim of this thesis is to provide the pavement engineer with information on the modulus and the fatigue characteristics of two local New Zealand asphalts. In doing so, good material handling practices are required during sample preparation to provide asphalt specimens that are replicable. Details of the materials and mix design used for modulus and fatigue testing are described in this chapter, as well as the sample preparation methods.

3.1 MATERIALS

3.1.1 Material Selection

This thesis investigates the modulus and fatigue characteristics of two typical New Zealand densely graded structural hot mix asphalts (HMAs).

- AC14 60/70
- AC14 80/100

AC14 represents the maximum nominal aggregate size (i.e. 14 mm) for the densely graded asphalt mixtures. 60/70 and 80/100 denote the penetration grade of the binder. The grade of the binder is known to effect the fatigue performance of the asphalt, so it will be interesting to see the effect of the fatigue life between these common New Zealand binders. 80/100 is the softer of the two binders, and thus it is hypothesised that this grade of bitumen will have a longer fatigue life than the 60/70 binder. Application of these asphalt mixes are for either heavy traffic or very heavy traffic classifications (New Zealand Transport Agency (NZTA), 2010).

3.1.2 Binder Properties

Binder's behaviour is dependent on its origin and distillation process, thus the source of bitumen is an important attribute. Both binder grades 60/70 and 80/100 were sourced from Downer, from Bitumen Supply Limited in Mount Maunganui, and where sent to the University of Canterbury's Transportation Laboratory.

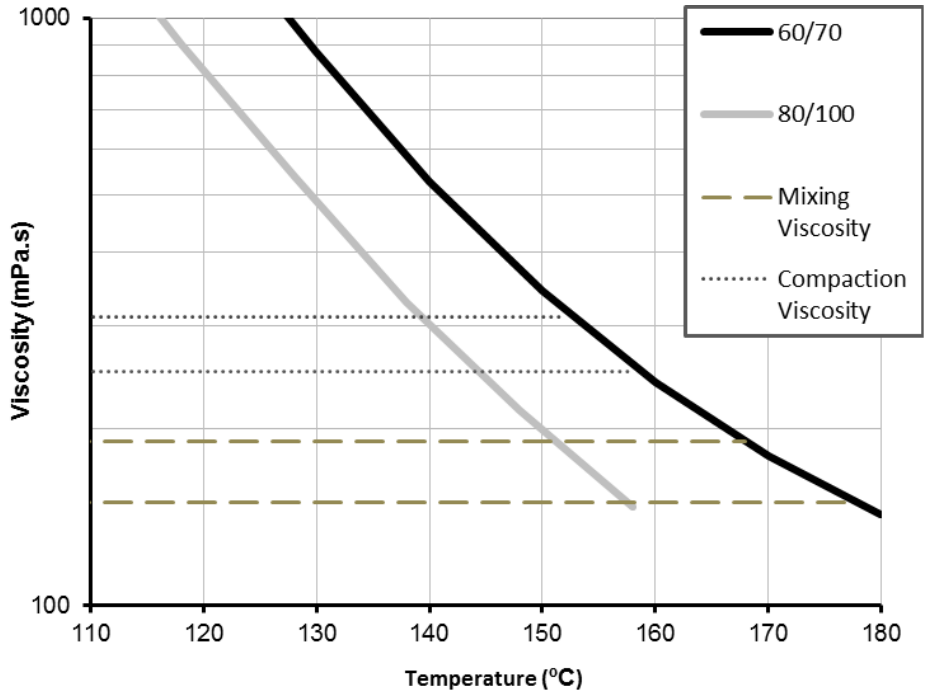

Figure 3.1 Temperature–viscosity relationship curve for both the 60/70 and 80/100 binders

Figure 3.1 plots the temperature–viscosity relationship for both the 60/70 and 80/100 binders. The plot of the viscosity and temperature relationship of the binder is a pivotal

property to determine the correct mixing and compaction temperatures for each binder. Mixing and compaction viscosity are juxtaposed on this figure showing their respective temperature ranges.

Mixing temperature corresponds to a viscosity range of 170 ± 20 mPa.s. Compaction temperature corresponds to a viscosity range of 280 ± 30 mPa.s. For the 80/100 binder, the mixing temperature was 155°C, and the compaction temperature was theoretically 142.5°C. In reality, temperature during compaction was around 120°C, measured by an infrared laser. However, the desired level of compaction was achieved as the samples were around target air voids – see Appendix B. For the 60/70 mix the contractor carried out all the sample preparation.

3.1.3 Aggregate Properties

The aggregate geology used throughout this thesis was basalt rock and was sourced from the Bombay Quarry, Auckland. This aggregate was provided by Downer. Basalt was used because it is a suitable rock for structural asphalt roads with either heavy traffic or very heavy traffic loads. These types of roads are more commonly constructed in Auckland than other parts of New Zealand.

Basalt rock is by nature an igneous rock. Good mechanical strength, durability, chemical stability, surface characteristics, hardness/toughness, surface texture and crushed shape properties are attributes of basalt rocks (AUSTROADS, Australian Asphalt Pavement Association, & Australian Road Research Board Transport Research, 1997). These properties are important in the design of pavements, particularly heavy duty structural pavements.

Details of the aggregate gradation, AC14 used for this thesis are presented in **Table 3.1**. The table shows the size of each aggregate used in this blend, the specifications limits, the proportion of each aggregate size in the final blend, and the specific gravity of each aggregate fraction. Three different aggregate sizes were blended together to provide the final blend. Coarse aggregates (52%), fine aggregates (42%), and sand aggregates (6%) were combined in the aggregate blend. The aggregate gradation complies with AUSTROADS AC14 dense graded HMA as shown graphically in **Figure 3.2**.

Table 3.1 Aggregate gradations, specific gravities and aggregate proportions in the mix

Sieve size (mm)	Coarse aggregate	Fine aggregate	Sand	AC14	Specification limits	
					Lower	Upper
19	100	100	100	100	100	100
13.2	98	100	100	99	90	100
9.5	67	100	100	83	72	83
6.7	18	99	100	57	54	71
4.75	1	87	100	43	43	61
2.36	1	60	100	32	28	45
1.18	0	40	96	23	19	35
0.600	0	28	76	16	13	27
0.300	0	20	33	10	9	20
0.150	0	15	5	7	6	13
0.075	0	12	0	5	4	7
Percentage in mix	52.0%	42.0%	6.0%	Combined		
Specific gravity	2.83	2.87	2.54	2.827		

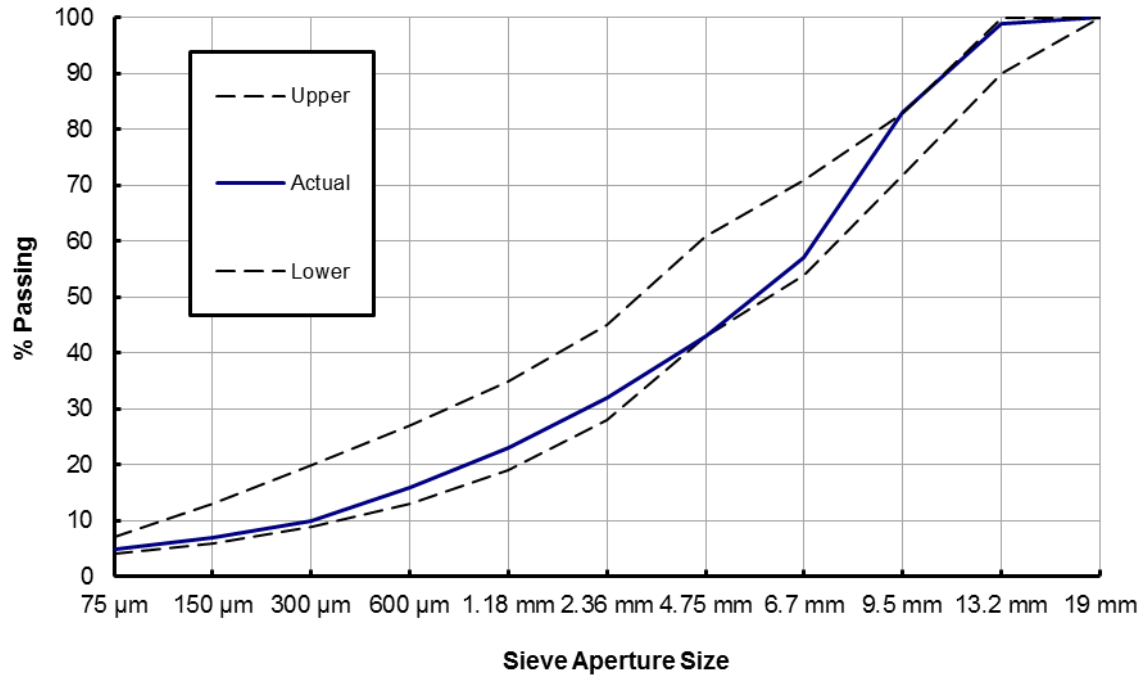

Figure 3.2 Combined aggregate gradation for the AC14 dense graded asphalt mixes

Volumetric properties of HMA plays a central role in the asphalt mix performance and are thus crucial to control in the mix design phase. Since the aggregate is a blend and is made up of a combination of crushed basalt rock, it is necessary to determine the bulk density from the individual aggregate sizes. To determine the bulk specific gravity of the AC14

mix based on the three proportions of the coarse, fine and filler aggregates, Equation 3–1 was applied.

$$G_{sb} = \frac{P_{coarse} + P_{fines} + P_{filler}}{\frac{P_{coarse}}{G_{coarse}} + \frac{P_{fines}}{G_{fines}} + \frac{P_{filler}}{G_{filler}}} \qquad \textbf{3–1}$$

where:

G_{sb} = bulk specific gravity of the combined aggregate blend
P_{coarse} = percentage of coarse aggregate in the total blend
P_{fine} = percentage of fine aggregate in the total blend
P_{filler}= percentage of filler aggregate in the total blend
G_{coarse} = specific gravity of the coarse aggregates
G_{fine} = specific gravity of the fine aggregates
G_{filler}= specific gravity of the filler aggregates

3.1.4 Mix Design Recipe

For both hot mixes of AC14 60/70 and AC14 80/100, the mix design was again completed by Downer. Before sample preparation can begin, the job mix formula (JMF) or mix recipe needs to be known. Details of the JMF are in **Table 3.2**.

Table 3.2 Mix design variables for the two different asphalt mixtures: AC14 60/70 and AC14 80/100

Variable	AC14 60/70	AC14 80/100
P_b	5.02%	5.02%
G_{mb}[i]	2.519	2.465
G_{mm}	2.652	2.595
G_{sb}	2.827	2.827
Target VTM[ii]	5.00%	5.00%
VMA[iii]	15.368%	17.182%
VFB[iv]	20%	20.06%

[i] Asphalt mix bulk specific gravity
[ii] Air voids in total mix (%)
[iii] Voids in mineral aggregate (%)
[iv] Voids filled with bitumen

For the asphalt mixtures, the optimum binder content, P_b, was determined as 5.02 per cent for the AC14 60/70, and was determined from the Marshall mix design method. For the AC14 80/10, the optimum binder content was also assumed to be the same as the AC14 60/70. The fabric of the aggregate gradation was also assumed to remain unchanged, since it is only the binder that coats the aggregate and gules the asphalt mixture; in addition, the design was made for a Level 1 mix, thus binder type does not play a role. The G_{mm}, however, differs between the two binders types. The G_{mm} for the AC14 60/70 was measured by Downer, and the G_{mm} for the AC14 80/100 was measured at the University of Canterbury's Transportation Lab.

Target air voids for the mix were 5.0 ± 0.5 per cent. The air void requirement for densely graded asphalt for very heavy traffic in New Zealand is between of 3–5 per cent (NZTA, 2010). In addition, it is recommended by AUSTROADS Pavement Research Group (APRG) that 5 per cent air voids are used for specimens for fatigue testing; although, it is acknowledged that the level of air voids affects the asphalt's fatigue performance (AUSTROADS, et al., 1997).

Another key variable in asphalt mix design is the maximum density of asphalt G_{mm} because it calculates the JMF volumetrics. To calculate G_{mm} the standard AS 2981.7.1 uses the water displacement method, also known as the Rice method. G_{mm} represents the 100 per cent density in an asphalt mix that has no air voids.

3.2 SAMPLE PREPARATION METHODOLOGY

Good sample preparation techniques are important to ensure that the intrinsic properties of the HMA are consistent and homogeneous. This section describes the process for turning the mix design into asphalt beams for modulus and fatigue testing, and is illustrated in **Figure 3.3**. Manufacturing of asphalt beams is simple and follows standard procedures. The document: Commentary to AG: PT/T220 – Sample Preparation – Compaction of Asphalt Slabs Suitable for Characterisation (2005) was also referred to in the preparation.

Figure 3.3 Sample preparation flow chart: from mixing to compaction

The mixing and blending of the binder and aggregate was carried out according to AS 2891.2.1 – 1995 and the APRG (AUSTROADS, et al., 1997). The amount of aggregate and binder calculated for each slab was based on the target air void content for the mix design; the calculation for the AC14 80/100 is presented in Appendix C. The calculation for the AC14 60/70 is not presented as this was prepared by Downer.

One of the problems when binder is exposed to high temperatures (particularly during mixing) is that the asphalt is prone to oxidation. As the mixing and compaction temperature depends on a set viscosity value oxidation causes the binder's viscosity to increase and this is undesirable. Oxidation changes the chemical composition of the binder

and thus its physical and mechanical properties. Therefore, during sample preparation a consistent technique is mandatory. For each slab preparation, the mixing time was two minutes and 30 seconds.

For each slab, the total batch for each slab was mixed as two parts and then these parts were combined in the mould before compaction. Conditioning time was for 60 minutes at 150^{o}C. In total, 24 asphalt slabs were prepared as two sets of 12. The first set for the AC14 60/70 mix were prepared by Downer; the second 12 slabs for the AC14 80/100 mix were prepared at the University of Canterbury's Transportation Laboratory.

During slicing of the slabs into beams, it was decided to deviate from the specified dimensions of the beams. The AUSTORADS (2008a) guidelines recommend trimming the beams to a cross section of 55 mm (high) by 63mm (wide) specimen. However, because 24 slabs were prepared for this thesis, in order to increase the number of beams for fatigue testing, the beams were cut to 55 mm (high) by 55 mm (wide). **Figure 3.4** gives a comparison of the two cross section sizes to scale. **Figure 3.4** (a) shows dimensions recommend by AUSTROADS and **Figure 3.4** (b) is dimensions used in this thesis. Previous it was noted that the Shell researchers used even thinner beams compared to those used in this research (Van Dijk & Visser, 1977).

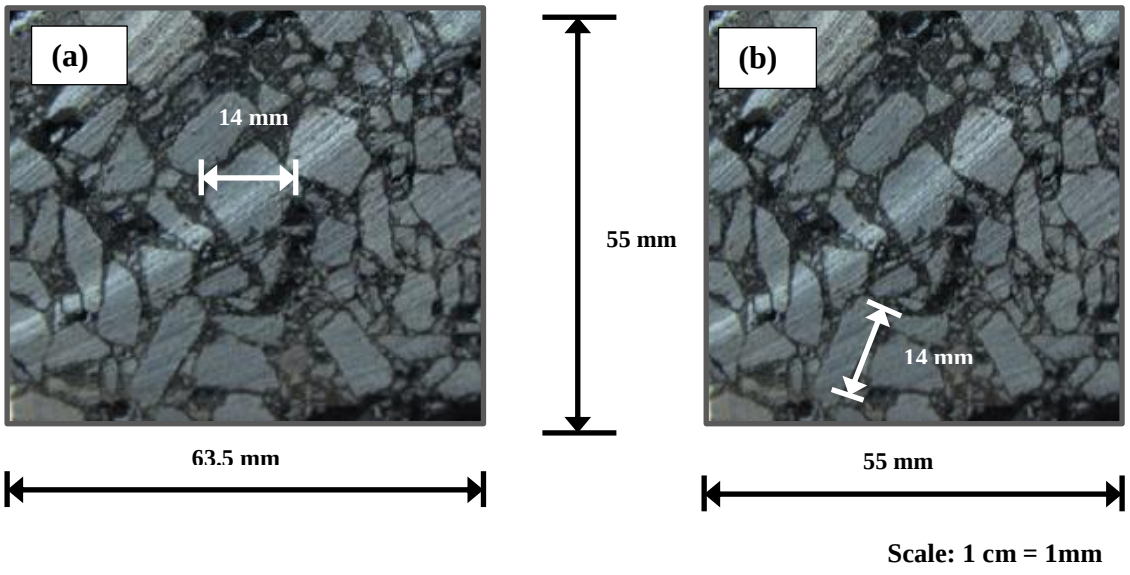

Figure 3.4 Cross-sectional comparison of the standard beam (a) and the experimental beam (b)

For the AC14 60/70 asphalt mixture, one slab was prepared and cored into six cylinders for indirect tensile testing to measure the resilient modulus. Otherwise, slabs were cut into beams.

Summary

This chapter describes the materials and sample preparation methodology needed to prepare asphalt specimens for modulus and fatigue testing. Details on the aggregate blend and binder properties of the AC14 60/70 and AC14 80/100 HMAs been provided. Method of preparing the various asphalt cores and beams has also been outlined. From the preparation of asphalt samples, they are now ready for both modulus and fatigue characterisation.

4

CHARACTERISATION OF ASPHALT'S MODULUS

Asphalt's modulus and fatigue transfer functions govern asphalt layer thicknesses in the AUSTROADS (2008a) pavement design guidelines. Understanding the characteristics of both the modulus and fatigue performance is fundamental in a pavement design, particularly for different environmental conditions.

Stiffness modulus for a given material is the ability to resist stress, principally from traffic loads in pavement engineering. Asphalt's modulus is a fundamental parameter in pavement design because it is required in mechanistic analysis to calculate the stresses and strains that the pavement layers sustain. These responses are induced by either traffic loads or temperature effects, and over time cause the pavement structure to fail.

Within New Zealand there is insufficient modulus data that characterises pavement response over a range of conditions common to New Zealand's climate. Moreover, the modulus also affects the fatigue life of asphalt and its effect is not well understood in New Zealand as well as other parts of the world. Hence, the objective of this chapter is to characterise the asphalt modulus for a range of the different climatic conditions. Chapter

results will be integrated with the fatigue analysis in Chapter 5 to provide a more accurate fatigue damage assessment and will be discussed in Chapter 6.

Four sections are covered in this experimental chapter. A literature review, which defines the asphalt's modulus, its properties, and the different laboratory methods to characterise the material response is presented in the first section. Experimental procedure for measuring the asphalt's modulus and the methodology to construct a modulus master curve is described in Section Two. The third section presents the results of the measured moduli as functions of temperature and frequency. Master curves for the different moduli are constructed in the final section.

4.1 LITERATURE REVIEW

4.1.1 Background

One of asphalt's most basic engineering properties is its modulus. Yet characterising modulus response under different loading and temperature conditions is complicated and this behaviour is not fully understood and this is clear from the forgoing discussion. This literature review provides an overview of the theory to compute asphalt modulus for different loading and temperature conditions. As there are numerous methods to calculate asphalt's modulus, some alternative methods common to AUSTROADS are also discussed.

4.1.2 Asphalt's Modulus Definition

An important variable in pavement design is asphalt's modulus because it is an input into multi-layer programs. Multi-layer programs calculate stresses, strains and deflections that are endured by the pavement; the objective of the pavement engineer is to ensure that these responses do not cause the pavement to fail for the required performance period. These programs are often based on elastic theory, and thus the asphalt material is also assumed to behave elastically. However at moderate to high temperature, asphalt does not behave elastically. In fact, after each loading application some permanent deformation remains within the material. If this load is small compared to the strength of the material for a large number of loading applications and the permanent deformation under each load is

completely recoverable, the material can be considered elastic (Huang, 2004). The elastic modulus E based on the recovered deformation is called the resilient modulus M_R and is given as Equation 4–1.

$$E \approx M_R = \frac{\sigma_d}{\varepsilon_r} \qquad \textbf{4–1}$$

where:

E = elastic modulus (MPa)
M_R = resilient Modulus (MPa)
σ_d = deviator stress (MPa)
ε_r = recoverable strain (mm/mm)

4.1.3 Laboratory Modulus Characterisation

There are a number of ways to measure the elastic modulus of asphalt concrete including the bending (or flexural) test, the indirect tensile test (ITT), and the uniaxial compressive testing. **Figure 4.1** (a) and (b) illustrates the four-point bending loading scheme and the ITT respectively. Each of these different tests creates a different state of stresses, thus measures a different modulus. The ITT measures the resilient modulus, M_R; the flexural bending test measures the stiffness modulus, S_{mix}; and the uniaxial compressive test measures the dynamic (or complex) modulus, $|E^*|$. Although each alternative test measures a *different* modulus, they are all said to be analogous to the elastic modulus.

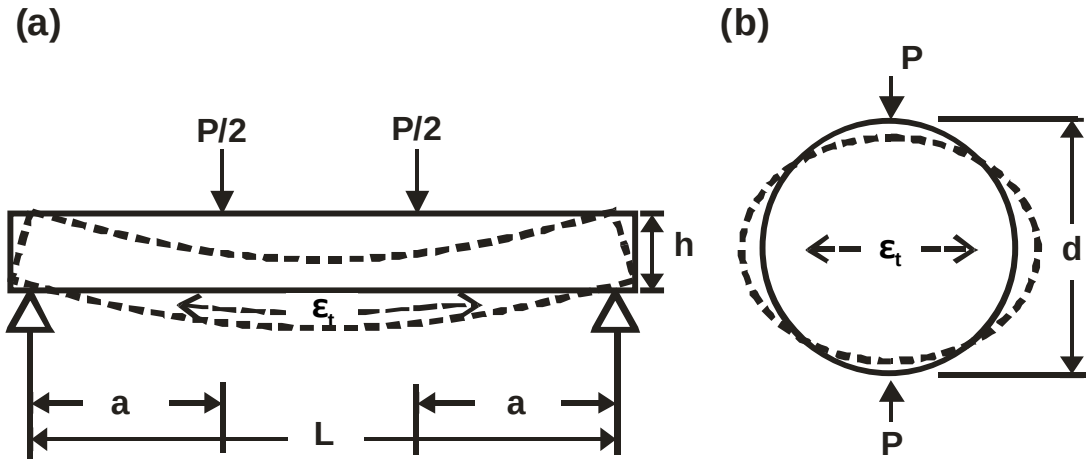

Figure 4.1 Loading setups: (a) four-point bending and (b) indirect tensile testing

Indeed, previous researchers including Shu and Huang (2010), Adhikari et al. (2009), Peploe (2008), Lacroix et al. (2007), and Jian (2006) have highlighted these differences. The flexural stiffness is said to be the preferred option because the procedure 'reproduces the actual behaviour of an asphalt layer (Austroads, 2010). Nonetheless, the ITT is most commonly carried by practitioners because of its simplicity and ease of application (Alba, Barksdale, Khosla, Lambe, & Rahman, 1997).

In addition to the various states of the stresses the asphalt can be under, the modulus can differ by the method of sample preparation. Laboratory test specimens (or mix designs) can be fabricated by: static compaction, impact compaction, kneading compaction, gyratory compaction, or rolling-wheel compaction. Tangella et al. (1990) gives an excellent comparison of the different compactions method. Rolling-wheel compaction is said to closely simulate field compaction conditions (Bonnot., 1986; Van Dijk., 1975; Von Quintus., Scherocman., Hughes., & Kennedy., 1988), and therefore is the favoured option.

The loading shape is a further variable that influences the modulus response of the asphalt. Applied load can have different shapes or durations. Different shapes can either be: haversine, exponential, sinusoidal, uniform, or triangular. The shape represents the loading pulse induced by a heavy vehicle. Haversine is the preferred shaped (AUSTROADS, 2008b).

In the ITT, the resilient modulus is calculated by Equation 4–2 and, in the flexural four-point bending test, the stiffness modulus is calculated by Equation 4–3. These tests assume that the asphalt behaves as an elastic and homogeneous material. However, it is well established that asphalt is a viscoelastic material.

$$M_r = \frac{P(\upsilon + 0.2734)}{\delta t} \qquad \textbf{4–2}$$

$$S_{mix} = \frac{23PL^3}{108bh^3\Delta} \qquad \textbf{4–3}$$

where:

P = applied load or force (N)
υ = Poisson ratio – typically between 0.35–0.40 for hot mix asphalt
δ = total recoverable deformation (mm)
t = thickness of the specimen (mm)
L = length of the asphalt beam (mm)
b = specimen width (into the page) (mm)
h = specimen height (mm)
Δ = deflection of the beam measured at the centre (mm)

4.1.4 Asphalt's Response

Asphalt is not strictly an elastic material. Instead asphalt behaves as a viscoelastic material (Huang, 2004), meaning asphalt's response is time dependent. Asphalt also behaves as a thermoplastic material (Whiteoak, 1990) and thus its response is also temperature dependent. It is observed that at lower temperatures and high loading rates the asphalt becomes stiffer, and at high temperatures and low loading rates the asphalt becomes softer.

To characterise the asphalt's time-temperature dependence, a master curve can be constructed using the principle of time-temperature superposition. A master curve gives the relationship between the asphalt mix modulus, loading rate, and pavement temperature, such that for any pavement temperature and any loading frequency the asphalt's modulus can be predicted. This ability to understand asphalt's modulus response at different temperatures and loading rates can be necessary to prevent different distress failures.

4.1.5 Master Curve Construction

Master curves characterise the asphalt's modulus for any given pavement temperature and loading rate (frequency) of a particular asphalt mix. Implementing the time-temperature superposition principle, the modulus measured at any temperature T for different levels of frequency f can be "shifted" to a reference temperature T_{ref} by a shift factor a_t. The modulus frequency curves for each level of temperature are aligned to form a single master curve. The shift factor is given by Equation 4–4, and is defined as "a constant by which the frequency is multiplied to get a reduced frequency" Pellinen et al. (2002).

$$f_{red} = a_t f \quad \textbf{4–4}$$

where:

f_{red} = reduced frequency
a_t = shift factor
f = loading frequency (Hz)

Within the literature, the most common shift functions are the empirical Williams Landel Ferry (WLF) equation and the Arrhenius equation. Pellinen et al. (2002) found that the Arrhenius shifting equation was the best shifting factor for over sixty mixes. The Arrhenius equation is given by:

$$\log a_t = \frac{E_a}{2.303R}\left(\frac{1}{T} - \frac{1}{T_{ref}}\right) \quad \textbf{4–5}$$

where:

E_a= apparent activation energy (J/mol)
R = universal gas constant = 8.314 (J/mol°K)
T = experimental temperature (°K)
T_{ref} = reference temperature (°K)

The apparent activation energy is associated with the relaxation process for amorphous polymers below the glass transition temperature. Various values for the apparent activation energy have been found in the literature. Pellinen et al. (2002) found that the average for conventional mixtures was 205 kJ/mol and values ranged from 156-227 kJ/mol. Whereas Lytton et al. (1993) found this value as high as 250 kJ/mol and Jacobs (1995) cited it as low as 147 kJ/mol.

The master curve can be constructed by fitting either a sigmoidal or polynomial model, but most commonly the sigmoidal model is employed, and is defined by:

$$\log E = \delta + \frac{\alpha}{1 + e^{\beta - \gamma \log \zeta}} \quad \textbf{4–6}$$

where:

δ = minimum modulus value (MPa)
α = span of modulus values (MPa)
β and γ = shape parameters
ζ = reduced frequency (Hz)

To fully characterize the modulus master curve with a sigmoidal function (i.e. capture the lower and upper ends of the curve) the modulus must be measured at high temperatures $\geq$ 45°C and low temperatures $\leq$ -5°C.

4.1.6 Asphalt's Modulus in AUSTROADS

To determine asphalt's field modulus based on the AUSTROADS pavement design guidelines (2008a), three parameters are required: laboratory modulus and two non-dimensional factors f_{temp} and f_{speed}. Each factor reflects the design conditions, that is: "What are the pavement temperature and vehicle speed for a section of road?" Based on these conditions, the adjustment factors can then be determined from using the charts presented in the Austroads (2008a). A standardised resilient modulus also needs to be measured in the laboratory. Equation 4–7 is then used to correct the standard laboratory measured modulus for the field.

$$E_{field} = E_{standard} \times f_{temp} \times f_{speed} \qquad \textbf{4–7}$$

where:

E_{field} = field resilient modulus (MPa)
$E_{standard}$ = laboratory resilient modulus (MPa)
f_{temp} = non-dimensional factor adjustment based on WMAPT
f_{speed} = non-dimensional factor adjustment based on vehicle speed

4.1.7 Design Problems with the Different Moduli

Often, asphalt's modulus is an input into the mechanistic empirical design for pavement response calculations and for damage analyses such as fatigue and rutting performance models and other deterioration criteria, such the Shell fatigue transfer function. One of the

problems in modelling asphalt fatigue cracking is that practitioners replace flexural stiffness S_{mix} with the resilient modulus M_r; however, the measured values of these moduli are not equal ceteris paribus. Substitution happens because the resilient modulus is much easier and simpler to measure. Therefore, another motivation of this thesis is to provide practitioners with a relationship between the resilient modulus and the flexural stiffness for any level of frequency and temperature, so that knowing one modulus can lead to the other.

4.2 EXPERIMENTAL METHOD

To characterise asphalt's modulus in the laboratory two different testing methods were carried out; the ITT to measure the resilient modulus and four-point bending to measure the stiffness modulus. For each test, various combinations of testing conditions of different temperatures and loading rates were used.

4.2.1 Modulus Testing

The resilent modulus was measured by the ITT with the IPC global universal testing suit (UTS) model UTS 3, and the test was carried out in accordance with the Australian Standard AS 2891.13.1—1995e. The ITT is shown in **Figure 4.2** (a), below. For the purpose of this research, the standard test temperature and loading frequency were modified. Each core specimen was tested at a range of different temperatures: -5°C, 1°C, 5°C, 10°C, 20°C, 25°C, and 45°C. For each temperature, the loading width pulse (frequency) was changed at different levels: 1000 ms (1 Hz), 500 ms (2 Hz), 100 ms (10 Hz), and 67 ms (15 Hz). All tests were carried out at a standard pulse repetition period of 3 s and a recovered horizontal strain of 50 ± 20 με. For each combination of test temperature and test frequency, the modulus was measured at least five times, with the average being plotted in the results.

Flexural modulus testing was measured using the IPC global universal testing machine (UTM) model UTM 21 stand-alone fatigue apparatus. Like the ITT, this bending beam apparatus is also placed in the controlled temperature cabinet, as in **Figure 4.2** (b). Because the load is applied dynamically, the stiffness modulus is also referred to as the *dynamic* flexural modulus test, not to be confused with the complex modulus test. The initial flexural stiffness is obtained using a four-point loading scheme under a range of

different loading conditions. The initial flexural stiffness is measured at the end of the 50th loading cycle. The *dynamic* modulus is measured at the end of the 200th loading cycle. Each beam was tested with a haversine loading pulse of: 5000 ms (0.2 Hz), 1000 ms (1 Hz), 200 31 ms (5 Hz), 100 (ms), and 67 ms (15 Hz). For each frequency level, each beam was tested under a range of different temperatures: 5°C, 10°C, 20°C, 25°C, 30°C, 40°C, and 45°C. All tests were carried out at a standard pulse repetition period of 100 ms and a constant strain of 400με. Beams were allowed to adjust to their testing temperature for at least 60 minutes before being loaded.

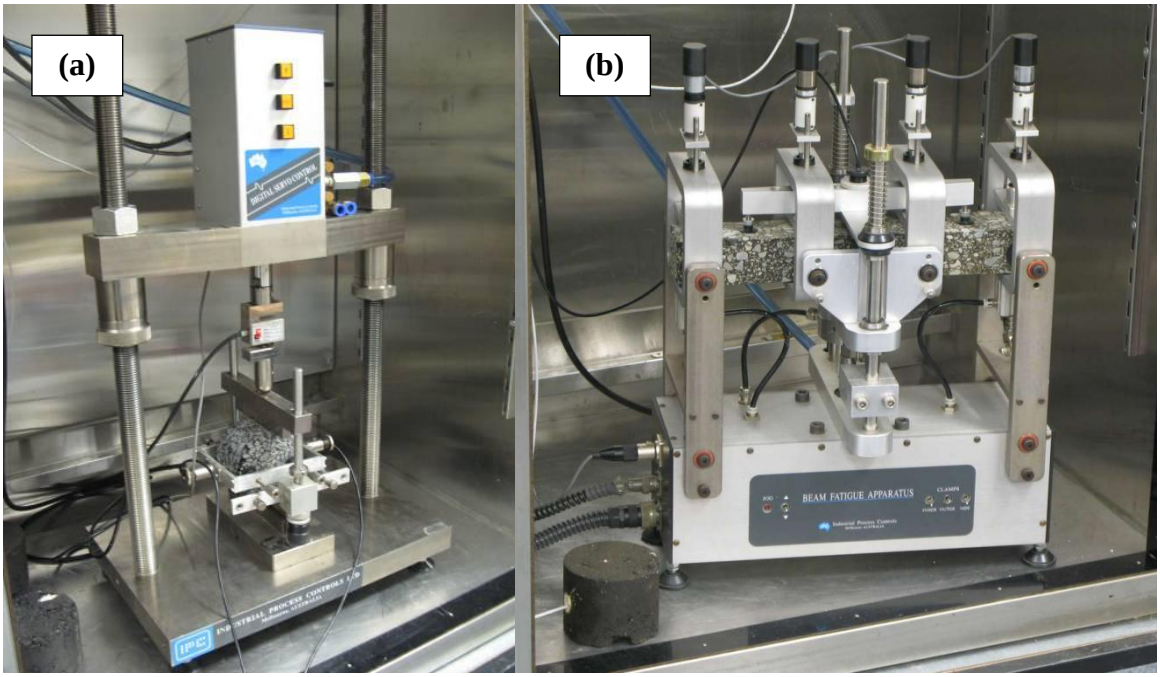

Figure 4.2 Laboratory testing setups at the University of Canterbury's transportation lab: (a) indirect tensile test and (b) four-point bending test

4.2.2 Master Curve Construction

A master curve was constructed for both the resilient modulus and flexural stiffness with a designated reference temperature of 20°C (=293K). The average measured modulus at various temperatures was then shifted using Equation 4–4 and Equation 4–5 (until the curves aligned into a single curve. The merged data was then fitted with a sigmoidal function (a standard form of the master curve) as defined by Equation 4–8 and Equation 4–9. The regression parameters, a, b and c, were computed by minimising the sum of squared errors. Brown (2001) gives an excellent account to perform this non-linear regression

analysis in Excel. The model parameters of Equation 4–8 and Equation 4–9 that were used in the regression analysis are presented in Equation 4–13, Equation 4–14, and Equation 4–15 — further on.

$$\log M_R = \log M_{R_{min}} + (\log M_{R_{max}} - \log M_{R_{min}}) \left(\frac{a}{1 + be^{-c*\log f_{red}}}\right) \quad \textbf{4–8}$$

$$\log S_{mix} = \log S_{mix_{min}} + (\log S_{mix_{max}} - \log S_{mix_{min}}) \left(\frac{a}{1 + be^{-c*\log f_{red}}}\right) \quad \textbf{4–9}$$

where:

M_R = laboratory resilient modulus (MPa)
$M_{R_{min}}$ = laboratory measured minimum resilient modulus value (MPa)
$M_{R_{max}}$ = laboratory measured maximum resilient modulus value (MPa)
S_{mix} = laboratory stiffness modulus (MPa)
$S_{mix_{min}}$ = laboratory measured minimum stiffness modulus value (MPa)
$S_{mix_{max}}$ = laboratory measured maximum stiffness modulus value (MPa)
a, b and c = regression coefficients
f_{red} = reduced frequency (Hz)

To construct the master curve the shift factor needs to be determined for each temperature level. **Figure 4.3** plots the shift factor based on the Arrhenius Equation 4–5 as a function of temperature. The activation energy, for the Arrhenius equation for both 60/70 and 80/100 binders was determined to be 200 kJ/mol. This was calculated by the non-linear regression analysis. Depending on the testing temperatures the required shift can be determined from this figure.

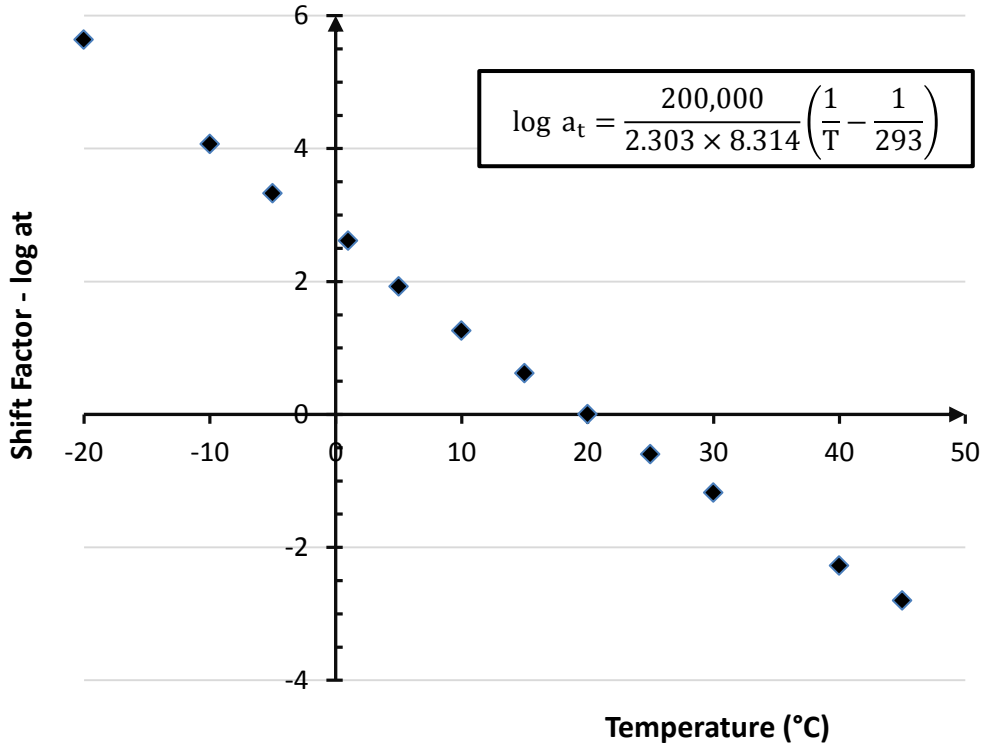

Figure 4.3 The temperature dependency of the Arrhenius shift factor a_t

4.3 RESULTS

The asphalt moduli for the two different mixtures were characterised as a function of temperature and frequency. The first section presents the data of the measured resilient modulus of the AC14 60/70 hot mix asphalt (HMA). The second section presents the measured stiffness modulus as a function of both temperature and frequency for the two different HMAs: AC14 60/70 and AC14 80/100. The final section compares the differences between measured resilient modulus against the stiffness modulus for the same mixes and loading conditions.

4.3.1 Resilient Modulus – AC14 60/70 HMA

Figure 4.4 and **Figure 4.5** present the average measured resilient modulus of the AC14 60/70 asphalt mix for the different temperature and frequency conditions. In **Figure 4.4**, the resilient modulus is depicted as a function of temperature a fixed frequency level, whereas in **Figure 4.5**, the resilient modulus is portrayed as a function of frequency for a

fixed temperature level. The data in each of these plots are the same, but just plotted differently. As expected, resilient modulus increases with decreasing temperature and increasing frequency. **Figure 4.4** shows resilient modulus is largely temperature dependent; indeed, the modulus roughly doubles for a drop in temperature of 10°C, for each testing frequency. The effect of temperature on resilient modulus is greater than the effect of frequency.

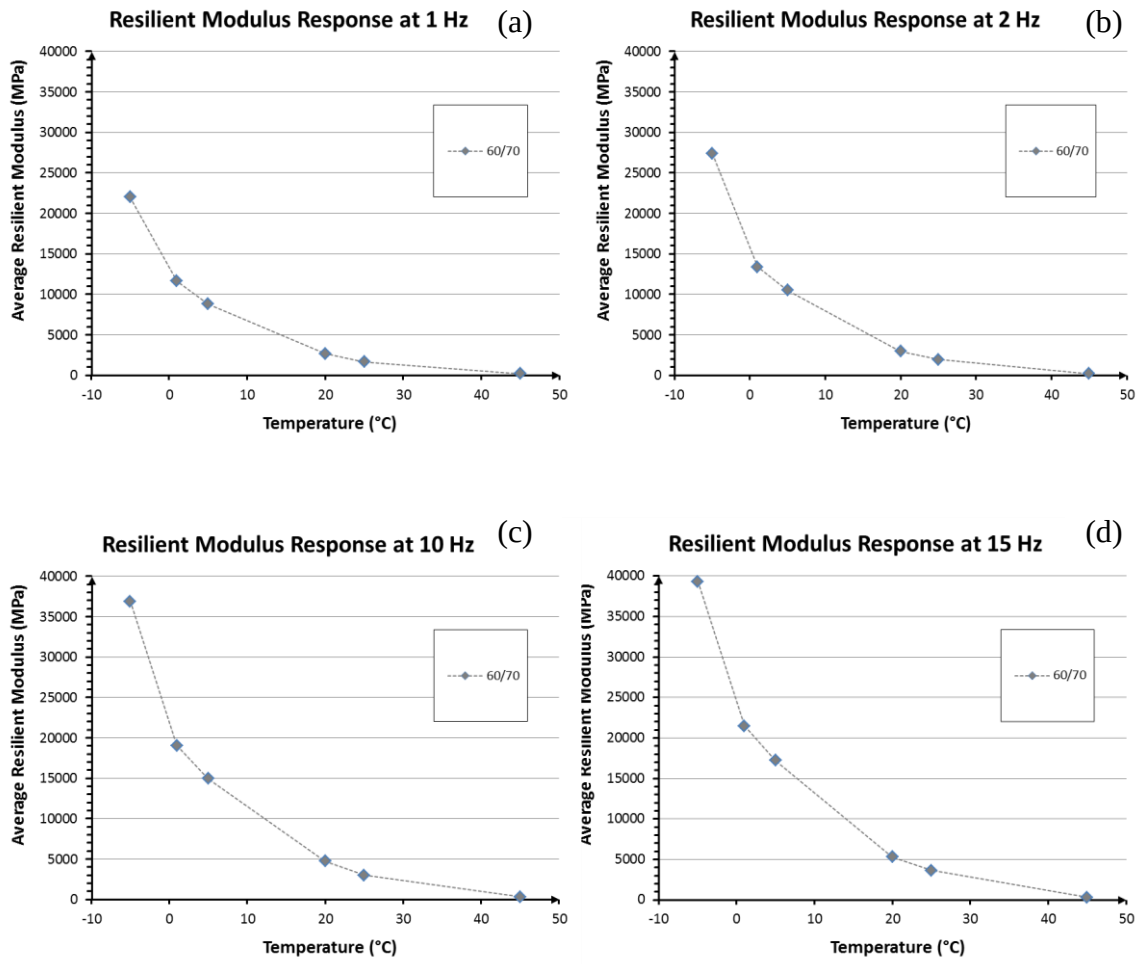

Figure 4.4 The effect of temperature on the measured resilient modulus for the AC14 60/70 mix for different frequency levels: (a) 1 Hz, (b) 2 Hz, (c) 10 Hz, and (d) 15 Hz

Figure 4.4 illustrates that the resilient modulus as a function of temperature can be modelled as an exponential function, Equation 4–10. Other researchers have also found a similar relationship for the stiffness modulus, but within a temperature range of 5–25°C (Deacon., Coplantaz, Tayebali, & Monismith, 1994). Other exponential models were

explored, using non-linear regression analysis, but were discounted to keep the model simple.

$$E = a \times e^{-b\,T} \qquad \textbf{4–10}$$

where:

E = modulus, either resilient or stiffness moduli (MPa)
T = temperature (°C)
a and b = empirical coefficients

The coefficients, a and b in Equation 4–10 were obtained from the numerous plots in **Figure 4.4** and have been tabulated in **Table 4.1** for their respective frequency levels.

Table 4.1 Resilient modulus regression coefficients a and b in Equation 4–10 for different frequencies for AC14 60/70 Mix

Frequency level	*a*	*b*	R^2
1 Hz	1.422×10^4	0.092	0.995
2 Hz	1.698×10^4	0.094	0.995
10 Hz	2.431×10^4	0.093	0.989
15 Hz	2.751×10^4	0.094	0.981

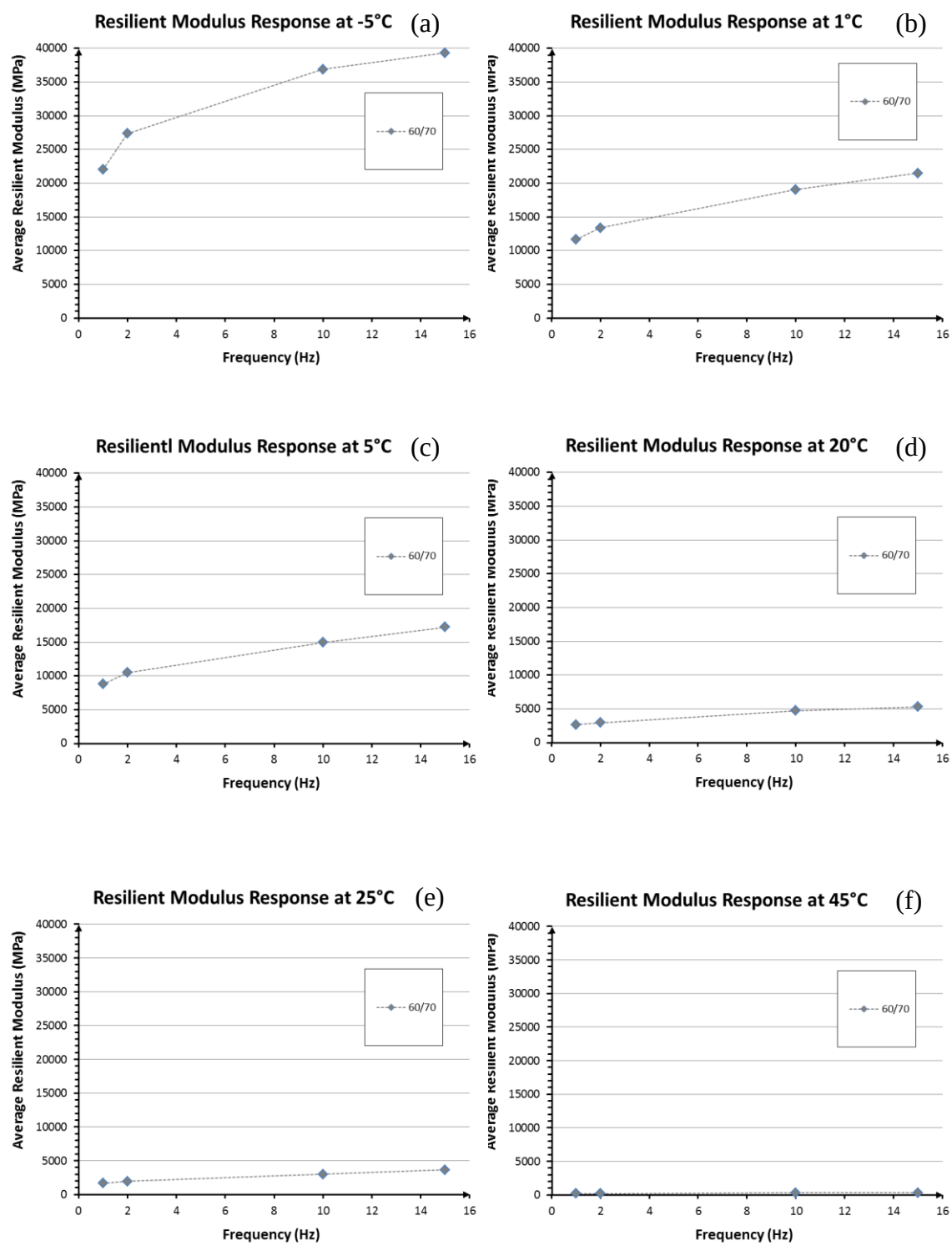

Figure 4.5 The effect of frequency on the measured resilient modulus for the AC14 60/70 mix for various temperature levels: (a) -5°C Hz, (b) 1°C, (c) 5°C, and (d) 20°C, (e) 25°C, and (f) 45°C

Resilient modulus is also a function of frequency, and can be modelled using the power law for different temperature levels as in Equation 4–11. Jahromi and Khodaii (2009)

stated that it is quite common to use the generalized power law to define the frequency dependent behaviour of bituminous material at low and moderate temperatures. **Table 4.2** presents the empirical coefficients a and b for Equation 4–11 for each measured temperature level.

$$E = a \times f^{b} \qquad \textbf{4–11}$$

where:

E = modulus, either resilient or stiffness moduli (MPa)
f = loading frequency (Hz)
a and b = empirical coefficients

Table 4.2 Resilient modulus regression coefficients a and b in Equation 4–11 for different temperatures

Temperature	a	b	R^2
-5°C	22.736×10^3	0.208	0.987
1°C	11.532×10^3	0.225	0.998
5°C	8.815×10^3	0.240	0.996
20°C	2.258×10^3	0.264	0.991
25°C	1.610×10^3	0.289	0.990
45°C	0.198×10^3	0.167	0.984
-5°C	22.736×10^3	0.208	0.987

4.3.2 Stiffness Modulus – AC14 60/70 HMA and AC14 80/100 HMA

The average measured laboratory stiffness modulus is plotted in **Figure 4.6** as a function of temperature for the various frequency levels: 0.2 Hz, 1 Hz, 2 Hz, 5 Hz, 10 Hz, and 15 Hz. Similar to the resilient modulus, the stiffness modulus decreases with increasing temperature and with decreasing frequency. On average, the stiffness modulus drops by 50 per cent for an increase in 10°C; this is a significant effect. The binder class is also a variable affecting stiffness modulus. The stiffer binder (i.e. lower binder grade) shows an increase in stiffness modulus. As metioned in section 4.1.6, Shell researchers found that the binder stiffness correlates to the mixtures stiffess based on the volumetric properties of the asphalt mix (Shell International Petroleum Company Ltd., 1978). For each combination

of temperature and frequency condition, the stiffness modulus difference between the two binder grades is non-uniform as the lines in **Figure 4.6** are not parallel.

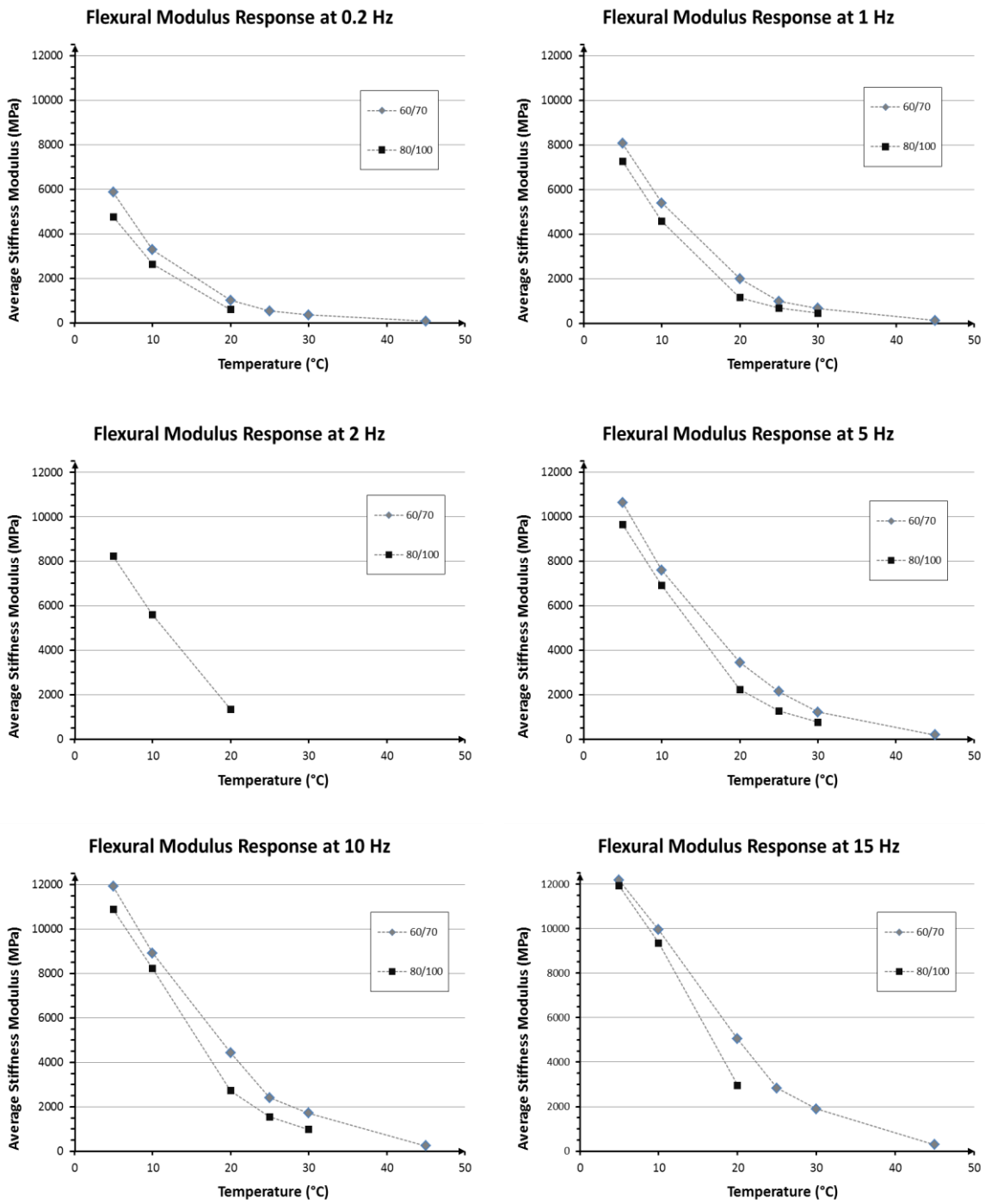

Figure 4.6 Effect of temperature on the measured stiffness modulus response on both AC14 60/70 and AC14 80/100 for numerous frequency levels: (a) 0.2Hz, 1 Hz, (b) 1 Hz, (c) 2 Hz, (d) 5 Hz, (e) 10 Hz, and (f) 15 Hz

The average measured laboratory flexural modulus is plotted in **Figure 4.7** as a function of frequency for the different temperature levels: 5°C, 10°C, 20°C, 25°C, 30°C, and 45°C. It is observed that the stiffness modulus decreases with increasing temperature and with decreasing frequency. On average, the stiffness modulus drops by 50 per cent for an increase in 10°C; this is a significant effect.

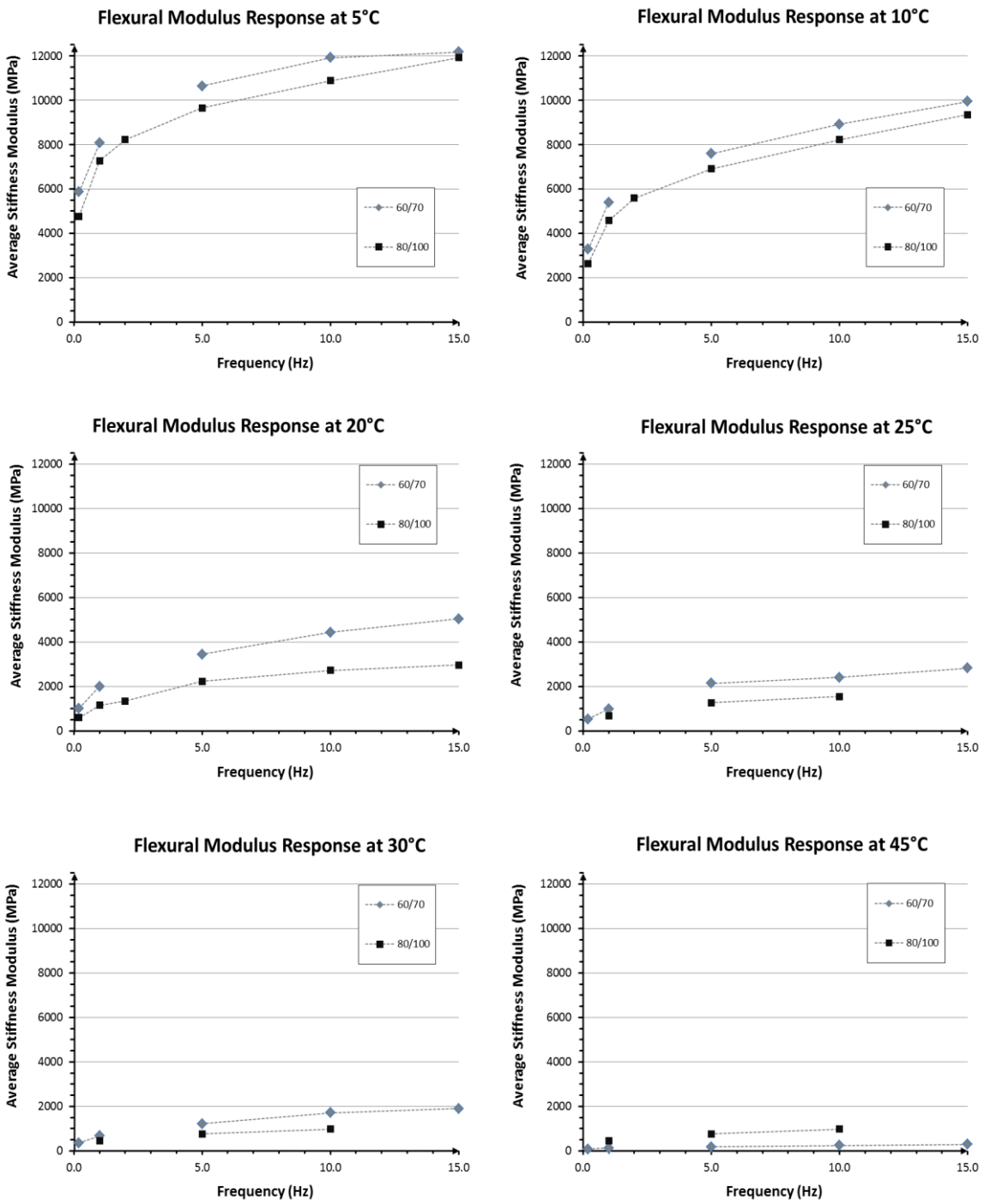

Figure 4.7 Effect of frequency on the measured stiffness modulus response for both the AC14 60/70 and the AC14 80/100 asphalt mixtures for different temperature levels: (a) -5°C Hz, (b) 1°C, (c) 5°C, (d) 20°C, (e) 25°C, and (f) 45°C

Coefficients a and b for Equation 4–10 and Equation 4–11 are displayed in **Table 4.3**, **Table 4.4**, **Table 4.5**, and **Table 4.6**. Additionally, the R^2 values for the various curves are

given. Modulus values can be taken with reasonable certainty as each modulus measurement was repeated at least five times.

Table 4.3 Flexural Stiffness coefficients of a and b in Equation 4–10 for **Figure 4.6** – AC14 60/70

Frequency level	a	b	R^2
0.2 Hz	0.922×10^4	0.108	0.996
1 Hz	1.492×10^4	0.106	0.997
2 Hz	NA	NA	NA
5 Hz	2.188×10^4	0.101	0.982
10 Hz	2.462×10^4	0.097	0.975
15 Hz	2.577×10^4	0.094	0.970

Table 4.4 Flexural stiffness coefficients of a and b in Equation 4–11 for **Figure 4.7** – AC14 60/70

Temperature level	a	b	R^2
5°C	7.899×10^3	0.173	0.993
10°C	5.085×10^3	0.250	0.994
20°C	1.896×10^3	0.369	0.998
25°C	1.015×10^3	0.392	0.992
30°C	0.664×10^3	0.394	0.999
45°C	0.458×10^3	0.326	0.989

Table 4.5 Flexural stiffness coefficients of a and b in Equation 4–10 for **Figure 4.6** – AC14 80/100

Frequency level	a	b	R^2
0.2 Hz	0.999×10^4	0.140	0.997
1 Hz	1.313×10^4	0.115	0.993
2 Hz	NA	NA	NA
5 Hz	1.776×10^4	0.105	0.996
10 Hz	1.984×10^4	0.100	0.994
15 Hz	2.119×10^4	0.096	0.971
0.2 Hz	0.999×10^4	0.140	0.997

Table 4.6 Flexural stiffness coefficients of a and b in Equation 4–11 for **Figure 4.7** – AC14 80/100

Temperature level	a	b	R^2
-5°C	6.924×10^3	0.206	0.990
1°C	4.369×10^3	0.286	0.993
5°C	1.114×10^3	0.378	0.991
20°C	0.694×10^3	0.355	0.997
25°C	0.458×10^3	0.322	0.998
45°C	0.124×10^3	0.283	0.989

4.3.3 Correlation between Resilient Modulus and Stiffness Modulus

It was found that there is a difference between the measured resilient modulus and stiffness modulus for the AC14 60/70 HMA. A correlation between the two has been presented in **Figure 4.8**, so for the given asphalt mixture the pavement engineer can predict the value of either stiffness moduli knowing the resilient moduli or vice versa. The two moduli are compared for the same temperature, loading rate (frequency), and pulse width The resilient modulus was found to be 1.26 times greater than the flexural stiffness for a temperature range of 5—45°C, as seen in Equation 4–12. The coefficient of determination R^2 value for this correlation is 0.9843. In addition, the figure illustrates that this relationship holds for the various testing temperatures, and they are not biased against each other.

$$M_R = 1.2665 \times S_{mix} \qquad \textbf{4–12}$$

where:

M_R = asphalt resilient modulus (MPa)
S_{mix} = asphalt stiffness modulus (MPa)

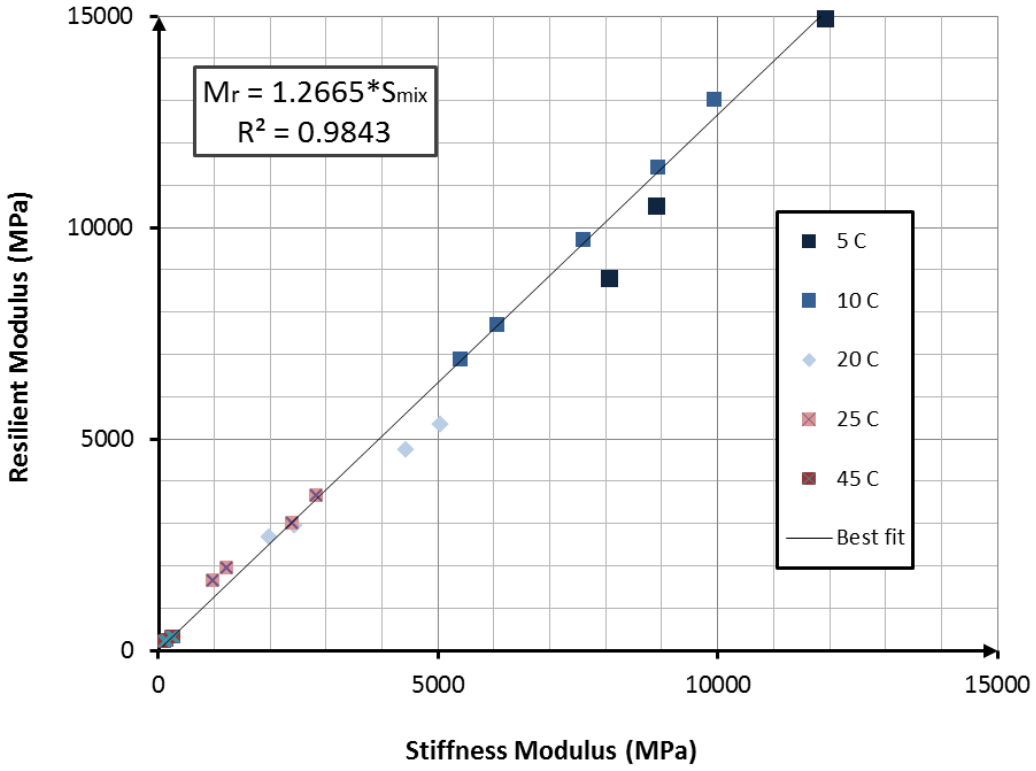

Figure 4.8 A comparison of the measured resilient modulus versus the measured stiffness modulus for the AC14 60/70 asphalt mixture

Comparing the two moduli, the resilient modulus was greater than flexural stiffness because for the flexural stiffness test, the tensile strain is induced by a moment and thus the tensile stress distribution is non-uniform (triangular in nature). Whereas in the ITT the horizontal tensile strain is induced by a compressive force and thus the horizontal tensile stress distribution is reasonably uniform – as is the compressive dynamic modulus test. Simply said, HMA materials are relatively weaker in flexure than indirect tension. However, a full fundamental analysis could be explored to explain this difference.

4.4 MASTER CURVE CONSTRUCTION

4.4.1 Resilient Modulus Master Curve

Figure 4.9 illustrates that the resilient modulus master curve for the AC14 60/70 HMA, defined by Equation 4–13. The master curve shows the variability of the asphalt modulus

response over a range of temperatures and loading rates. The next step for the practioner is to correctly convert the reduced frequency into a vehicle speed to evaluate the modulus of the asphalt at any particular highway speed. A recommended procedure is provided in Jameson and Hopman (2000).

$$\log M_R = 0.6329 + 3.9340\left(\frac{1.074}{1 + 0.5626e^{-0.3945*\log f_{red}}}\right) \qquad \textbf{4–13}$$

where:

M_R = resilient modulus (MPa)
f_{red} = reduced loading frequency (Hz)

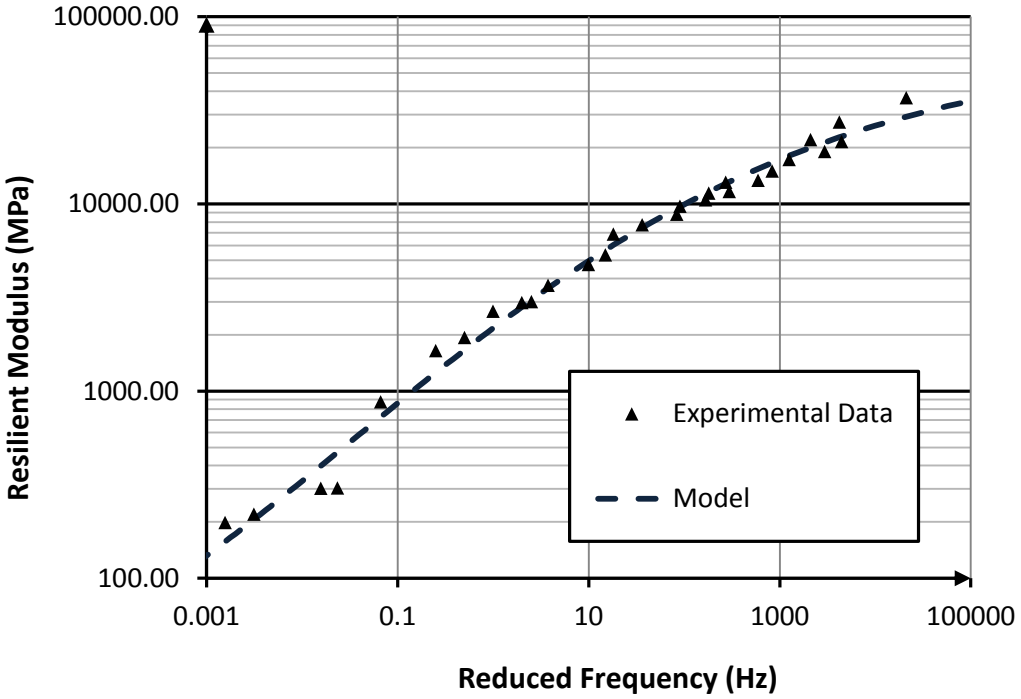

Figure 4.9 Predicted resilient modulus master curve for the AC14 60/70 HMA based on the experimental measurements

The resilient modulus master curve gives reasonable certainty when predicting the resilient modulus as in **Figure 4.10**. The figure shows the resilient modulus measurements are fairly evenly distributed about the line of equality, demonstrating that the model is unbiased. However, the model does under estimate the resilient modulus at around 37,000 MPa, which was measured at -5°C.

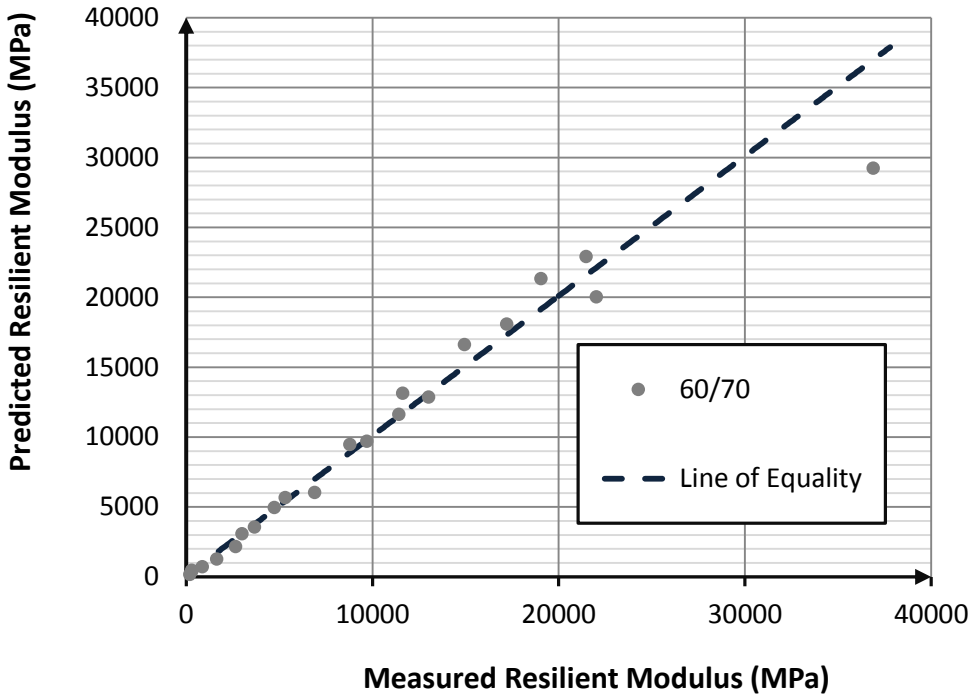

Figure 4.10 Predicted resilient modulus master curve model of the AC14 60/70 HMA against the measured modulus

4.4.2 Stiffness Modulus Master Curve

Sigmoidal stiffness modulus master curves are constructed for the AC14 60/70 and AC14 80/100 asphalt mixtures. The models are superposed against the experimental data. Equation 4–14 and Equation 4–15 give the function of each of these curves respectively. The R^2 values for each of these equations are 0.995 and 0.996 respectively.

AC14 60/70

$$\log S_{mix} = 1.2029 + 1.9645\left(\frac{1.5586}{1 + 0.4396e^{-0.6055*\log f_{red}}}\right) \qquad \textbf{4–14}$$

AC14 80/100

$$\log S_{mix} = 2.4218 + 1.07897\left(\frac{1.6352}{1 + 1.80296e^{-1.04259*\log f_{red}}}\right) \qquad \textbf{4–15}$$

where:

M_R = stiffness modulus
f_{red} = reduced loading frequency (Hz)

The master curves illustrate the expected range of the asphalt's modulus over different temperatures and traffic speeds. For example, for the 60/70 binder class, the asphalt mix modulus can be as low as 100 MPa when pavement temperature is 45°C and the traffic has stopped at a red light. On the other hand, the modulus can be as high as 12,000 MPa when the pavement temperature is 5°C and the traffic is travelling freely on the open road. As a pavement engineer, it is important to understand this variability to prevent the pavement from breaking up.

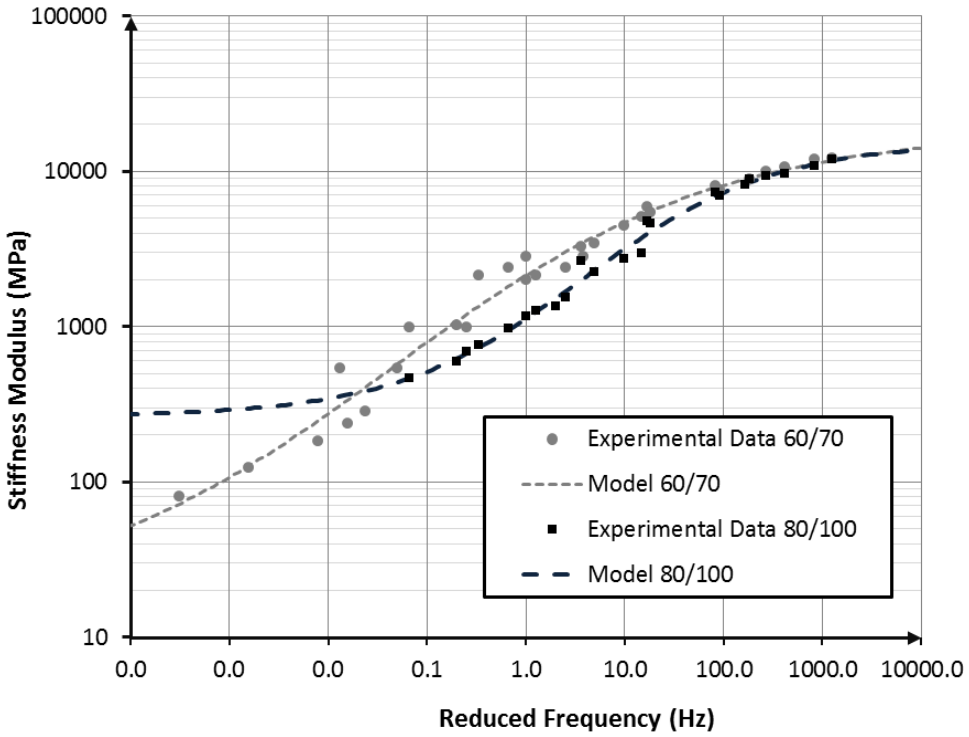

Figure 4.11 Stiffness modulus master curves of both the 60/70 and the 80/100 binder grades, and the experimental data.

Theses stiffness modulus master curves can predict the experimental data with reasonable certainty as illustrated in **Figure 4.12**. The measured data is evenly distributed about the line of equality, demonstrating that the model is unbiased against the results as neither model underestimates nor overestimates the data, implying that the model is accurate.

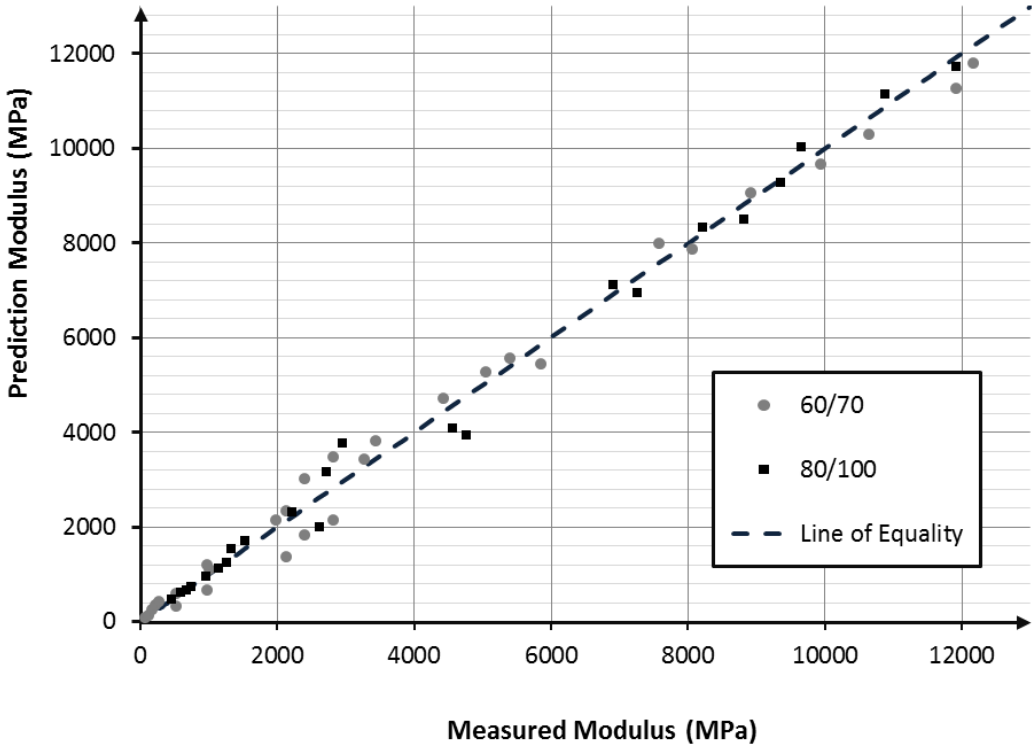

Figure 4.12 Stiffness master curves against the measured flexural modulus measurements of the two different asphalt mixtures AC14 60/70 and AC14 80/100

Summary

Chapter 4 has characterised the resilient modulus for the AC14 60/70 asphalt mix, and characterised the stiffness modulus for the AC14 60/70 and AC14 80/100 asphalt mixes. Measurements have been carried out over a range of temperatures and loading frequencies representing realistic pavement temperatures and traffic speeds.

Although this chapter is secondary to the principal goal of this thesis, the results of this chapter will improve understanding of New Zealand's modulus values for asphalt mixes and of the factors affecting fatigue behaviour. Furthermore, this knowledge for a range of different conditions will facilitate a more rigorous pavement design using an incremental damage analysis.

5

ASPHALT FATIGUE: FACTORS AND CHARACTERISATION

5.1 INTRODUCTION

5.1.1 Context

Structural asphalt concrete layers are favoured for heavy duty and durable pavement construction, and in their design they are built to withstand fatigue cracking. The current AUSTROADS pavement design guidelines for predicting structural asphalt fatigue cracking is the Shell fatigue transfer function (FTF) (2008a). Adoption of the Shell FTF into the AUSTROADS mechanistic empirical (ME) pavement design (MEPD) has been a problem for some time and gives rise to two areas of concern.

First, this FTF does not specifically characterise the fatigue behaviour of New Zealand's asphaltic concrete mixes. Second, the Shell FTF underestimates the fatigue life of the country's asphalts mixes, and thus thicker asphalt layers are unnecessarily constructed to

compensate for this underestimation. Consequently, structural asphalt roads, designed according to the Shell FTF, are prohibitively expensive. As a result, when comparing other pavement design alternatives in an economic evaluation, such as unbound granular pavements, structural asphalts are often not constructed.

The aim of this experimental chapter is to characterise the fatigue behaviour of two common New Zealand structural asphalts. Difficultly arises in understanding asphalt fatigue behaviour because it is affected by a number of factors. A greater understanding of the factors affecting fatigue behaviour is necessary to characterise the fatigue behaviour of the material. Since New Zealand's main roads are under increasing strain because of heavier traffic loading, increasing volumes, and pressure for rapid construction, structural hot mix asphalts (HMAs), if well designed, will become an increasingly advantageous option especially if thinner layers could be engineered.

Given such complexity, it is no wonder the asphalt fatigue cracking phenomenon is not fully understood. Fatigue has been under investigation for a number of decades, and still remains at the forefront of international research because this phenomenon has not been completely solved. Instead, good engineering judgment is required to tackle this problem from a practitioners view.

5.1.2 Predicting Asphalt Fatigue Cracking

Fatigue cracking is caused by the cumulative damage of heavy axle loads. To predict the number of heavy axle loads until fatigue cracking in the field, FTFs are commonly employed. FTFs are central to pavement design as they determine the asphalt's thickness to support this traffic demand. Laboratory testing or analyses of historical data are used to develop FTFs. These functions are commonly expressed in the form of Equation 5–1 and Equation 5–2.

$$N_f = a\left(\frac{1}{\varepsilon_t}\right)^b \qquad \textbf{5–1}$$

$$N_f = a\left(\frac{1}{\varepsilon_t}\right)^b \left(\frac{1}{S_{mix}}\right)^c \qquad \textbf{5–2}$$

where:

N_f = number of loading cycles to fatigue failure
ε_t = tensile strain (mm/mm)
S_{mix} = asphalt mix modulus (MPa)
a, b, c = laboratory regression coefficients

These types of equations after field calibration are referred to as transfer functions because they relate the structural response of the pavement, in this case strain, to the required number of axles until failure. Compared with dissipated energy fatigue models, these types of transfer functions are advantageous because they can be implemented in multilayer elastic analysis programs, such as CIRCLY, widely adopted in Australia and New Zealand.

Constants a, b, and c in Equations 5–1 and Equation 5–2 are specific to factors affecting fatigue and asphalt mixes; accordingly, these laboratory derived models are not applicable to a range of asphalt mixes, and are only applicable to those derived mixes (Di Benedetto, de Roche, Baaj, Pronk, & Lundstrom, 2004). Furthermore, these models have other assumptions.

For example, traditional fatigue studies examine the effects of temperature, frequency, strain, and other variables *individually* (i.e. one variable at a time). Too often, fatigue models are largely developed using a single temperature and frequency. Investigating this individual effect reduces the number of fatigue tests to be carried out, reducing the cost and the time of testing. However, because this traditional approach focuses on the effect of strain at one particular condition, it fails to consider the impacts of interaction between strain and other factors affecting the fatigue life.

Investigating the factors affecting fatigue – their individual and interactional effects – is the major research output of this thesis. The work is original: this type of assessment on asphalt fatigue has not been carried out in New Zealand before. Understanding the factors affecting fatigue will allow for better characterisation and ultimately better engineered roads in New Zealand. To carry out this research, a general factorial design of experiment (DOE) will be used.

5.1.3 Factorial Design of Experiments

In experiments, factorial DOEs are a powerful tool to understand complex physical phenomena. Factorial DOEs are a method for evaluating both the individual and the

interactional effects of different experimental variables. All experimental variables (or testing factors) are varied simultaneously; therefore, the joint effects (or interactions) between factors are additionally considered. Traditional experimental design is limiting because only one factor at a time is investigated while all other factors are held constant. Hence it fails to detect the interactional effect of variables.

5.1.4 Chapter Goals and Organisation

Chapter 5 investigates how combinations of loading, temperatures, traffic speeds (i.e. loading frequency), and binder types affect the fatigue behaviour of two typical New Zealand mixes. The effects of different combinations will be assessed using a DOE. Individual and interactional effects will then be investigated and their level of significance will determined from the DOE.

Following the identification of influencing variables, the chapter also aims to characterise the fatigue behaviour as a function of these variables. Characterisation will be carried out by building a laboratory fatigue life prediction model. The developed models can then act as a surrogate fatigue model to the Shell FTF. Two fatigue models will be custom built to characterise the fatigue life of AC14 60/70 and AC14 80/100 HMA

Six sections are covered in this experimental chapter, which addresses the factors and characterisation of asphalt fatigue behaviour. In the second section, background information on the factors affecting asphalt fatigue behaviour and the factorial DOEs are reviewed. Experimental procedures for the fatigue testing and DOE are described in Section Three. In Section Four, the results of the fatigue testing from factorial DOE are analysed and discussed in three parts. In the first part, the results from the factorial DOE are presented. Both atypical behaviour during fatigue testing and the stiffness reduction during testing are discussed in the second and third parts respectively. Fatigue models are developed in the sixth section, which also has three parts. Analysis Of Variance (ANOVA) is statistically examined in the first part. Part two presents the fatigue models and part three compares these fatigue models with the Shell FTF. Conclusions are given in the final section.

5.2 BACKGROUND INFORMATION

Further context is provided in this section, and is covered in two parts. The various factors affecting asphalt fatigue are reviewed in the first part, and methods of experimental designs to access these factors are addressed in the second part.

5.2.1 Factors Affecting Asphalt Fatigue

There are numerous variables that influence asphalt's fatigue life. Such factors include loading criteria, environmental elements, construction parameters, and material characteristics. These various effects are illustrated in a schematic diagram in **Figure 5.1**.

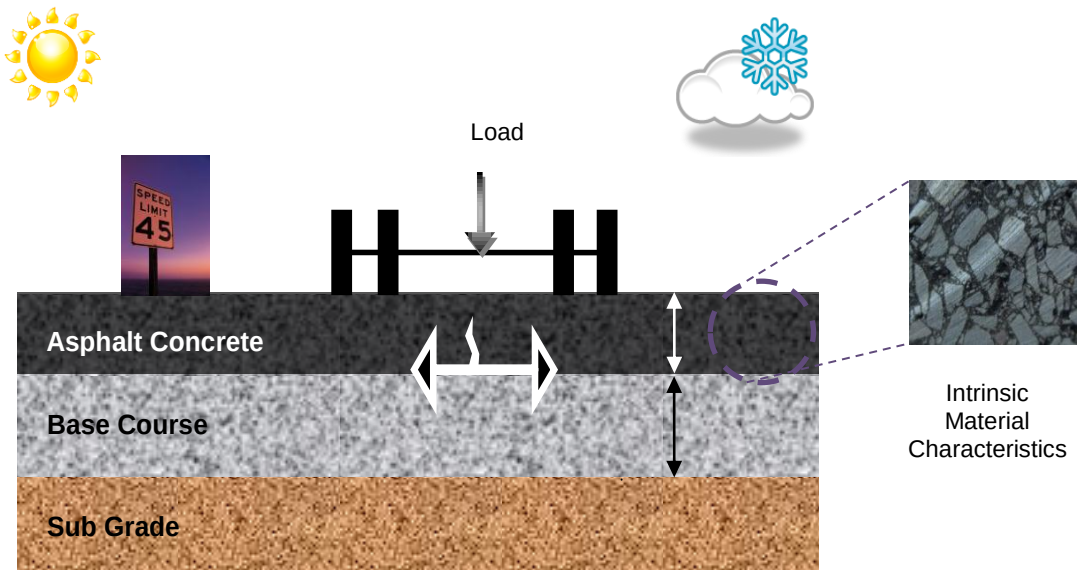

Figure 5.1 Factors affecting asphalt fatigue cracking

Amongst these factors include the parameters used in the design of pavement layers. Variables include pavement layer thickness, axle configurations, modulus values of the different pavement layers, moisture in the pavement, pavement temperature, and speed of the traffic.

In addition to pavement design variables affecting asphalt's fatigue life, there are also the various intrinsic properties of the asphalt mixture. Bitumen content, grade, source,

viscosity, film thickness; air voids; aggregate gradation, shape, geology, angularity; and asphalt's tensile strength all contribute the mix fatigue life.

Complicating matters further are the effects of environmental factors: ageing, temperature fluctuations, and crack healing. Ageing influence depends on the selection of the binder in the mix, as well the interconnecting air voids. Greater interconnecting air voids increase the oxidation (ageing) potential. Furthermore, since asphalt is a time and temperature dependent material, and due to the intermittent nature of traffic loading, asphalt cracks heal during rest periods and at high temperatures, thus impacting fatigue life.

With such complexity, good engineering judgement is required to design a mix that not only has durability and good cracking resistance, but good deformation resistance as well.

5.2.2 Design of Experiments (DOE)

An experimental design is a practical and an empirical method to understand various phenomena. In particular, factorial designs help to explain the effects of simultaneous factors influencing a certain response variable. Factorial DOEs can be time consuming, given the size of some experimental designs. For example, an experiment involving five different factors k=5 with three levels n requires $n^k = 3^5 = 243$ tests. If each test was to be repeated three times to ensure repeatability then there will be 243 x 3 = 729 tests to run. A further limitation with DOEs is that all experimental tests need to be completed before any analysis can begin.

There are different types of factorial designs, each with advantages and disadvantages. Types of factorial designs include traditional experiments, 2^k, 3^k, n^k, general factorial designs, fractional factorial designs, and Plackett-Burman designs. A drawback to traditional experiments is that they only access the effect of a single variable, and therefore are suited to less complex problems.

2^k DOEs are particularly useful to screen effects, since the number of tests required to complete the experiments are not as large as others. Moreover, fractional factorial DOE can be employed to reduce the number of tests due to the symmetric nature of the design. However, a concern of only doing two levels for a particular factor instead of three or more levels is the assumption of linearity in the factor effects (Montgomery, 2001). When a

variable has a non-linear response, testing only two levels will not highlight such a relationship. To combat any second or higher order effects in a two level design a centre-point is tested. However, with a multi-dimensional and non-linear problem, like fatigue, centre points cannot solve the 'big-picture'.

Multivariate type problems can be solved using a general factorial design. Unlike n^k DOE, a general factorial design allows for multiple factors with multiple levels, so that more a sensitive variable can have a greater number of levels than a less sensitive variable, keeping the number of experiments to a minimum. A general factorial design works by having k number of factors, and each factor has n different levels. An issue with such designs is that the number of tests required to complete the experiment can grow very quickly. A further disadvantage of the general factorial design is that if the designer wishes to reduce the number of tests in the experiment, a fractional factorial design cannot be implemented due to its asymmetric nature.

In this chapter, a general factorial design will be used to carry out this investigation. Section 5.3.2 explains the number of factors and levels of factors used within the design.

5.3 EXPERIMENTAL PROCEDURE

5.3.1 Fatigue Testing

All fatigue testing was carried out with the universal testing machine UTM 21 beam fatigue apparatus – shown in **Figure 5.2**. Each fatigue test was conducted using the controlled strain (displacement) mode, rather than the controlled stress (load) mode. Four different controlled strain levels of 300, 400, 500, and 600 με were chosen. These were selected to provide a range of strain levels and to capture the nonlinear behaviour effect of the strain amplitude on fatigue, as in Equation 5–1. Fatigue tests at lower levels were not carried out because of the length of time required to gather results.

Figure 5.2 The bending beam fatigue apparatus within temperature cabinet

As testing was carried out in the controlled strain mode, where the asphalt loses its stiffness during cyclic loading because of the growth of micro cracks, the beam never snaps. Therefore, failure needs to be defined. In this case, fatigue failure was defined as a 50 per cent reduction in the initial flexural stiffness of each beam. Initial stiffness is measured at the end of the 50^{th} loading cycle.

To control the temperature during fatigue testing, the beam fatigue apparatus is placed in a temperature cabinet as in **Figure 5.2**. Temperatures of 10°C, 20°C, and 30°C were selected to give a range of fatigue behaviour that is common in New Zealand's climate. Since fatigue occurs at the intermediate temperatures, there is no need to test at higher or lower temperatures as other modes of failure are more common than fatigue.

Another control variable is the loading frequency (or loading rate). The loading frequency is to mimic the different traffic speeds. To convert the loading frequency to a vehicle speed a correlation is used, however, they often depend on the depth of the asphalt layer. Loading frequencies of 5 Hz and 10 Hz were selected as they roughly represent a traffic speed of 45 km/h and 90 km/h respectively. Ideally, a third frequency level would have been tested as well, but was omitted to save time and resources.

For each testing condition, fatigue measurements were measured twice to ensure repeatability. Variations in measured fatigue lives are well known to occur in fatigue tests

because of asphalt's inherent heterogeneities. Good sample preparation techniques are therefore important to help reduce such inconsistencies.

5.3.2 General Factorial Design

A summary of the various fatigue testing conditions are presented in **Table 5.1**. The levels of each factor are also given.

Table 5.1 Different testing factors and their levels for the factorial design

Testing factors	Levels of factors
Temperature	10, 20, and 30°C
Loading frequency	5 and 10 Hz
Binder grade	60/70 and 80/100
Strain amplitude	300, 400, 500, and 600 $\mu\epsilon$

Temperature, loading frequency, binder grade, and strain amplitude were the four factors selected in this investigation. Three levels of temperature, two levels of frequency, two grades of binder with one binder content, and four levels of strain amplitude were chosen for this study. The generalised factorial design therefore becomes 3 x 2 x 2 x 4 = 48 tests. As there are two repeats, 96 beams are prepared for testing. **Table 5.2** shows the factorial design in matrix form and indicates schematically how factorial designs work.

Table 5.2 Factorial design: matrix of factors and levels to be tested

Asphalt mix (1): AC14 60/70																							
Temperature 10°C								**Temperature 20°C**								**Temperature 30°C**							
Frequency 5 Hz				Frequency 10 Hz				Frequency 5 Hz				Frequency 10 Hz				Frequency 5 Hz				Frequency 10 Hz			
300 με	400 με	500 με	600 με	300 με	400 με	500 με	600 με	300 με	400 με	500 με	600 με	300 με	400 με	500 με	600 με	300 με	400 με	500 με	600 με	300 με	400 με	500 με	600 με

Asphalt mix (2): AC14 80/100																							
Temperature 10°C								**Temperature 20°C**								**Temperature 30°C**							
Frequency 5 Hz				Frequency 10 Hz				Frequency 5 Hz				Frequency 10 Hz				Frequency 5 Hz				Frequency 10 Hz			
300 με	400 με	500 με	600 με	300 με	400 με	500 με	600 με	300 με	400 με	500 με	600 με	300 με	400 με	500 με	600 με	300 με	400 με	500 με	600 με	300 με	400 με	500 με	600 με

5.4 ANALYSIS OF FATIGUE BEHAVIOUR DATA

5.4.1 Presentation of Fatigue Results

Figure 5.3 and **Figure 5.4** present the fatigue life measurements. **Figure 5.3** (a) gives the results for the mixes prepared with the 60/70 and 80/100 binders at 10°C, whereas **Figure 5.3** (b) is for 20°C for both binders. By making a comparison between **Figure 5.3** (a) and (b) the salient points are: for both grades of binder, the higher temperature of 20°C has a greater fatigue life compared with 10°C; and the softer binder 80/100 has a greater fatigue life than the 60/70 bitumen grade for the same temperature. Asphalt also has a longer fatigue life at lower strain levels, which is expected.

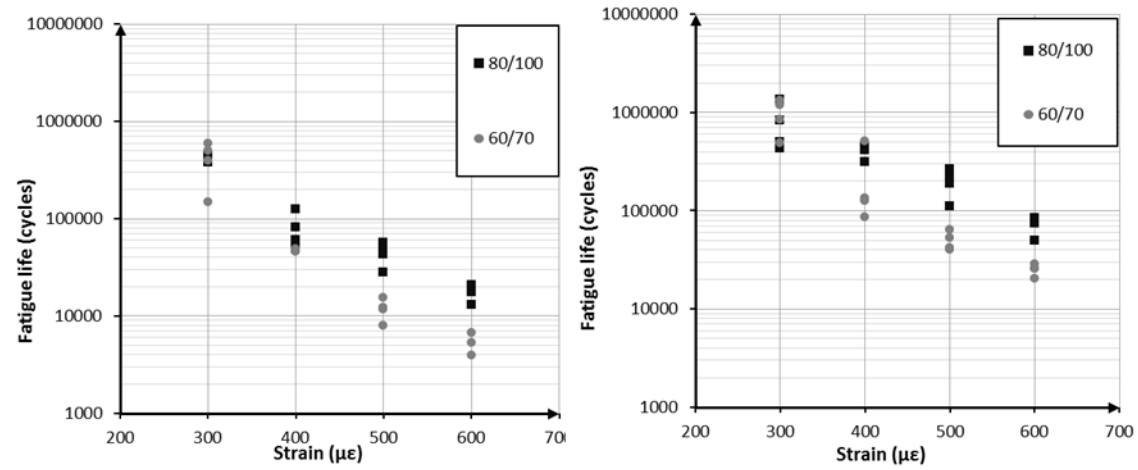

Figure 5.3 Fatigue life plots versus strain: (a) measurements taken at 10°C for both binders, and (b) measurements taken at 20°C for both binders

In addition, **Figure 5.3** illustrates the interaction effect of binder and strain on fatigue life. Irrespective of temperature, bitumen grade has a greater effect on fatigue with increasing strain levels. At lower strain levels, the effect of grade of bitumen on the fatigue life is not as significant as other factors. Section 5.5.1 later quantifies the effect of binder strain interaction on fatigue life.

Like **Figure 5.3**, **Figure 5.4** also illustrates the effect of temperature on asphalt fatigue life. **Figure 5.4** (a) and (b) show that higher temperatures increase fatigue life, regardless of the binder grade. Similar to the joint effect of binder and strain, the combined effect of strain

and temperature on fatigue life is more pronounced at greater strain levels. Once again, Section 5.5.1 quantifies this interaction.

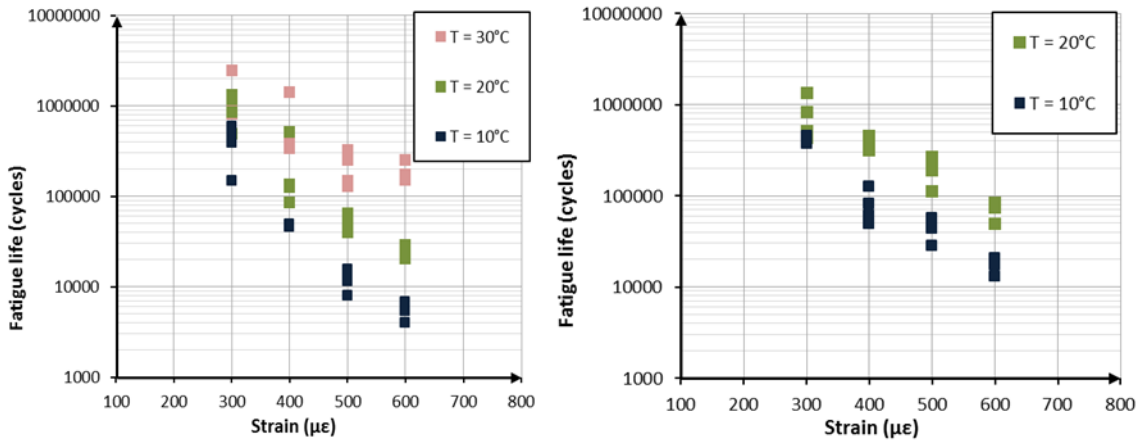

Figure 5.4 Fatigue life plots versus strain: (a) fatigue measurements for the 60/70 binder at 10°C, 20°C, and 30°C; and (b) fatigue measurements for the 80/100 binder at 10°C and 20°C

For **Figure 5.4** (b) the fatigue measurements at 30°C are excluded, Section 5.4.2 explains the reasons for this exclusion.

Variability with the measurements is important to disclose. As only two measurements were taken for each testing condition, due to time constraints, there is a lack of data, resulting in an inability to carry out statistical type tests to quantify this spread, such as the t-test. In some cases, the minimum fatigue life at one strain is the maximum fatigue life at a higher strain level, demonstrating this scatter. Given the inherent variability nature of asphalt, this level of scatter is not surprising. Moreover, even for homogeneous materials, like aluminium and steel, scatter of fatigue results exists (Oliver & Alderson, 2001). Indeed fatigue damage is recognised to have a stochastic nature. Due to its probabilistic nature, at least 8–12 measurements are recommended to develop a fatigue characteristic curve (Huang, 2004).

5.4.2 Atypical Behaviour

Fatigue tests of the AC14 80/100 at 30°C exhibited nonconforming behaviour, irrespective of loading frequency. Thus, for the interpretation and analysis of the fatigue data, at this

particular temperature, all fatigue life measurements were ignored. Atypical behaviour occurred because elastic beam theory was violated, and this theory is the basis for this analysis. Essentially, at higher temperatures, the viscoelastic asphalt behaves more viscous than elastic.

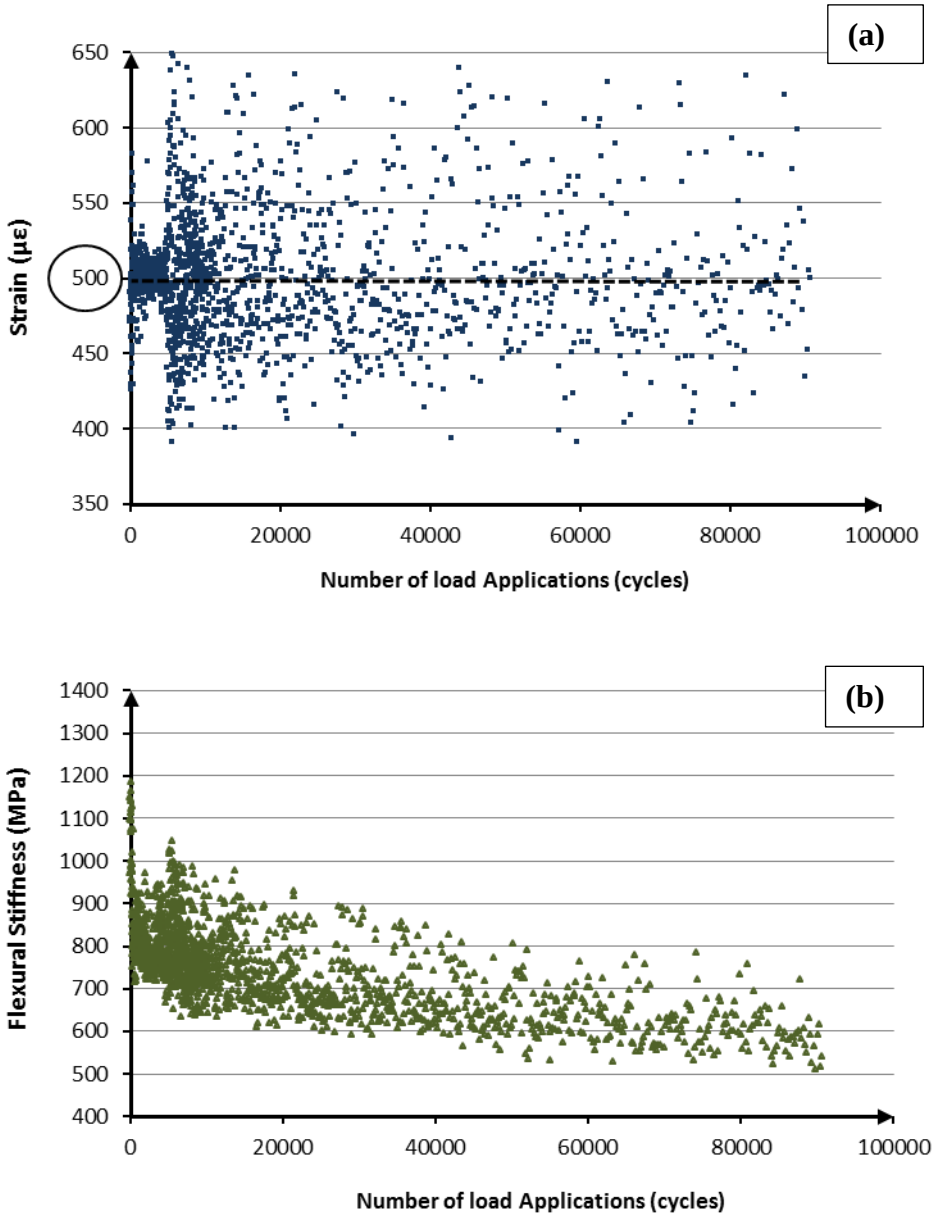

Figure 5.5 A typical cyclic loading (fatigue) test at 30°C for the 80/100 binder: (a) attempting a constant strain of 500 με, and (b) the flexural stiffness evolution curve

For example, **Figure 5.5** demonstrates a typical fatigue test's inability to maintain a constant strain, in this case 500 με. For a normal fatigue test, the strain is within 5 με of the target level; however, **Figure 5.5** (a) illustrates the test is well outside this prescribed tolerance, at times deviating by 150 με. As each new load cycle is applied at 30°C, the deformation does not fully recover before the next load is applied; in addition, at this temperature, the 80/100 binder cannot sustain a constant deflection as given by Equation 5–3. Because strain is directly proportional to the applied deflection by a geometric factor, the asphalt mix cannot maintain a constant strain. Moreover, for each consecutive load, the bending beam machine wants to calculate how much load to apply to maintain a fixed level of strain, but because the deflection is "out" the next calculated load is also out. Subsequently, the flexural stiffness measurements, which are function of strain, for each load cycle, are also scattered as in **Figure 5.5** (b).

$$\varepsilon_t = \frac{12h\Delta}{3L^2 - 4a^2} \qquad \textbf{5–3}$$

where:

ε_t = extreme fibre strain
h = specimen height (mm)
Δ = deflection measured at the beam's centre (mm/mm)
L = span length (mm)
a = third of the length L

Given that elastic theory is violated for the fatigue testing, no direct interpretation of the fatigue life – strain relationship can be inferred. Indeed, **Figure 5.6** illustrates poor correlation between fatigue life and strain amplitude. Furthermore, since the reading of the asphalt's stiffness' are incorrect because the strain measurements are erroneous for a particular loading cycle, the termination stiffness is also astray, resulting in a pseudo fatigue life.

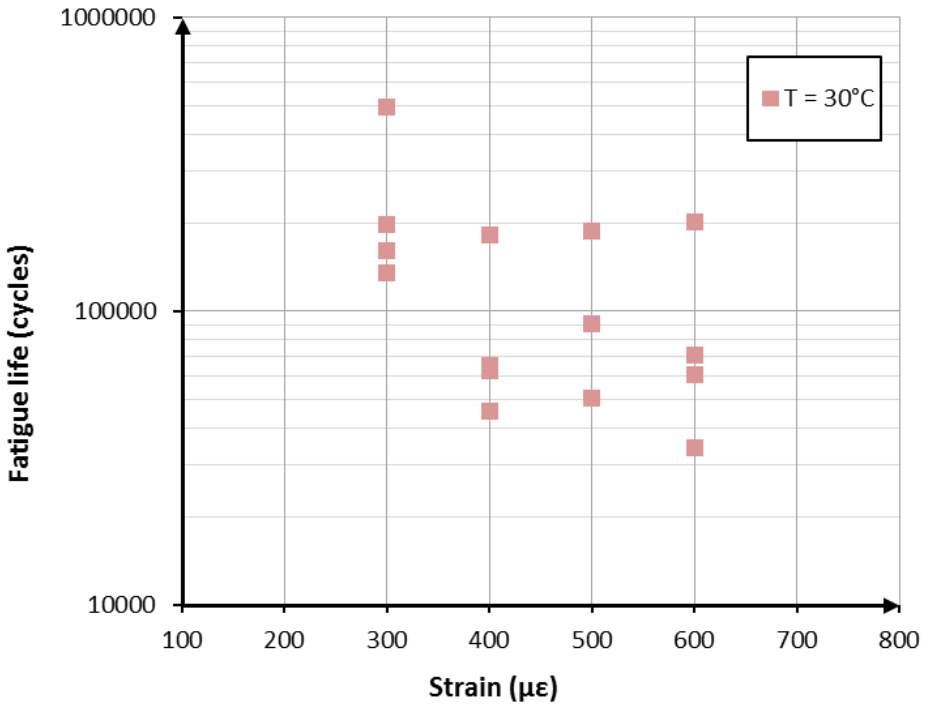

Figure 5.6 Fatigue life data measurements for the AC14 80/100 asphalt mix at 30°C

Although a very weak correlation between fatigue life and strain could be concluded for the AC14 80/100 mix at 30°C, it does not mean poor fatigue performance. Conforming behaviour occurred for the 60/70 at 30°C because during continuous loading this binder behaved more elastic than viscous; however, violation could happen at higher temperatures with the 60/70 bitumen grade.

5.4.3 Stiffness Evolution Curves

The rate at which the asphalt loses its stiffness modulus in a controlled strain mode environment is an indication of the rate at which asphalt fatigues. By plotting the stiffness evolution curve as in **Figure 5.7**, this rate loss can be examined. Several stiffness evolution curves are plotted within the figure for the different binder types 60/70 and 80/100; testing strain levels 300με, 400 με, 500 με, and 600με; and testing temperature 10°C, 20°C, and 30°C for the one testing frequency 5Hz.

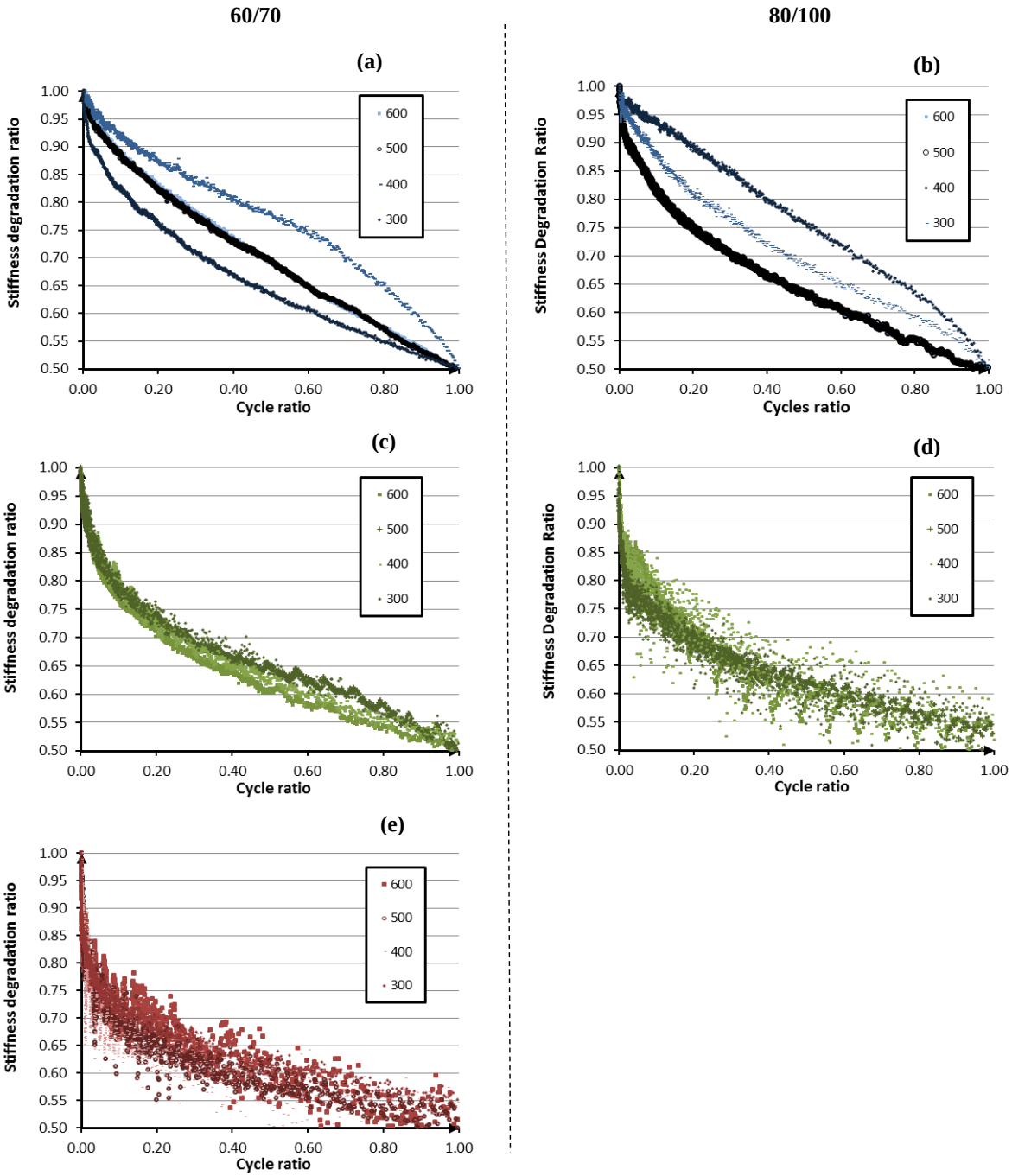

Figure 5.7 Stiffness modulus evolution curves for the different binders 60/70 and 80/100 for the various temperatures: (a) and (b) 10°C; (c) and (d) 20°C; and (e).

Three salient points can be discussed regarding the stiffness evolution. First, different stiffness evolution curve exist for each fatigue test condition. This is not surprising. During the cyclic loading of asphalt there are four phenomena that explain this effect: nonlinearity,

heating, thixotropy, and fatigue (Di Benedetto, Ngugen, & Sauzéat, 2010). For the two binder grades, the four testing strain levels, and the three testing temperatures, the viscoelastic response of the asphalt differs. These four phenomena can be modelled using mathematical relationships, but are beyond the scope of this thesis. Second, the stiffness evolution curve becomes erratic as the asphalt material behaves more viscoelastic due to increasing temperatures and softer binders. At these conditions, asphalt does not behave as an elastic material, rather as a viscoelastic material, hence their irregular response. Third, no single fatigue test exhibits the complete crack growth – as expected as the test is in the controlled strain mode. In fracture mechanics, three phases describe crack growth: initiation, propagation, and disintegration (Paris & Erdogan, 1963). Initiation progresses hairline cracks or micro cracks; propagation develops macro cracks; and disintegration breaks the specimen. Since the fatigue testing terminates when asphalt flexural stiffness reaches 50 per cent of its initial flexural stiffness, the asphalt does not fracture by fatigue. Rather, the specimen fatigues once flexibility is lost. Nonetheless, this failure criterion of 50 per cent is widely adopted for strain fatigue testing as this reduces the length of time required for testing.

5.5 PROPOSED FATIGUE MODELS

5.5.1 Two-Way ANOVA

Based on the fatigue life measurements as presented in Section 5.4.1, excluding the atypical behaviour at 30°C, a Two-Way Analysis Of Variance (ANOVA) was carried out. A Two-Way ANOVA compares the effect of two factors on the response variable simultaneously. Any interaction affect from two variables are therefore highlighted. Coupled with the Two-Way ANOVA, the fatigue measurements were first analysed as a factorial DOE using the Design-Expert software (Stats-Ease Inc., 2009). In the DOE analysis both the applied strain and measured fatigue life were transformed using a natural logarithmic function; a best-fit model was developed followed by the Two-Way ANOVA.

Strain, temperature, binder, strain–temperature interaction, and binder–strain interaction has a statistically significant effect on asphalt fatigue behaviour. **Table 5.3** presents a summary of the Two-Way ANOVA analysis of these fatigue life measurements. The higher the F–value or the lower the P–value the higher the significance of the factor

(Montgomery, 2001). If the P–value is very small, that is, less than 0.05, then that factor has a significant effect on fatigue life at a level of significance α of 5.0 per cent. In contrast, P–values greater than the level of significance have insignificant effects on fatigue life. Therefore, in this case, the factors listed in **Table 5.3** have a significant effect. Frequency and all other higher level interactions have a statistical insignificance. Thus these insignificant effects were excluded from the developed fatigue model.

Table 5.3 Summary Statistics of two factor interaction model

Source	F–Value	p–Value
Model	200.51	<0.0001
A - Binder	53.32	<0.0001
B - Strain	433.24	<0.0001
C - Temperature	341.46	<0.0001
AB - Binder-strain	21.16	<0.0001
BC - Strain-temperature	37.63	<0.0001

From the Two-Way ANOVA and using a natural logarithmic transformation of the fatigue life and strain, a fatigue model was constructed. The Model's F–Value of 200.51 implies that the model is significant as there is only a 0.01% chance that a "Model F–Value" this large could occur due to noise.

It was originally hypothesised that frequency would have a significant effect on fatigue. Yet this was not present. The joint effect of temperature and frequency interaction was also believed to perhaps have a contributing role. Again, this was not apparent. These variables, due to asphalt's viscoelastic nature, were thought to influence fatigue as they significantly affect asphalt's modulus, which subsequently affects fatigue.

The effects of stiffness modulus on fatigue behaviour were also accessed, but not directly by the factorial DOE and Two-Way ANOVA. Since the stiffness is a dependent variable, control of its value is impossible. However, there was a 17 per cent correlation between stiffness and fatigue life. Non-linear least square regression modelling of Equation 5–2, where strain and stiffness are a function of fatigue life, showed poor results. Although stiffness is known to affect fatigue, Harvey and Tsai (1996) found that "stiffness should not be included in regression for fatigue life models for mix design unless there is a clear understanding of the effects of other variables in the model that correlated with both

fatigue life and stiffness." In this case, frequency did not correlate well will both fatigue and stiffness, but only with stiffness.

5.5.2 Fatigue Models

Least squares regression modelling of the experimental fatigue response data found that the two-factor interaction model had the highest correlation with the experimental data; hence, Equation 5–4 and Equation 5–5 were developed. The predicted coefficient of determination R^2 value for the models is 0.946. Equation 5–4 is for the AC14 60/70 HMA and Equation5–5 is for the AC14 80/100 HMA. Equation 5–5 is not valid for temperatures greater than 30°C. It is also unknown at which temperatures above 20°C that Equation 5–5 is no longer valid.

AC14 60/70

$$\ln N_f = (57.2623 - 0.8167T) - (7.924 - 0.1555T) \ln \varepsilon_t \quad \textbf{5–4}$$

AC14 80/100

$$\ln N_f = (47.28938 - 0.81668T) - (6.15559 - 0.15516T) \ln \varepsilon_t \quad \textbf{5–5}$$

where:

N_f = laboratory fatigue life (cycles)
ε_t = applied tensile strain (με)
T= asphalt temperature (°C)

Figure 5.8 depicts Equation 5–4, and **Figure 5.9** depicts Equation 5–5. Fatigue behaviour is highly sensitive to strain and temperature. Indeed, Bodin et al. (2010), Deacon et al. (1994), and Tayebali et al. (1993) among others have also found this to be true. In particular, these researchers have further shown temperature dependency for the slope of the strain life relationship. Equation 5–4 and Equation 5–5 agree that the variables a and b in Equation 5–1 are temperature dependent.

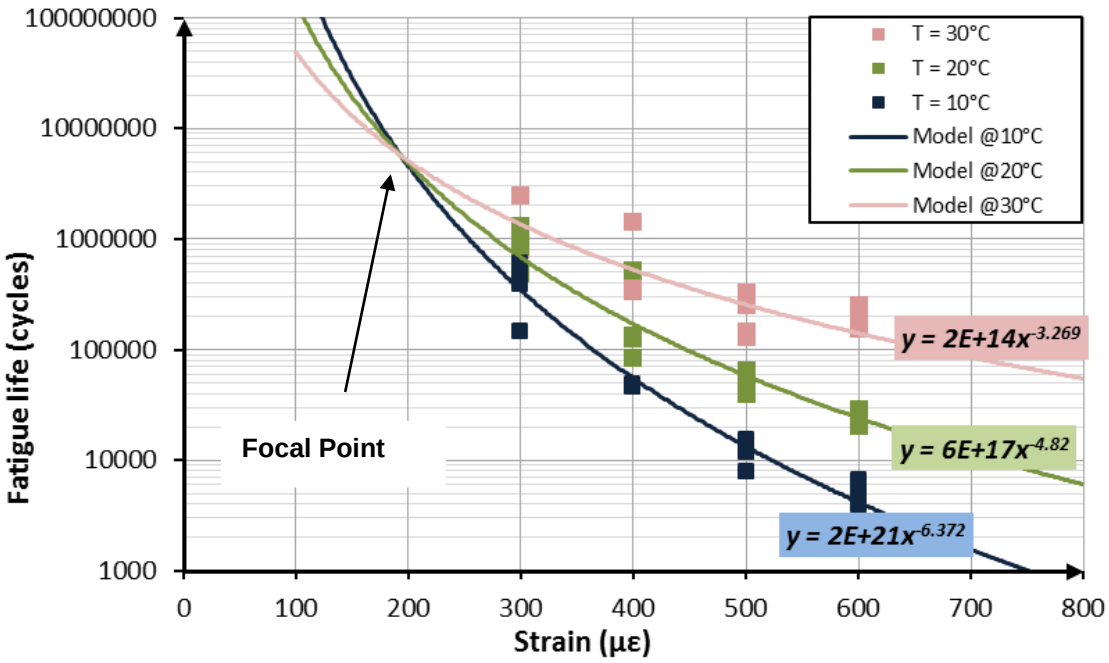

Figure 5.8 Family of curves for Equation 5–4 at different temperatures for the AC14 60/70 HMA, superposed against the fatigue life measurements

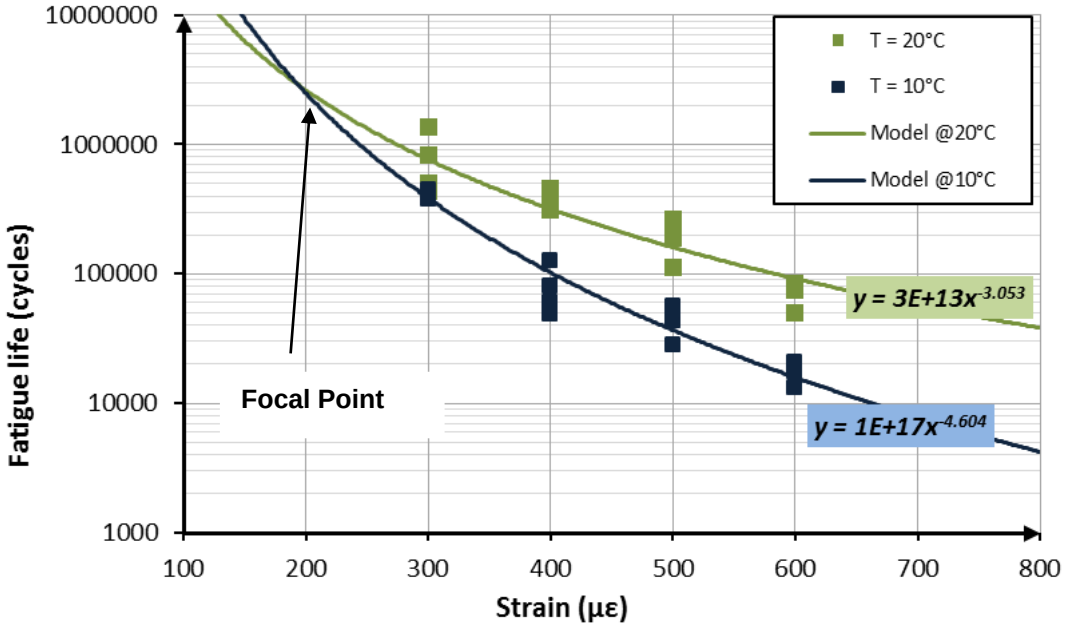

Figure 5.9 Family of curves for Equation 5–5 at different temperatures for the AC14 80/100 HMA, superposed against the fatigue life measurements

In **Figure 5.8**, for each temperature 10°C, 20°C, and 30°C the experimental fatigue results are juxtaposed with their respective theoretical fatigue lines (or family of curves) derived

from Equation 5–4. Given a set temperature value (i.e. 10°C), each curve illustrates Equation 5–4.

In addition, **Figure 5.8** shows that this family of curves intersect at 191 με. This point of intersection or focal point is presented in **Figure 5.8** and **Figure 5.9**. The focal point illustrates an idea that if the strain level is at the focal-strain then the same fatigue life is achieved independent of the temperature, for a particular asphalt mix. Generally, fatigue life increases with increasing temperature; however, if the strain is less than the focal-strain, then perhaps fatigue life decreases with increasing temperature. Fatigue tests at strain below the focal-strain are required to validate this hypothesis, since this statement is based on extrapolation. Nevertheless, testing with low strain levels may cause the fatigue test reach to a perpetual state known as the endurance limit testing.

The endurance limit is a concept when the asphalt pavement layer does not fatigue because the strains induced are low enough to maintain the pavement's structural integrity. Various United States and European research institutes, as well as the Australian Asphalt Pavement Association (AAPA) are in search for this limit. In New Zealand, searching for the endurance limit would also make an excellent research programme in New Zealand.

A contour plot of the developed fatigue life model Equation 5–4 for the AC14 60/70 is presented in **Figure 5.10**, with strain on the x-axis and temperature on the y-axis. As observed and expected the fatigue life is greatest at low strain levels and high temperatures. If the contour lines in **Figure 5.10** were linear, then there would be no interaction; rather, the curvature of these contours shows the interdependencies of strain and temperature on asphalt fatigue. However, this joint effect is not as significant as the individual effects of strain and temperature as demonstrated by the higher F–values in **Table 5.3**. In addition, the contour plot shows that different combinations of strain and temperature can have the same fatigue life. For example, both these conditions 600 με and 30ºC, and 343 με and 10ºC have a fatigue life of approximately 150,000 cycles.

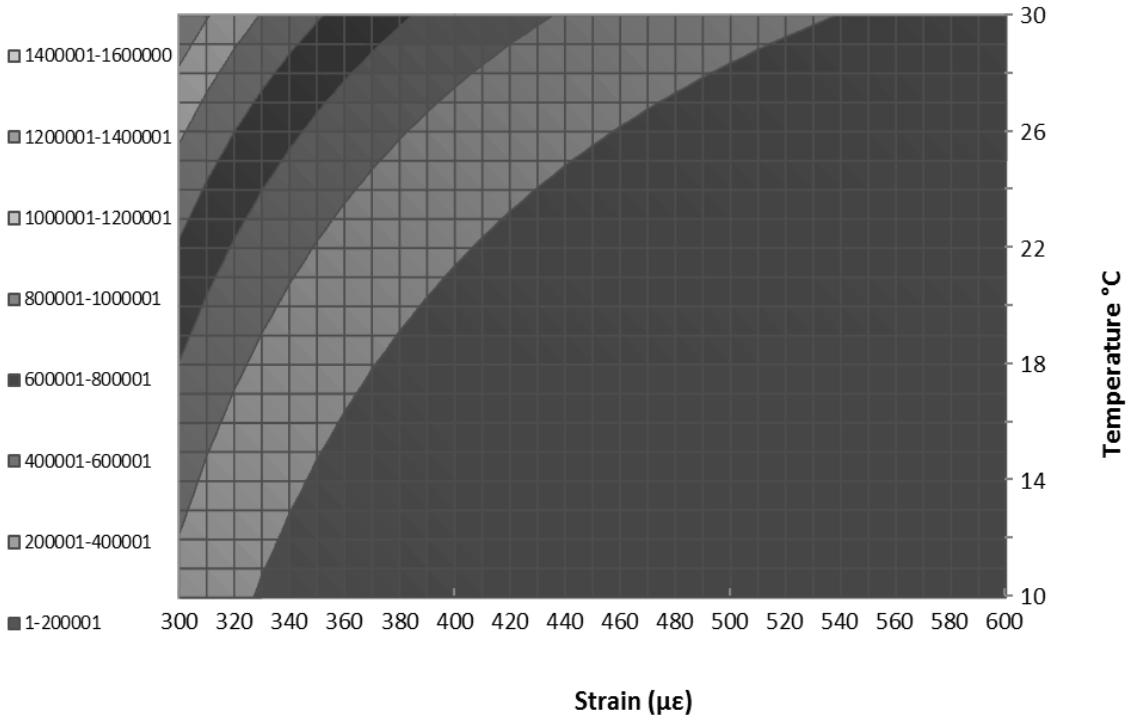

Figure 5.10 Fatigue life contour plot as a function of strain and temperature for the AC14 60/70

Figure 5.11 illustrates the goodness of fit of Equation 5–4 and Equation 5–5.

The goodness of fit of Equation 5–4 and Equation 5–5 are illustrated in **Figure 5.11**. This figure plots the relationship between these regression models and the actual measured fatigue life. The models for the AC14 60/70 and AC14 80/100 are unbiased because the scatter of data are evenly distributed about the line of equality, suggesting that the model is accurate.

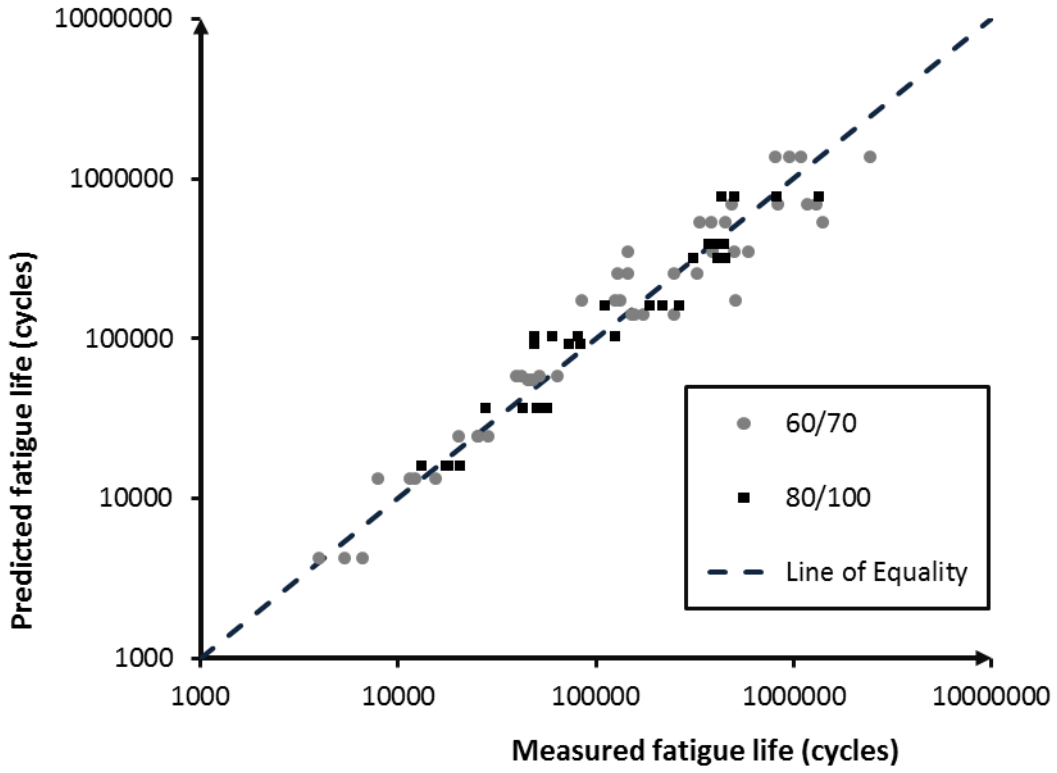

Figure 5.11 Prediction accuracy of the fatigue models: Equation 5–4 and Equation 5–5 against the measured experimental data.

5.5.3 Comparison of Models with the Shell FTF

Given that one of the central arguments in this thesis is the validity of the Shell FTF, the fatigue life measurements of both the AC14 60/70 and AC14 80/100 are compared with the prediction of the Shell FTF. Section 2.1.3 showed that the Shell FTF underestimates the fatigue life of New Zealand asphalts in the laboratory. In particular, Stubbs et al. (2010) showed that the Shell FTF under predicts the same asphalt mix AC14 60/70 by 5.5 times (range 3.1–8.9). Validity of the Shell FTF is one of the central arguments in this thesis.

Figure 5.12 superimposes the predicted fatigue life of the Shell FTF onto **Figure 5.11**, showing the Shell FTF inability to predict the fatigue life of both the AC14 60/70 and AC14 80/100. **Figure 5.12** illustrates that the predicted fatigue life from the Shell FTF underestimates the fatigue life of these mixes, since the majority of the data points are below the line of equality. Thus, for these mixes, the Shell FTF is biased. A 95 per cent confidence interval found that the Shell FTF underestimates the fatigue life of these two mixes between 2.06 and 2.71 times, with an average of 2.39 times.

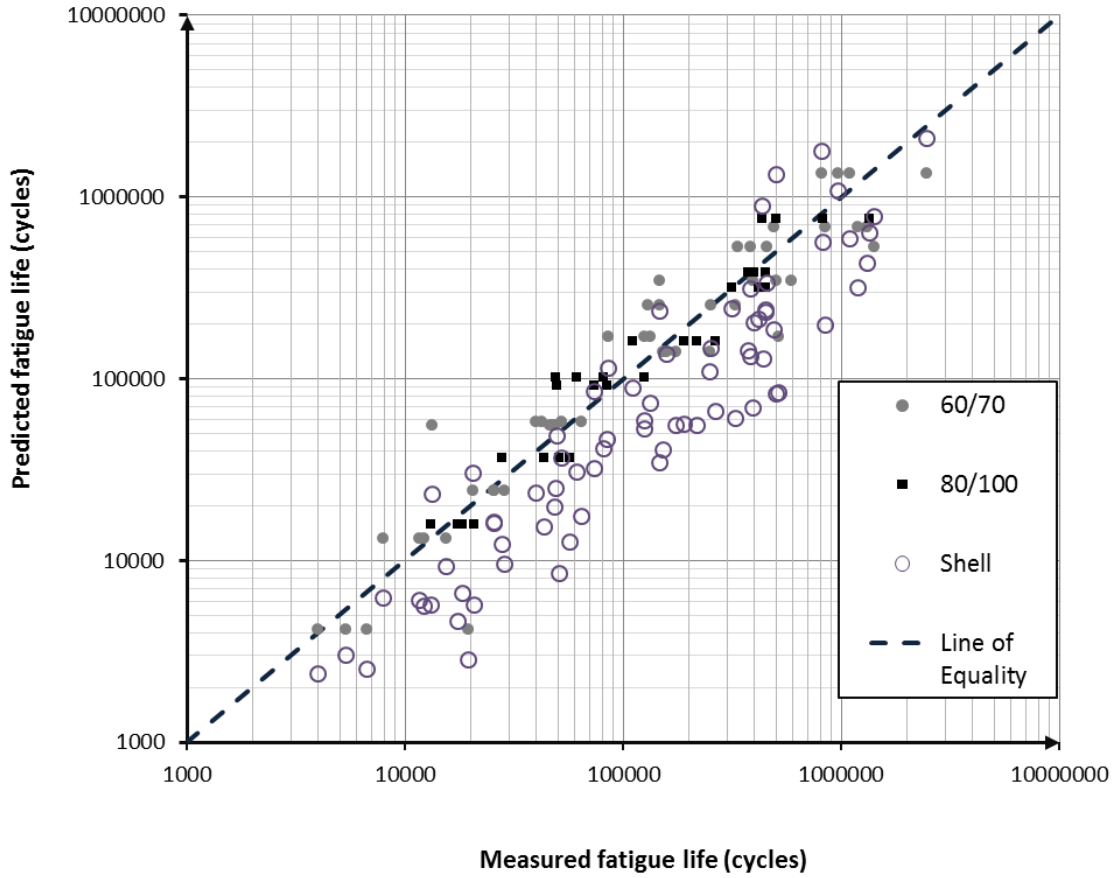

Figure 5.12 Comparison of Equation 5–4 and Equation 5–5's ability to predict fatigue life with the Shell FTF

The fatigue measurements of the AC14 60/70 taken from this thesis and the previous cited work show that some discrepancies indeed exist despite the fact that both measurements are from the same asphalt mix and the same fatigue test apparatus. Differences between measured fatigue life results are attributed to the specimen size for two reasons. **Figure 5.13** compares the specimen dimensions between the two studies. First, fatigue life relates to the bending stiffness, EI. Mathematically, bending stiffness is the product of asphalt's modulus E and inertia I. Due to the different widths between the specimens, their inertias are different. Second the "disturbance" differs between the samples. In order to maximise the number of specimens manufactured per slab for a more extended factorial DOE, each slab was sawn into five beams, instead of four. In the former study, Stubbs et al. (2010), four beams were cut. It is hypothesised that sawing fives beam caused greater disturbance to the aggregate fabric structure compared with sawing four beams. However, disturbance is believed to be a secondary contribution to the differences in inertia.

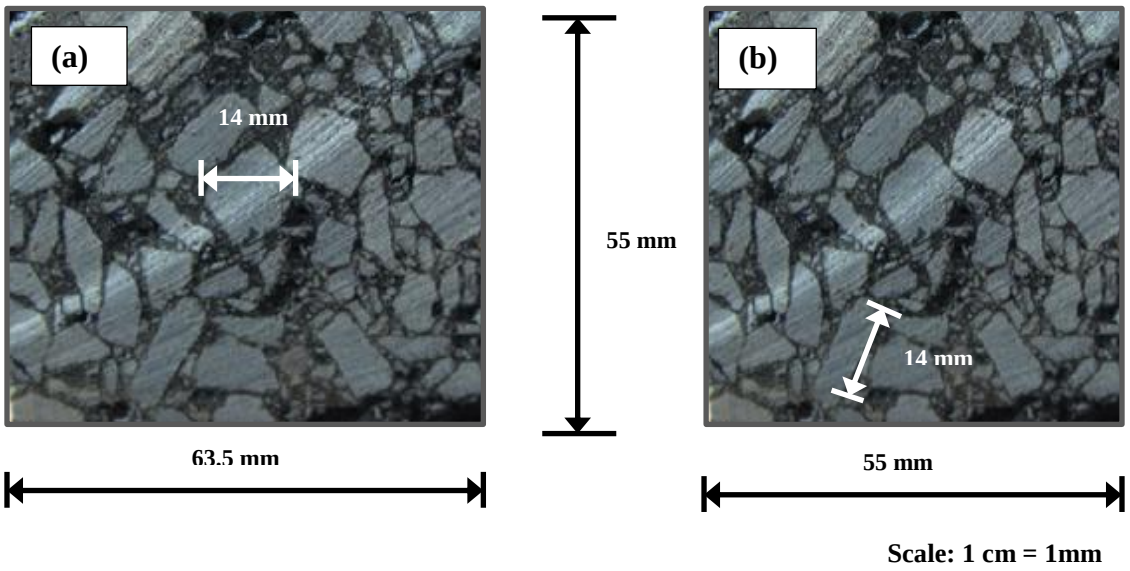

Figure 5.13 Cross-sectional comparison of the standard beam (a) and the experimental beam (b)

Having another dimension, inertia, affecting fatigue behaviour makes it absolutely tougher to analyse asphalt fatigue. Given that the sample size has been shown to additionally affect fatigue, there is therefore reason to understand the effect of specimen geometry on fatigue. Indeed, previous researchers such as Molenaar (2007), Bodin et al. (2006), and Di Benedetto (2004) have shown the influence of test geometry, loading mode, and specimen size on asphalt fatigue. In light of this, a potential study could investigate whether there is a critical geometry and specimen size that no longer affects fatigue, so that the more fundamental parameters affecting asphalt fatigue can be better understood.

Although this comparison shows some differences in the values measurements compared with the previous research with the AC14 60/70 asphalt mix, the primary argument of this thesis remains valid. The Shell FTF consistently underestimates the fatigue life for these two New Zealand asphalt mixes.

5.6 CONCLUSIONS

The following conclusions can be made from the factorial DOE:

(i) Statistically significant individual factors were on fatigue strain amplitude, temperature, and binder

(ii) Interaction between strain and temperature, and strain and binder has a statistically significant effect on fatigue life.

(iii) The main effect frequency had a statistically insignificant effect on fatigue life.

Summary

The effect of different variables affecting fatigue behaviour has been assessed. Fatigue models that characterise these effects for the AC14 60/70 and AC14 80/100 HMAs have also been developed. Laboratory results confirm that the Shell FTF consistently underestimates the fatigue life of this mixes by an average of 2.39 times.

Having a fatigue life model that includes temperature as a variable enables pavements designers to account for fatigue damage due to different temperatures. The following chapter discusses a method to address this damage by carrying out an incremental damage analysis.

6

INCREMENTAL DAMAGE ANALYSIS: ACCOUNTING FOR SEASONAL EFFECTS IN PAVEMENT DESIGN

6.1 INTRODUCTION

Pavements are subjected to seasonal and temperature variations. Yet, in the AUSTROADS mechanistic-empirical (ME) pavement design (MEPD) procedure, asphalt layers are designed for a single temperature, that is, Weighted Mean Annual Pavement Temperature (WMAPT). Furthermore, both the modulus and fatigue transfer functions (FTFs) of asphalt mixes are not only two important parameters in pavement design, but are extremely temperature dependent. Lack of temperature dependent models for both modulus and fatigue behaviour of asphalt mixes is a problem for the AUSTROADS (2008a) guidelines. Without these relationships, a more rigorous pavement design that accounts for seasonal variation cannot be performed.

The objective of this chapter is to integrate the models developed in Chapter 4 and Chapter 5 into a methodology for an incremental damage analysis. An incremental damage

analysis could be included in the AUSTROADS MEPD. Five sections are covered in this chapter. Background theory to the MEPD and the incremental damage analysis procedure are covered in the second section. A method of integrating the incremental damage analysis into the AUSTROADS MEPD is presented in Section Three, with a demonstration in Section Four. The final section discusses future improvements to the incremental design analysis framework.

6.2 BACKGROUND THEORY

6.2.1 Mechanistic-Empirical Pavement Design

MEPD is the most advanced pavement design procedure and it combines both mechanistic and empirical techniques. The mechanistic aspect determines the structural response such as stresses, strains and deflections due to loading. Through empirical transfer functions these responses are related to the performance of the pavement. Performance can then be classified into different failures, such as fatigue cracking. A schematic of the MEPD approach is shown in **Figure 6.1**.

Unlike traditional empirical pavement design methods, the MEPD connects the pavement structural response to the effects of traffic, material properties, and climatic effects. MEPD provides a comprehensive process that adequately underpins these effects.

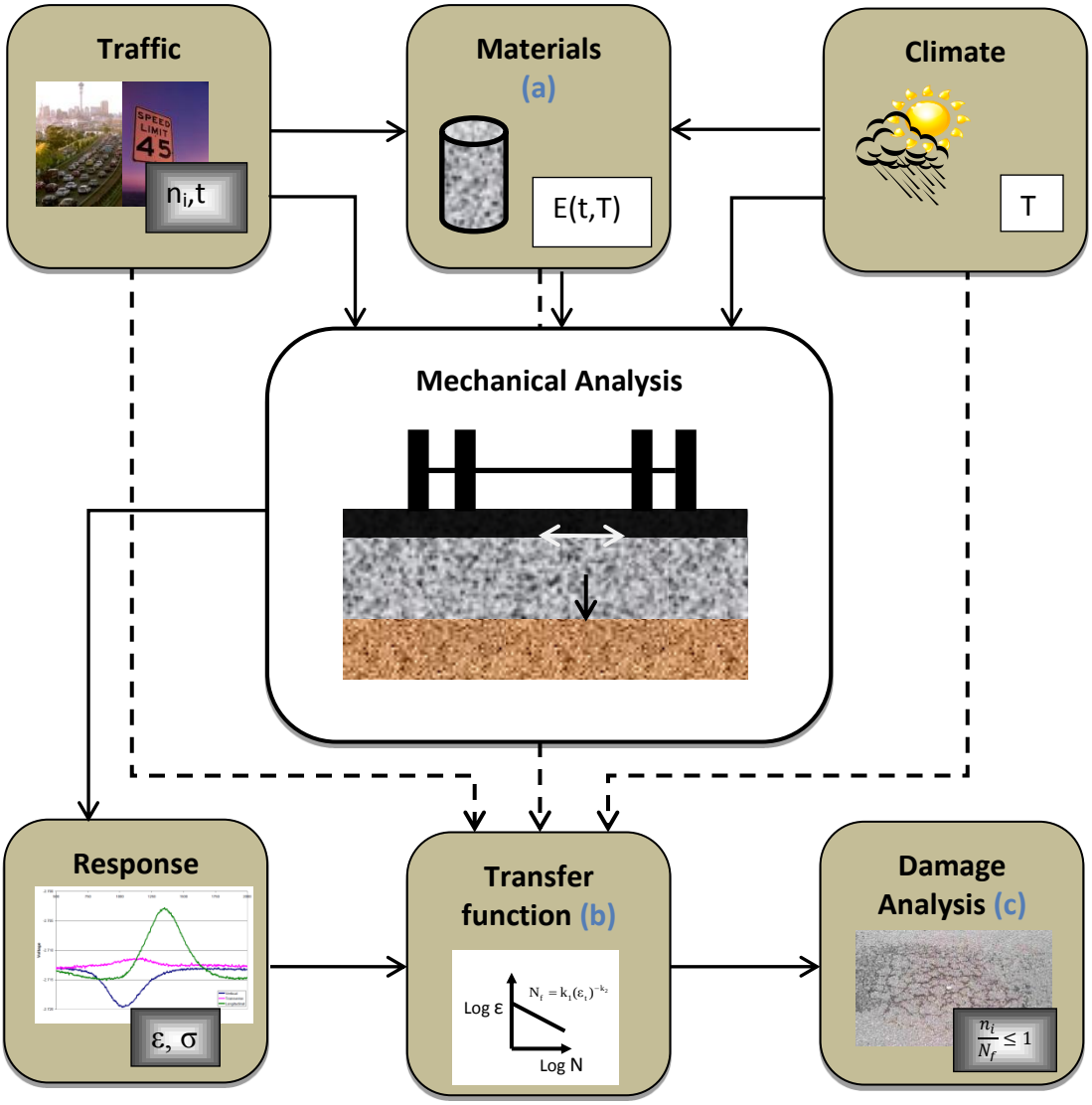

Figure 6.1 Schematic of the ME pavement design process: (a) characterisation the asphalt's modulus in Chapter 4; (b) development of the asphalt FTFs in Chapter 5; and (c) implementation of the incremental damage analysis in this chapter

Pavement design is tricky because all the design variables interact with each other. Because of this complexity, many New Zealand pavements are either over designed and fail later than their design life, or are under designed and fail earlier than their design life. Indeed, Arampamoorthy and Patrick (2010) illustrated that unbound granular pavements with an open graded porous asphalt (OGPA) surfacing has a high probability of early failure; in contrast, full depth asphalt concrete with an OGPA surfacing had a high probability of late failure. Therefore, a better understanding of the interaction and dependency between design variables is needed to overcome some of the deficiencies that

exist in the AUSTROADS design guidelines, so appropriate design lives are achieved. At present, the AUSTROADS design procedure for asphalt pavements does not fully utilise the MEPD capability. For example, the response of the asphalt layer due to loading is dependent on its modulus; however, the modulus is dependent on material characteristics, asphalt temperature, and the rate at which the load is applied (i.e. vehicle speed). This dynamic response throughout the change in seasons alters the asphalt performance. In addition, the material characteristics evolve; over time asphalt oxidises and hardens. Fatigue characteristics, and others, are hence continually changing. To date, AUSTROADS design procedure for asphalt pavements has not addressed this complexity. Rather a more practical approach is taken in the design by selecting a single WMAPT. The intensive research effort of the National Center for Asphalt Technology (NCAT), the National Cooperative Highway Research Program (NCHRP), and the National Asphalt Pavement Association (NAPA) in the latest US ME design guide actually adheres to this complexity by undergoing an incremental damage analysis.

6.2.2 Incremental Damage Analysis

Incremental pavement damage analysis is an iterative process, and terminates when the cumulative damage factor (CDF) mathematically equals one as shown in **Figure 6.2**. The CDF theoretically determines whether the pavement structure has reached the end of its design life.

In the current AUSTROADS MEPD, the pavement layer thicknesses are based on a single increment, with certain assumptions. Assumptions include: a standard axle configuration and axle load; only one season or temperature considered, the WMAPT; and an *unchanging* modulus. Yet all these conditions are continually altering over the pavement's design life. For simplicity, one set of conditions remains.

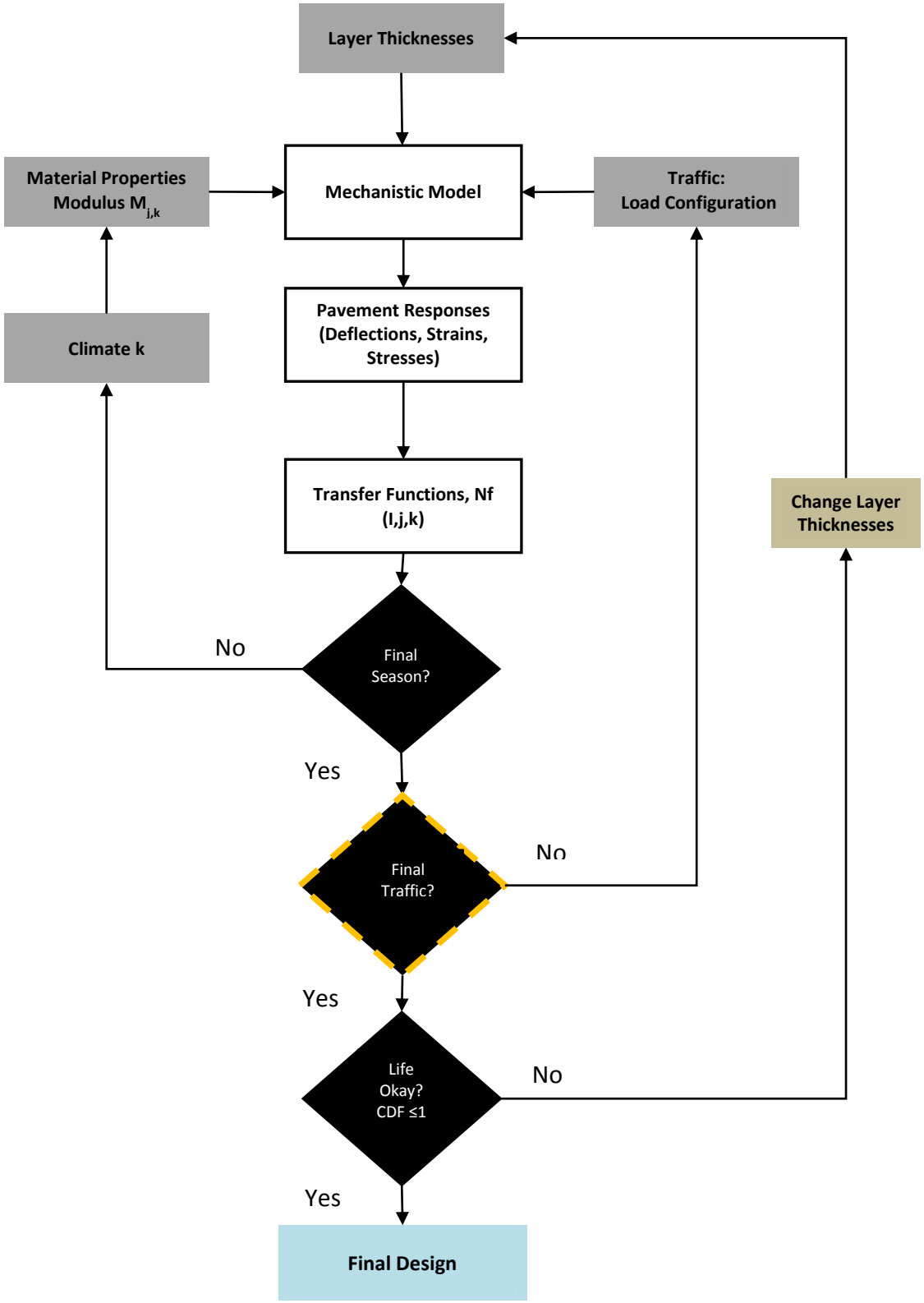

Figure 6.2 Flow chart of the ME incremental damage analysis process

To improve the AUSTROADS MEPD, an iterative process using the incremental damage analysis can be integrated. Damage per season and per axle loading configuration can be

computed. Links between temperature, material properties, load, and damage are needed to complete this incremental damage analysis. One aim of this thesis is to provide these relationships between temperature, material properties, and fatigue, thus facilitating the damage analysis.

Theoretical damage occurs when the number of heavy axle passes n_i equals or exceeds the allowable number of load repetitions N_i for the different failure modes and is based on Miner's hypothesis (Miner & Calif, 1945). The CDF parameter is calculated according to Equation 6–1.

$$CDF = \sum_{i=1}^{n} \frac{n_i}{N_f} \qquad \textbf{6–1}$$

where:

n_i = number of heavy axle repetitions from i to n for a given failure mode
N_f = allowable number of loading repetitions until fatigue cracking failure

In theory, Miner's hypothesis calculates the point in time when fatigue cracking damage occurs. However, this hypothesis fails to address the probabilistic nature of asphalt fatigue cracking. Pavements are rehabilitated once a certain per cent of cracking exists. Failure could indeed be initiated when Miner's hypothesis is less or more than one; thus field calibration is essential. For practical pavement design purposes, the CDF is assumed to equal one.

Currently, AUSTROADS calculates the CDF by Equation 6–1. If expanded, this is identical to Equation 6–2. Explicitly, Equation 6–2 shows that the total design life traffic is divided over the allowable number of loading repetitions. Since this allowable traffic is calculated through transfer functions that are temperature dependent, the CDF can now be calculated as Equation 6–3. The equation calculates the damage per season, i, for up to k increments. The total damage over the design life is the sum of damage per season.

$$CDF = \sum_{i=1}^{k} \frac{n_i}{N_f} = \frac{n_1 + n_2 + \cdots + n_k}{N_f} \leq 1 \qquad \textbf{6–2}$$

$$CDF = \sum_{i=1}^{k} \frac{n_i}{N_{fi}} = \frac{n_1}{N_{f_1}} + \frac{n_1}{N_{f_2}} + \cdots + \frac{n_k}{N_{f_k}} \leq 1 \qquad \textbf{6–3}$$

where:

n_i = number of loading repetitions per increment i for a given failure response
N_{fi} = allowable number of loading repetitions for fatigue failure for each season i
k = total number of increments

6.3 SEASONAL PAVEMENT DESIGN PROCEDURE

Outlined in this section is the incremental damage analysis procedure to account for seasonal variations in asphalt pavements. The procedure requires six steps. Schematically, the framework is shown in **Figure 6.3** and the iterative steps in this process are shown in the flowchart, **Figure 6.2**. This design procedure, like the AUSTROADS (2008), assumes the axle configurations are identical throughout the incremental seasons.

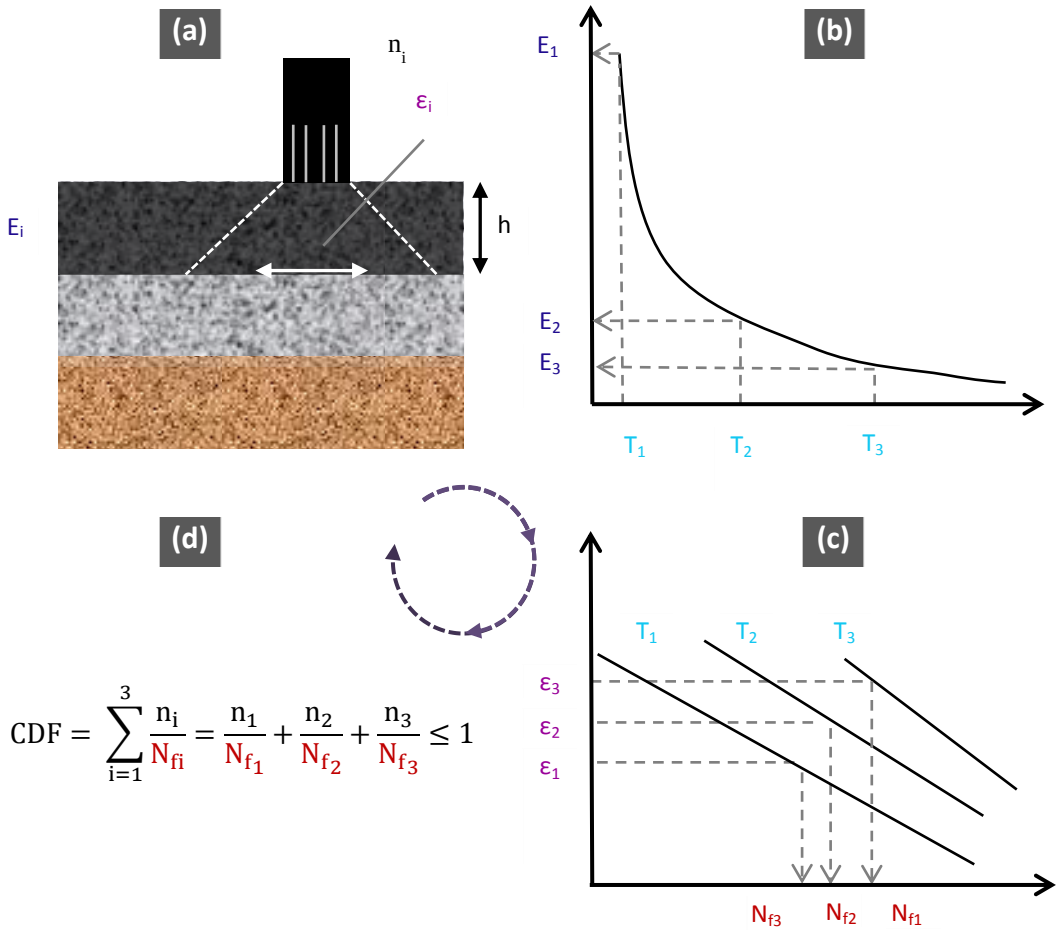

Figure 6.3 Incremental damage analysis process: (a) estimate the pavement thicknesses and thus the structural responses; (b) from the various incremental temperatures, determine the asphalt's respective moduli; (c) determine the fatigue life for each increment; (d) calculate the fatigue damage per increment. This is a cyclic process until the CDF is equal to one.

Any seasonal pavement design procedure can be divided into any number of increments (e.g. four seasons, 12 months). Seasons in other countries might be divided into dry, wet, frozen, and thawing; and each season will have a different length. Increasing the number of increments increases the rigour of the analysis; however, it also increases the amount of data needed. For pavement design engineers, this trade-off needs to be made; in addition, this framework should be coupled with engineering judgement and experience with specific local issues. The selection of materials that can endure the change in seasons is an example.

6.3.1 Step 1: Traffic Spectrum

The number of equivalent standard axle repetitions (SARs) for each increment needs to be determined. If insufficient data is present, the engineer could divide the SAR by the number of increments to ascertain the number of SARs per increment; however, this could also be dependent on the increment's length.

6.3.2 Step 2: Pavement Temperature

Instead of using a single pavement temperature, WMAPT, the different seasonal increments are assigned a pavement temperature. Now a problem arises. Without instrumentation, as in thermocouples, accurate pavement temperatures are difficult to ascertain; moreover, asphalt temperatures are a function of pavement depth making this complicated.

However, pavement temperature can be linked with air temperature. For example, Super Performing Asphalt Pavements (SUPERPAVE) correlates air temperature with pavement temperature at a depth of 20 mm below the surface based on the geographical latitude of the road, as defined in Equation 6–4 (Asphalt Institute, 1995). If this regression equation is to be transferable to New Zealand's climate, calibration is needed.

$$T_{20mm} = (T_{air} - 0.00618 \times Lat^2 + 0.2289 \times Lat + 42.2) * (0.9545) - 17.78 \quad \textbf{6–4}$$

where:

T_{20mm} = pavement temperature at a depth of 20 mm (°C),
T_{air} = seven-day average high air temperature (°C), and
Lat = geographical latitude of the project in degrees

6.3.3 Step 3: Asphalt's Modulus

Given the pavement temperatures, the asphalt moduli can be calculated from the modulus temperature relationships developed in Chapter 4, and this step is shown in **Figure 6.3**.

6.3.4 Step 4: Mechanistic Analysis

From the above steps the structural responses of the pavement layers for each incremental season can be calculated mechanistically.

6.3.5 Step 5: Failure Criteria

The next step determines the number of load cycles to fail for each increment using the temperature dependent fatigue models developed in Chapter 5.

6.3.6 Step 6: Damage

The final step is to calculate the damage factor for each increment and sum them together to determine the CDF. This calculation is shown in Equation 6–3. If the CDF does not equal one, the thicknesses of the layers are adjusted as shown in **Figure 6.2** and **Figure 6.3** by undergoing iterations until the scenario is solved.

6.4 INCREMENTAL DAMAGE ANALYSIS CASE STUDY

To demonstrate the incremental damage analysis procedure in the AUSTROADS pavement design, a case scenario is studied. In this demonstration, a structural asphalt layer is constructed with AC14 60/70 hot mix asphalt (HMA). Modulus and fatigue models developed in the earlier chapters of this thesis for this particular asphalt mix are integrated into this incremental pavement design approach.

A hypothetical pavement design scenario has been adapted from the Mount Wellington Highway, Auckland test site. Information from Jackson et al. (2003) has been borrowed to perform this design. The construction of the structural asphalt is to support a traffic volume of six million equivalent standard axles (ESAs) during the design life of 25 years. For the purpose of demonstrating the incremental damage analysis, the base course and subgrade layers were assumed to have certain properties, common to a structural asphalt design, illustrated in **Figure 6.4**.

Instead of selecting a single asphalt modulus, the modulus is varied, and this depends on the increment's temperature. For the analysis, the pavement temperatures were borrowed on measurements taken from the thermocouples installed in the Mount Wellington Highway test site. Based on these measurements and to keep the demonstration simple, it was decided to divide the analysis into three increments summer, winter, and spring and autumn.

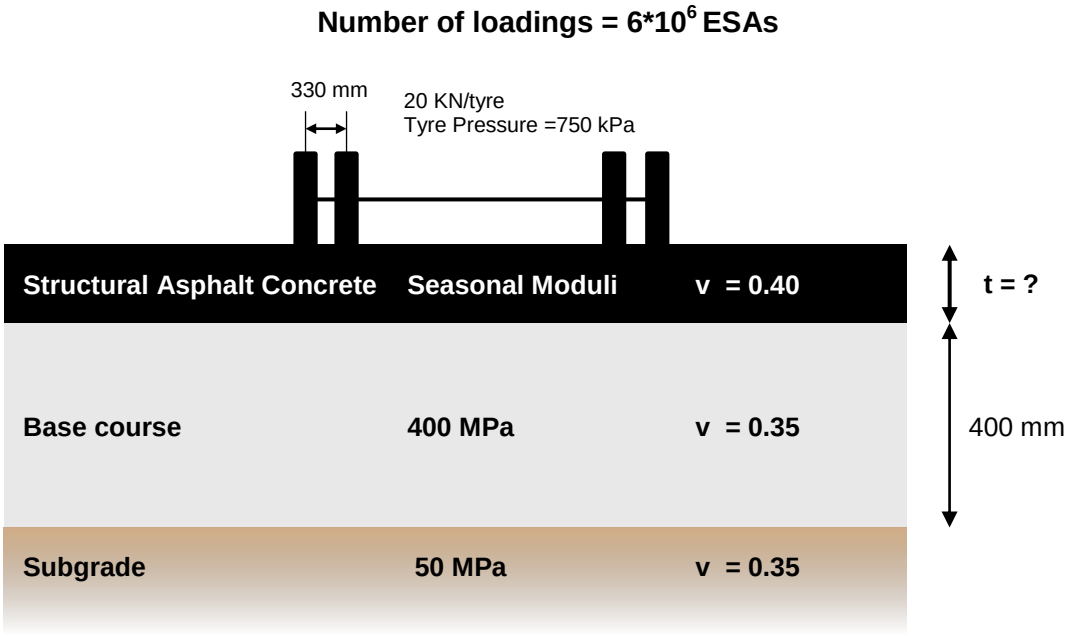

Figure 6.4 Pavement cross section and material properties for the case study

6.4.1 Step 1: Heavy Axles Passes

Six million ESAs was the total design traffic for the road. Although, Jones and Bell (2004) state that structural asphalt pavements are not economically viable unless the traffic for a 25 year period is greater than 14 million ESA, there was reason to have 6 million ESA. A discussion on this intention is written in Section 6.4.7. Depending on the length of the incremental season, the traffic volume is divided on a pro rata basis.

6.4.2 Step 2: Pavement Temperature

Figure 6.5 illustrates the yearly range of temperatures that are felt by the asphalt in the Mount Wellington Highway test site. In the graph, pavement temperatures vary from 8–40°C; hence for an AC14 60/70 HMA, the modulus could be between 500–11,500 MPa.

Based on **Figure 6.5**, the summer pavement temperature is about 30°C, and lasts for two months; the winter pavement temperature is 16°C, and also lasts for two months; and the spring and autumn pavement temperature is 22°C, and would last for eight months.

In the conventional AUSTROADS (2008a) pavement design approach the WMAPT for Auckland is 23°C.

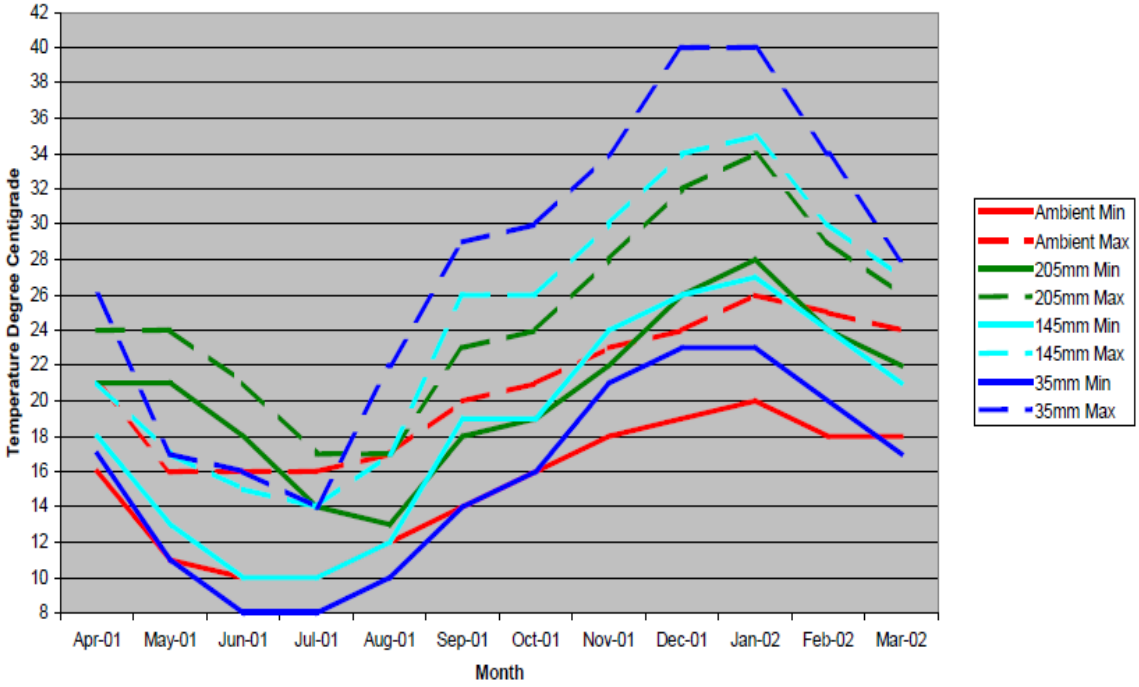

Figure 6.5 Annual maximum and minimum differential temperature for each pavement layer including the ambient temperatures versus each month from April 2001–April 2002 (Source Jackson et al. 2003)

6.4.3 Step 3: Asphalt's Modulus

The asphalt's modulus for each incremental temperature is calculated from the resilient modulus master curve developed in Chapter 4, reproduced as Equation 6–5. To apply this equation, for each increment, the following variables need to be determined first: frequency, shift factor, and reduced frequency. Reduced frequency is a function of the shift factor and the loading frequency.

$$\log M_R = 0.6329 + 3.9340\left(\frac{1.074}{1 + 0.5626e^{-0.3945\log f_{red}}}\right) \qquad \textbf{6–5}$$

where:

M_R = asphalt resilient modulus (MPa)
f_{red} = reduced loading frequency (Hz)

Frequency is calculated from Equation 6–6. Equation 6–6 relates the laboratory testing frequency with the vehicle speed and pavement depth (Jameson & Hopman, 2000). The laboratory testing frequency is for a loading pulse with a haversine shape. Although the resilient modulus master curve was developed using a loading pulse with an exponential shape, it is inferred that this shape would generate the equivalent resilient modulus. Saleh and Jian (2006) showed there was no statistical difference between the triangular and the sinusoidal loading patterns, thus providing a reason for the assumption.

$$\log f = 1 + 2.738 \log(0.981 + 0.352 \log S - 0.314 \log T) \quad \textbf{6–6}$$

where:

f = haversine test frequency (Hz)
S = design vehicle speed (km/h)
T = total asphalt layer thickness (mm)

The shift factor is calculated by the Arrhenius equation, as in Equation 6–7

$$\log a_t = \frac{200{,}000}{2.303 * 8.314}\left(\frac{1}{T} - \frac{1}{293}\right) \quad \textbf{6–7}$$

where:

a_t = shift factor (dimensionless)
T = experimental temperature (°K)

The logarithm of loading frequency and the logarithm of shift factor are added to calculate the logarithm of the reduced frequency, as in Equation 6–8. These calculations are completed for each increment.

$$\log f_{red} = \log a_t + \log f \quad \textbf{6–8}$$

where:

f_{red} = reduced frequency
a_t = shift factor
f = loading frequency (Hz)

6.4.4 Step 4: Mechanistic Analysis

Version five of CIRCLY was used to carry out the mechanistic analysis. CIRCLY is a multilayer elastic pavement design and analysis computer program, which can undergo a MEPD (Wardle, 2004). CIRCLY is recommended for pavement design and analysis in the AUSTORAD design procedure because of its ability to handle cross-anisotropic properties and sublayering AUSTROADS (2008). Cross-anisotropic materials are isotropic in the horizontal plane, but not in the vertical plane. This assumption is important for granular pavement materials. Given the thickness of each pavement layer and their respective engineering properties, the various responses in the pavement can be calculated.

6.4.5 Step 5: Failure Criteria

The failure criterion (or transfer function) for this analysis for the AC14 60/70 asphalt is based on Equation 5–4, reproduced as Equation 6–9. This relationship is a laboratory model, not a field fatigue model. However, as this equation is a function of temperature, the failure criteria can be defined for the given incremental temperature.

$$\ln N_f = (57.26231 - 0.81668T) - (7.9236 - 0.15516T) \cdot \ln \varepsilon_t \qquad \textbf{6–9}$$

where:

N_f = laboratory fatigue life (cycles)
ε_t = applied tensile strain ($\mu\varepsilon$)
T = asphalt temperature (°C)

Failure is also a function of the reliability factor. To keep the analysis simple the reliability factor was assumed to be one, with a desired project reliability of 95%. A project reliability factor of 95% can be used when the annual average daily traffic (AADT) is greater than 500 (AUSTROADS, 2008a).

6.4.6 Step 6: Damage

Given the above, the asphalt thickness is calculated based on the CDF equalling one, or as close to one as possible.

6.4.7 Demonstration Discussion

Table 6.1 and **Table 6.2** present the MEPD analysis for the incremental damage with three increments and a single increment respectively. For this demonstration, the more rigorous design with a triple increment predicts the asphalt as 220 mm, whereas the design with the single increment predicts the asphalt as 205 mm. Although the damage analysis with three increments shows a difference, this may or may not always be the case. The value of carrying out an incremental damage analysis versus a single increment at this stage is not certain. However, in this case, the demonstration highlights that it is not always safe to carry out a single increment, since the more rigours analysis requires a thicker layer to withstand fatigue life.

A drawback in carrying out this design with the developed fatigue life models is that if the asphalt strains are outside of 300 to 600 με, then they must be extrapolated. In this case, they are. It is uncertain exactly how the fatigue characteristic curve behaves outside this range of strain.

Table 6.1 Incremental damage analysis with temperature dependent models

Demonstrated Incremental Damage Analysis								**Asphalt thickness = 220 mm**	
Increment	**Duration per Year**	**Pavement Temperature**	**Modulus**	**Traffic**	**k**	**b**	**Strain**	**Fatigue Life**	**Damage**
1. Winter	2 months	16°C	6750 MPa	3,000,000	0.003370	5.441	86με	465,744,700	0.006
2. Autumn–Spring	8 months	22°C	3900 MPa	12,000,000	0.006080	4.510	125 με	40,599,600	0.296
3. Summer	2 months	30°C	1700 MPa	3,000,000	0.022530	3.269	206 με	4,621,123	0.649
								CDF	**0.95**

Table 6.2 Conventional pavement design with temperature dependent models with a single increment

Conventional Design								**Asphalt thickness = 205 mm**	
Increment	**Duration per Year**	**Pavement Temperature**	**Modulus**	**Traffic**	**k**	**b**	**Strain**	**Fatigue Life**	**Damage**
1. Annual	12 months	23°C	35000 MPa	18,000,000	0.006875	4.355	180	19,297,032	0.933
								CDF	**0.93**

6.5 FURTURE WORK

Advancement of the incremental damage analysis will require the generation of a comprehensive data collection. In this section, two methods to improve to the incremental damage analysis are described. The first method is another step to advancing the analysis by accounting for the damage per axle configuration. Both the Airport Pavement Structural Design System (APSDS) and Heavy Industrial Pavement Design System (HIPAVE) include the capability to analyse the cumulative damage for different axle configurations (Wardle, 2010). Currently, the inclusion of load spectra is accounted for in the US MEPD Guide (MEPDG). Furthermore, there is an international trend towards including different loading configurations into pavement designs, instead of the standard axle. (Wardle, 2010). With increasing axle weights, this becomes more important as the level of damage per axle increases. Equation 6–10, in Section 6.5.1, gives the method of calculating the CDF for the damage per seasonal increment per axle configuration. The second improvement advances the current state of practice for the incremental analysis by accounting for the degradation of the asphalt stiffness over time and is presented in Section 6.5.2.

6.5.1 Damage per axle configuration

$$\mathrm{CDF} = \sum_{j=1}^{m}\sum_{\mathrm{i}=1}^{\mathrm{n}} \frac{\mathrm{n_{ij}}}{\mathrm{N_{fi}}} = \frac{\mathrm{n_{11}}}{\mathrm{N_{f_1}}} + \frac{\mathrm{n_{12}}}{\mathrm{N_{f_2}}} + \cdots + \frac{\mathrm{n_{1n}}}{\mathrm{N_{f_2}}} \ldots + \frac{\mathrm{n_{21}}}{\mathrm{N_{f_1}}} + \frac{\mathrm{n_{22}}}{\mathrm{N_{f_2}}} + \cdots + \frac{\mathrm{n_{2n}}}{\mathrm{N_{f_2}}} \ldots + \frac{\mathrm{n_{m1}}}{\mathrm{N_{f_1}}} + \frac{\mathrm{n_{m2}}}{\mathrm{N_{f_2}}} + \cdots + \frac{\mathrm{n_{mn}}}{\mathrm{N_{f_2}}} \leq 1 \qquad \textbf{6–10}$$

where:

n_{ij} = number of loading repetitions per increment i, per axle configuration j, for a given failure mode

N_{fi} = allowable number of loading repetitions for fatigue failure for the given increment i

n = number of defined seasonal increments

m = number of axle configuration increments

6.5.2 Accounting for a Weakening Moduli

Pavements deteriorate over time due to adverse weather conditions and cumulative traffic loading. As a result, the asphalt modulus weakens as experimentally shown in Section 5.4.3. However, no MEPD procedure worldwide currently includes this effect. Rather the analysis procedure assumes the asphalt modulus remains constant throughout the pavements design life. Because of this assumption, the tensile strain developed in the asphalt layer is also fixed. Again, this is not true. Over time these strains will surely increase as the modulus decreases. Understanding this process must be coupled with the counter effect of healing and asphalt stiffness hardening due to the asphalt binder oxidising. To enable this, good long-term monitoring is required.

Summary

This chapter has discussed background theory to the MEPD and the incremental damage analysis procedure. A method of integrating the incremental damage analysis into the AUSTROADS MEPD has also been presented. The chapter combines both Chapter 4 and Chapter 5 to demonstrate the ability of carrying out an incremental damage analysis by accounting for temperature effects that are deeded important in pavement design. The following chapter concludes the thesis by providing a summary of the work and its application in pavement design.

7

CONCLUDING REMARKS

OUTCOMES, GENERAL DISCUSSION, AND FUTURE RESEARCH

> *An ideal pavement procedure is one which will predict a thickness and composition, which without being conservative, ensures that the pavement will not deteriorate beyond a tolerable level of serviceability in less than the design period.*
> *— NAASRA (1987) and AUSTROADS (1992)*

In the AUSTROADS (2008a) Mechanistic Empirical Pavement Design (MEPD) guidelines, structural asphalt layer thicknesses are governed by material properties (i.e. modulus) and fatigue transfer functions (FTFs). Having accurate characteristics of both modulus and fatigue performance are therefore an absolute in pavement design, particularly for different climatic conditions. Pavement engineers in New Zealand and Australia are, however, limited in their pavement design and analysis due to insufficient data on modulus and fatigue characteristics of local structural asphalts. Thus the purpose of this thesis is primary to improve the status quo.

Because of this lack of available data, AUSTROADS have adopted overseas research, specifically the Shell FTF to predict field fatigue cracking. Yet, the Shell FTF is a laboratory model (Jameson, et al., 1992). Predicting fatigue cracking in asphalt pavements is important because it is a major failure mode. Nevertheless, there is great uncertainty in the ability of the Shell FTF to predict fatigue in New Zealand. Additionally, since the Shell FTF was developed from overseas asphalt mixes, not New Zealand's structural asphalts, there is indeed a need to develop an FTF that is applicable for New Zealand's asphalts and one that is appropriate for a range of climatic conditions. Hence, the thesis aims to characterise the modulus and fatigue behaviour of two common structural asphalts to New Zealand AC14 60/70 ad AC14 80100.

Seven sections are discussed in this final chapter. Achievements of the thesis are presented in Section One. In the second and third sections, the work's significance and research limitations are addressed accordingly. Barriers to implementing the developed models for design practice are identified in Section Four. Finally, recommendations, future research, and conclusions are stated in sections five, six and seven respectively.

7.1 ACHIEVEMENTS

Based on the key research objectives outlines in Section 1.3, the following has been achieved.

(i) A resilient modulus master curve has been developed for the AC14 60/70 asphalt mix given by Equation 4–13. A stiffness modulus master has also been developed for the AC14 80/100 as well as for the AC14 80/100 as Equation 4–14 and Equation 4–15 respectively. These master curves can predict the laboratory modulus for a variety of temperature and vehicle speed conditions.

(ii) Strain amplitude, temperature, and binder types were found to have a statistically significant effect on fatigue behaviour. Additionally, the interaction of strain and temperature, and the interaction of strain and binder had a statistically significant influence on fatigue

behaviour. Frequency was statistically insignificant, as well as other second order and higher order interactions.

(iii) A fatigue characteristic curve was developed for the AC14 60/70 and AC14 80/100 asphalt mixes, which represents the behaviour of local available materials. The characteristic curve further accounts for the significant factors mentioned above in **(ii)** and their respective equations are Equation 5–4and Equation 5–5.

(iv) An incremental damage analysis procedure has been presented, which could be applied in the AUSTROADS guidelines for a more fundamental analysis. This procedure, for the AC14 60/70 and AC14 80/100, addresses the influence of strain, temperature, and vehicle speed in the pavement design

(v) Both the develop modulus master curves and fatigue models can be integrated into the incremental damage analysis. Thus enabling the assessment of fatigue damage per season.

7.2 SIGNIFICANCE OF THE STUDY

Work in this thesis has advanced the current state of practice and knowledge of asphalt pavement design in New Zealand. The research has addressed the current over-conservatism problems with the Shell FTF, and has presented alternative fatigue models that reflect both the availability of indigenous asphalt materials and some of the factors affecting fatigue performance.

A major ramification of this over-conservatism is that thicker asphalt layers are designed, which results in uneconomical pavements, and thus is prohibitively expensive. Consequently, when a pavement designer compares alternative pavements such as unbound granular pavements in an economic analysis and evaluation, the structural asphalt option appears less favourable against others. Cheaper options are therefore constructed;

however, these alternatives require greater maintenance costs and greater road user costs, particularly over the pavement's economic life.

Overall, the study has established greater certainty in laboratory fatigue behaviour of these common asphalt mixes. The developed models provide the New Zealand roading industry with both greater accuracy and cost savings when predicting fatigue cracking. Given that New Zealand's roading industry have requested characterisation of asphalt's modulus and fatigue behaviour (Gribble & Patrick, 2008), the developed fatigue and modulus models begins to respond to this call.

A further advantage of providing temperature dependent modulus and fatigue models for pavement design is that such models can be applied where fatigue is common to temperature variations. For example, inside a tunnel, the various pavement temperatures may be different from the outside pavement temperatures; the proportion of loads at these temperatures may be different, and thus the pavement design requires a first principles approach (AUSTROADS, 2008a). Another benefit of the developed temperature dependent models is it addresses the limitations of the Weight Mean Annual Pavement Temperature (WMAPT). For instance, the WMAPT assumes the traffic loads are applied uniformly throughout the day, with no allowance made for situation where the hourly loading varies with hourly asphalt temperatures (AUSTROADS, 2004). The incremental damage analysis enables such proportion of loads at different pavement temperatures.

7.3 LIMITATIONS

This thesis has by no means solved the asphalt fatigue cracking phenomenon or even established the true fatigue performance of asphalt concrete mixes. Instead, it has instigated a way forward from the current design of asphalt with the Shell FTF.

A major limitation of the developed fatigue models are they are developed between 300–600 με. Hence, for lower strain levels in a pavement design, extrapolation may be required. In addition, since only four different strain levels 300, 400, 500, and 600 με were tested, this does not completely capture the non-linearity effect of strain on asphalt fatigue behaviour. A greater number of levels would have solved this issue. Another limitation with these fatigue models is that for each particular strain and temperature condition, only four data points were measured to develop these models.

Although the developed fatigue models are accurate for the particular materials used in this thesis, the model requires field calibration.

7.4 BARRIERS TO CHANGING THE SHELL FTF IN THE AUSTROADS

Before the New Zealand and Australian roading industry will adopt newly developed fatigue models, field calibration is required. AUSTROADS (2008a) state that if using laboratory fatigue models, a correlation with field performance must be made. Industry experts, Rickards and Armstrong (2010) consistently stress the need for calibration of test methods before implementation. Interestingly, however, verification and calibration of the Shell FTF has still not been fully carried out in New Zealand, yet it is now understood that the Shell FTF is a laboratory fatigue model, not a *field* calibrated FTF (Jameson, et al., 1992).

The major barrier to providing the industry with field calibration is the enormity and cost of the required work. Classical fatigue cracking, by definition, tends to fail towards the end of a pavement's design life. Subsequently, it may be 15 to 30 years until the pavement fails by fatigue, thus it will take time to gather any conclusive results. Accelerated pavement testing is surely a step forward.

Another issue in challenging the Shell FTF for pavement design in New Zealand is the need to have a greater understanding of the previous performances of structural asphalt before the Shell FTF was introduced into the AUSTROADS pavements design guidelines. Evidence suggests that the former design criterion is still overestimating asphalt thicknesses (Transit New Zealand, 2007). Although this is not the answer, it could perhaps provide an alternative to the over-conservative Shell FTF in the interim, before an extensive research effort is carried out.

Despite this over-conservatism of thickness of asphalt layers, which is acknowledged by the New Zealand Transport Agency (NZTA), formerly Transit New Zealand, the New Zealand Supplement to the AUSTROADS continues to design asphalt pavements in accordance with the Shell FTF. For this reason, unbound granular pavement in New Zealand is seen to be the preferred option because they appear much less expensive than structural asphalts. As a result, much of the research focus from NZTA is directed towards

solving the chip sealing problems of flushing and chip loss. Yet despite the evidence to suggest that cheaper structural asphalt roads can be laid and still maintain an equivalent structural capacity over the performance period, there appears to be no major interest from the industry. Interestingly, back in 1982 Saunders states: "*A strong case would be made for research effort to establish design charts and formulae [regarding structural asphalts] for New Zealand conditions and materials*" (Saunders, 1982).

7.5 RECOMMENDATIONS

In the interim (before field or extensive laboratory testing is carried out), based on the results from this research, it is recommended a field shift factor (FSF) between 5 and 10 is applied to the Shell FTF, but depends on the asphalt mix. Therefore, this shift accounts for the Shell FTF's inherent over-conservatism. Confirming with this recommendation, Saleh (2010) additionally derived a shift factor of 5.7 for a common New Zealand hot mix asphalt AC14 60/70.

In addition, the author recommends that the New Zealand roading authority, currently the New Zealand Transport Agency (NZTA), need to decide on the maximum permitted level of fatigue cracking in the wheel path and or a suitable reduction in asphalt modulus that is deemed failure. Without this governing decision, there is nothing to calibrate field data to. The developed fatigue models in this study will provide better representations to New Zealand mixes and therefore it is recommended that these models will be field calibrated and validated.

7.6 FUTURE RESEARCH

In this research, only two types of binders (60/70 and 80/100) were studied and only one gradation AC 14 was considered. Nonetheless, there are many other gradations such as AC20, AC10 and stone mastic asphalts and different types of binders such as polymer modified binders. Fatigue behaviour of these different mixes will need to be investigated to provide a complete picture of the fatigue performance of the different mixes.

Research into investigating field observation from current asphalt pavement is also recommended. In particular, taking regular core samples and or falling weight

deflectometer readings over the pavement's design life of various sites. The modulus and strains can therefore be back calculated. An advantage of such a long term study enables the researcher to plot the deflection life curve, which can act as an empirical design chart or alternative performance transfer function. Furthermore, such a study would chiefly benefit the New Zealand roading industry because this curve would instantly give the fraternity the field calibration that it urgently needs.

Another excellent research project, which would see a jointly collaborative effort between key industry groups, would be to established a field calibration factor and a develop a new set of generation fatigue models that would be applied to New Zealand's asphalt materials and meteorological conditions. Such models would indeed not only provide an accurate representation of local conditions and indigenous materials, but more importantly provide the industry with better pavement engineering practices. Moreover, these models would enable a more cost effective solution for society, without money wasted on over design. In the interim, good engineering judgement must be applied.

Interestingly, back in New Zealand in 1989, it was stated in the State Highway Pavement Design and Rehabilitation Manual stated that "[t]he bridging of the gap between laboratory data and in-situ behaviour is one of the most urgent research problems in this field at the time of writing" (National Roads Board, 1989). Despite this, the gap still remains in the New Zealand roading industry. Since field calibration would take a long time, the time lost waiting to begin such a research effort only compounds the problem. To reduce this period, accelerated pavement performance testing is thus the next step forward.

7.7 CONCLUSIONS

To summarise, this study has characterised both the modulus and fatigue behaviour of two common hot mix asphalts in New Zealand for a range of temperatures and vehicle speeds, which are both important variables in the design of roads. The research has also developed temperature dependent models, thus enabling the design engineer to account for the incremental damage due to traffic axle loads at different climatic temperatures. While this study further demonstrates the inability of the Shell FTF to predict fatigue behaviour of two common asphalts in the laboratory, its inability to predict fatigue in the field must be even further removed. The current study has advanced our knowledge of hot mix asphalt

for pavement design in New Zealand. In doing so, it has addressed a small, but important part of the ever present quest for solving the asphalt fatigue cracking phenomenon, by improving our understanding of the effects of strain, temperature, vehicle speed and binder types on asphalt fatigue. In addition, the thesis has discussed the ability to design asphalt pavements to withstand fatigue cracking and prevent failure. Finally, although the work promotes the construction of asphalt pavements at a cost that now appears competitive with alternatives, designs engineers should not overlook options, such as stone mastic asphalts, rigid pavements, or even reclaimed asphalt pavements. Indeed, the final construction decision is primarily an economic one.

REFERENCES

Adhikari, S., Shen, S., & You, Z. (2009). Evaluation of Fatigue Models of Hot-Mix Asphalt Through Laboratory Testing. *Transport Research Board, 2127*, 36-42.

Alba, J., Barksdale, R. D., Khosla, N. P., Lambe, P. C., & Rahman, M. S. (1997). *Laboratory determination of resilient modulus for flexible pavement design*.

Anderson, D. (1982). *Study of asphalt fatigue relationships*: Report to working group National Assoication of Australian State Road Authorities.

Arampamoorthy, H., & Patrick, J. (2010). Failure probability of New Zealand pavements. Land Transport New Zealand Research Report 421.

AS 2891.2.1. (1995). Methods of sample and testing asphalt. Method 2.1: Sample preparation - Mixing quartering and conditioning of asphalt in the laboratory. Standards Australia.

AS 2891.7.1. (1995). Methods of sample and testing. Method 7.1: Determination of maximum density of asphalt—Water displacement method. Standards Australia.

Asphalt Institute. (1995). *Superpave Performance Graded Asphalt Binder Specifications and Testing*. Lexington, KY: Asphalt Institute.

AUSTROADS. (2004). *Technical Basis of Austroads Pavement Design Guide*. Sydney.

AUSTROADS. (2008a). *Guide to Pavement Technology Part 2: Pavement Structural Design*. Sydney, NSW: Austroads Incorporated.

AUSTROADS. (2008b). *Technical Basis of Austroads Guide to Pavement Technology Part 2: Pavement Structural Design AP-T98/08*. Sydney.

Austroads. (2010). *Guide to Pavement Technology Part 2: Pavement Structural Design*. Sydney, NSW: Austroads Incorporated.

AUSTROADS. (2011). About Austroads

AUSTROADS, Australian Asphalt Pavement Association, & Australian Road Research Board Transport Research. (1997). *Selection & design of asphalt mixes : Australian provisional guide* (1st ed.). Vermont South, Vic.: AUSTROADS.

Baburamani, P. (1999). *Asphalt Fatigue Life Prediction Models - A Literature Review* (No. ARR 334). Vermont South, Victoria: ARRB Transport Research Ltd.

Bodin, D., de Roche, C., & Pijaudier-Cabot, G. (2006). Size effect regarding fatigue evaluation of asphalt mixtures: Laboratory cantilever bending tests. *International Journal of Road Materials and Pavement Design, 7*, 181-200.

Bodin, D., Terrier, J.-P., Perroteau, C., Hornysch, P., & Marsac. (2010). *Effect of temperature on fatigue performance of asphalt mixes.* Paper presented at the 11th International Conference on Asphalt Pavements, Nagoya, Japan.

Bonnot., J. (1986). Asphalt Aggregate Mixtures. *In Transportation Research Record, Transport Research Board, 1096*, 42-50.

Boon, G. S. (1979). *Recommended Procedure for Design of Asphaltic Concrete Road Pavements for New Zealand*: Roading Division, Minstry of Works and Development.

Brown, A. M. (2001). A step-by-step guide to non-linear regression analysis of experimental data using a Microsoft Excel spreadsheet. *Computer Methods an Programs in Biomedicine, 65*, 191-200.

Claessen, A. I. M., Edwards, J. M., Sommer, P., & Ugé, P. (1977). *Asphalt Pavement Design: The Shell Method.* Paper presented at the Proceedings Fourth International Conference on Structural Design of Asphalt Pavements, Ann Arbor, Michigan, USA.

Deacon., J. A., Coplantaz, J. C., Tayebali, A. A., & Monismith, C. L. (1994). Temperature considerations in asphalt aggregate mixture analysis and design. *Transport Research Board, 1454*, 97-112.

Di Benedetto, H., de Roche, C., Baaj, H., Pronk, A. C., & Lundstrom, R. (2004). Fatigue of bituminous mixtures. *Materials and structures, 37*, 202-216.

Di Benedetto, H., Ngugen, Q. T., & Sauzéat, C. (2010). Nonlinearity, Heating, Fatigue and Thixotropy during cyclic loading of Asphalt Mixtures. *Road Materials and Pavement Design, X*.

Gerritsen, A. H., & Koole, R. C. (1987). *Sevens years' experience with the structural aspects of the Shell Pavement Design Manual.* Paper presented at the Proceedings Sixth International Conference on Structural Design of Asphalt Pavements, Ann Arbor, Michigan, USA.

Gribble, M., & Patrick, J. (2008). *Adaptation of the AUSTROADS Pavement Design Guide for New Zealands Conditions*.

Haora, K. (2011). *Effect of air voids on the fatigue behaviour of hot mix asphalt* Unpublished 3rd professional year project, University of Canterbury, Christchurch.

Harvey, J. T., & Tsai, B.-W. (1996). Effects of Asphalt Content and Air Voids Content on Mix Fatigue and Stiffness. *Transport Research Board, 1543*, 38-45.

Huang, Y. H. (2004). *Pavement Analysis and Design* (Second ed.). Upper Saddle River: Pearson Prentice Hall.

Hudson, K. (2006). *Top down cracking: a discussion*. Paper presented at the Transportation and the Pursuit of Excellence: NZIHT & Tansit NZ 8th Annual Conference.

Jackson, J., Peploe, R. J., & Vercoe, J. (2003). *The influence of pavement temperatures on predicted pavement performance*. Paper presented at the Proceedings of the 21st ARRB and 11th REAAA Conference. Transport. Our Highway to a Sustainable Future

Jacobs, M. M. J. (1995). *Scheurgroei in asfalt = [Crack growth in asphaltic mixes]*. Unpublished Thesis (Ph D), Delft, The Netherlands.

Jahromi, S. G., & Khodaii, A. (2009). Master Curves for Stiffness Asphalt Concrete. [Technical Paper]. *International Journal of Pavement Research and Technology, 2*(4), 148-153.

Jameson, G. W. (1999). *An Assessment of the Need to Incorporate Shift Factors for Predicting the Fatigue Life of Asphalt* APRG Document 99/43, December.

Jameson, G. W., & Hopman, P. (2000). *AUSTROADS Pavement Design Guide Chapter 6: Development of relationships between laboratory loading rate and traffic speed*: APRG Document 00/07, Australian Pavement Research Group.

Jameson, G. W., Sharp, K. G., & Vertessy, N. J. (1992). Full-depth asphalt pavement fatigue under accelerated loading: The Mulgrave (Victoria) ALF trial 1989/1991. *Australian Road and Research Board Ltd., Research Report No. 224*, 50.

Jones, A. & Bell, A, (2004) "A New Approach to Making Decisions About the Type of Pavement to be Adopted", Road Systems & Engineering Forum, Queensland, Australia.

Jian, S. J. (2006). *Investigation of factors affecting resilient modulus for hot mix asphalt.* University of Canterbury, Christchruch.

Lacroix, A., Khandan, A. A. M., & Kim, Y. R. (2007). Predicting the Resilient Modulus of Asphalt Concrete from the Dynamic Modulus. *Transport Research Board, 2001*, 132-140.

Lytton., R. L., Uzan., J., & Fernando., E. M. (1993). *Development and Validation of Performance Prediction Models and Specifications for Asphalt Binders and Paving Mixes*. SHRP/NRC, Washington DC: SHRP Report A-357.

Miner, M. A., & Calif, S. M. (1945). Cumulative Damage in Fatigue. *Journal of Applied Mechanics, 12*, A159-A164.

Molenaar, A. A. A. (2007). Prediction of fatigue cracking in asphalt pavements: Do we follow the right approach. *Transport Research Record*(2001), 155-162.

Montgomery, D. C. (2001). *Design and Analysis of Experiments*. New York: John Wiley & Sons.

National Asphalt Pavement Association (NAPA).

National Center for Asphalt Technology (NCAT).

National Cooperative Highway Research. (2010). *Validating the Fatigue Endurance Limit for Hot Mix Asphalt*. Washington D.C: Transportation Research Board.

National Cooperative Highway Research Program (NCHRP).

National Roads Board, N. Z. (1989). *State Highway Pavement Design and Rehabiliation Manual*.

New Zealand Transport Agency (NZTA). (2009). State Highway Traffic Volumes 1975-2010.

New Zealand Transport Agency (NZTA). (2010). *Draft specification for dense graded, stone mastic, and fine graded asphalt paving materials: Draft NZTA M/10: 2010*.

Oliver, J. W. H., & Alderson, A. (2001). *Examination of the Precision of the Beam Fatigue Apparatus Using Aluminium and Plastic Beams*. Melbourne: ARRB Transport Research, Contract Report RC1577- A. For Australian Asphalt Pavement Association.

Paris, P. C., & Erdogan, F. (1963). A Critical Analysis of Crack Propagation Laws. *Journal of Basic Engineering, 85*, 528-534.

Paterson, W. D. O. (1972). *Traffic Compaction of Asphalt Concrete Surface Courses.* University of Canterbury, Christchurch.

Pell, P. S., & Copper, K. E. (1975). The effect of testing and mix variables on the fatigue preformance of bituminous materials. *Proceedings Assoication of Asphalt Paving Technologists, 44*, 1-37.

Pellinen, T. K., Christensen Jr., D. W., Rowe, G. M., & Sharrock, M. (2004). Fatigue-Transfer Functions: How Do they Compare? *Transport Research Board, 1896*, 77-87.

Pellinen, T. K., Witczak, M. W., & Bonaquist, R. F. (Eds.). (2002) Proceedings of the Pavement Mechanics Symposium at the 15th ASCE Engineering MechanicsConference (EM2002). Columbia University, New York, NY.

Peploe, R. J. (2008). *Flexural modulus of typical New Zealand structral asphalt mixes*: Land Transport New Zealand Report 334.

Pidwerbesky, B. (2009). AUSTROADS Pavement Design Guide 2004. Lecture notes for Pavement Engineering, ENCI 415, University of Canterbury.

Pidwerbesky, B. (2010). Personal commuications.

Pierce, L. M., & Mahoney, J. P. (1996). Asphalt Concrete Overlay Design Case Studies. *Transport Research Board, 1543*, 3-9.

Rickards, I., & Armstrong, P. (2010). *Long term full depth asphalt pavement performance in Australia.* Paper presented at the 24th ARRB Conference, Melbourne.

Roa Tangella, S. C. S., Craus, J., Deacon., J. A., & Monismith, C. L. (1990). *Summary Report on Fatigue Response of Asphalt Mixtures*. University of California at Berkeley, California: TM-UCB-A-003A-89-3, Prepared for Strategic Highway Research Program Project A-003-A.

Saleh, M. (2010). Methodology for the calibration and validation of the Shell fatigue performance function using experimental laboratory data. *Road & Transport Research, 19*(4).

Saleh, M., & Jian, S. J. (2006). *Factors affecting resilient modulus*. Paper presented at the 10th International Conference on Asphalt Pavements (ICAP 2006), 12-17 Aug 2006.

Saunders, L. R. (1982). The foundations of modern pavement design: a preliminary report.

Shell International Petroleum Company Ltd. (1978). *Shell pavement design manual - : asphalt pavements and overlays for road traffic*. London, UK.

Shu, X., & Huang, B. (2010). *A Practical Method for Converting Resilient Modulus to Dynamic Modulus of Asphalt Mixtures.* Paper presented at the 11th International Conference on Asphalt Pavement, Nagoya, Japan.

Stats-Ease Inc. (2009). Design Expert version 8. Minneapolis, MN.

Stubbs, A. (2010). Personal Communication at 24th ARRB Conference. Mebourne, Australia.

Stubbs, A., Saleh, M., & Jeffery-Wright, H. (2010). *An Investigation into the Validation of the Shell Fatigue Transfer Function*. Paper presented at the IPENZ Transportation Conference.

Tayebali, A. A., Deacon., J. A., Coplantaz, J. C., & Monismith, C. L. (1993). Modeling fatigue response of asphalt-aggregate mixtures. *AAPT, 62*, 385-421.

Thom, N. (2006). Asphalt cracking: A Nottingham Perspective. *Engenaria Civil/Civil Engineering, 26*, 75-84.

Transit New Zealand. (2005). New Zealand Supplement to the Document, Pavement Design - A Guide to the Structural Design of Raod Pavements (Austroads, 2004). In T. N. Zealand (Ed.). Wellington.

Transit New Zealand. (2007). New Zealand Supplement to the Document, Pavement Design - A Guide to the Structural Design of Road Pavements (Austroads, 2004). Wellington, Transit New Zealand.

Van Dijk, W., & Visser, W. (1977). The energy approach to fatigue for pavement design. *Proceedings Assoication of Asphalt Paving Technologists, 46*, 1-40.

Van Dijk., W. (1975). Practical Fatigue Characterization of Bituminous Mixes. *Proceedings Assoication of Asphalt Paving Technologists, 44*, 38-74.

Von Quintus., H. L., Scherocman., T. A., Hughes., C. S., & Kennedy., T. W. (1988). *Development of Asphalt-Aggregate Mixtures Analysis System: AAMAS*. Austin: Brent Rauhut Engineering, Inc.

Wardle, L. J. (2004). CIRCLY (Version Version 5). Web: www.minicad.com.au: Mincad Systems, Australia.

Wardle, L. J. (2010) CIRCLY and Mechanistic Pavement Design: The Past, Present and Towards the Future. Minicad Systems, Australia.

Whiteoak, D. b. (1990). *The Shell bitumen handbook*. Chertsey: Shell Bitumen U.K.

APPENDIX A – JOB ADVERT

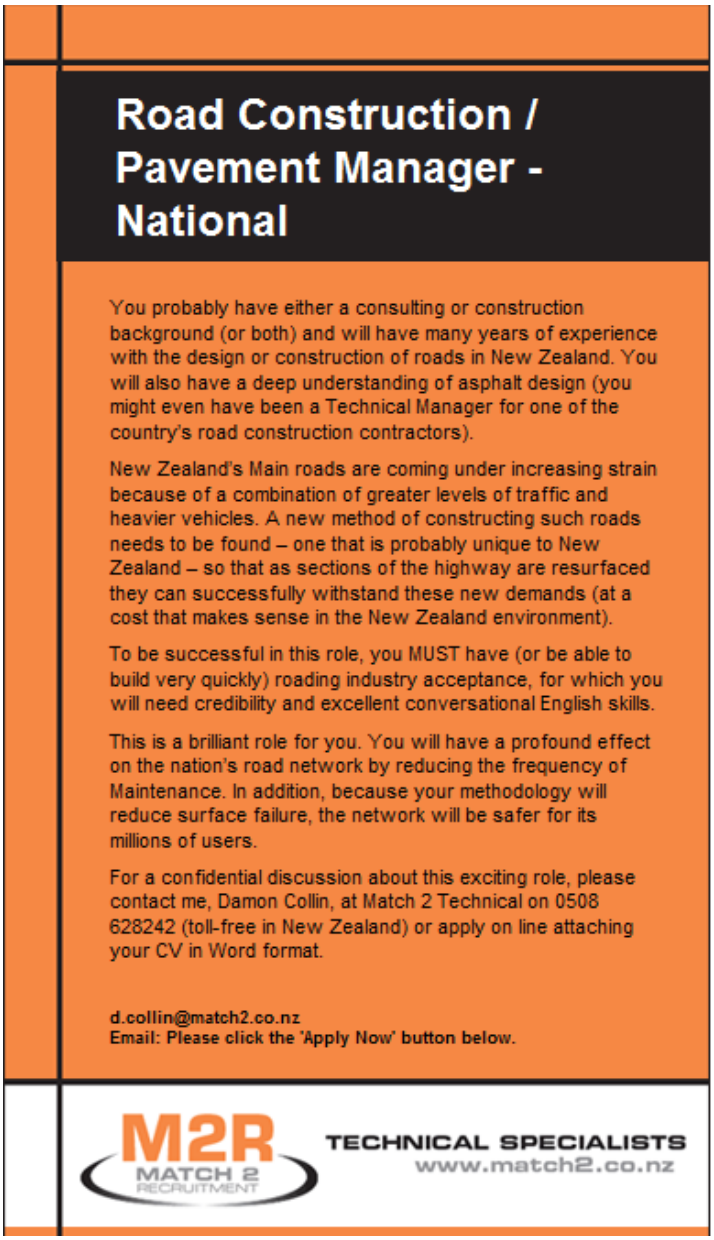

Road Construction / Pavement Manager - National

You probably have either a consulting or construction background (or both) and will have many years of experience with the design or construction of roads in New Zealand. You will also have a deep understanding of asphalt design (you might even have been a Technical Manager for one of the country's road construction contractors).

New Zealand's Main roads are coming under increasing strain because of a combination of greater levels of traffic and heavier vehicles. A new method of constructing such roads needs to be found – one that is probably unique to New Zealand – so that as sections of the highway are resurfaced they can successfully withstand these new demands (at a cost that makes sense in the New Zealand environment).

To be successful in this role, you MUST have (or be able to build very quickly) roading industry acceptance, for which you will need credibility and excellent conversational English skills.

This is a brilliant role for you. You will have a profound effect on the nation's road network by reducing the frequency of Maintenance. In addition, because your methodology will reduce surface failure, the network will be safer for its millions of users.

For a confidential discussion about this exciting role, please contact me, Damon Collin, at Match 2 Technical on 0508 628242 (toll-free in New Zealand) or apply on line attaching your CV in Word format.

d.collin@match2.co.nz
Email: Please click the 'Apply Now' button below.

Figure A Job advertisement for a National Road Construction / Pavement Manager. (Source Trademe Jobs, September 2011)

APPENDIX B – ASPHALT BEAM VOLUMETRICS

Table B.1 Volumetric properties for the various asphalt beams for the AC14 60/70 HMA

Sample #	A[i]	B[ii]	C[iii]	G_{mb}[iv]	G_{mm}[v]	G_{sb}[vi]	VTM[vii] (%)	VMA[viii] (%)	VFB[ix] (%)	P_b[x] (%)	V_b[xi] (%)
1	2974.20	2980.19	1795.40	2.510	2.652	2.827	5.342	15.660	65.884	5.02	12.35
2	3278.41	3286.23	1970.16	2.491	2.652	2.827	6.069	16.307	62.785	5.02	12.26
3	2995.09	3000.29	1808.23	2.513	2.652	2.827	5.259	15.585	66.257	5.02	12.37
4	3082.44	3085.99	1859.36	2.513	2.652	2.827	5.244	15.572	66.325	5.02	12.37
5	2834.90	2858.23	1705.56	2.459	2.652	2.827	7.262	17.370	58.194	5.02	12.10
6	3025.00	3015.00	1819.24	2.530	2.652	2.827	4.609	15.006	69.286	5.02	12.45

[i] Dry mass (grams)
[ii] Saturated surface dry mass (grams)
[iii] Submerged mass in water (grams)
[iv] Asphalt bulk specific gravity
[v] Maximum theoretical specific gravity
[vi] Stone specific gravity
[vii] Air voids in total asphalt mix
[viii] Voids in mineral aggregate
[ix] Voids filled with binder
[x] Percentage of binder, by mass
[xi] Percentage of binder, by volume

Sample #	A	B	C	G_{mb}	G_{mm}	G_{sb}	VTM (%)	VMA(%)	VFB(%)	P_b (%)	V_b (%)
7	3010.26	3034.00	1816.73	2.473	2.652	2.827	6.751	16.915	60.088	5.02	12.17
8	2977.82	2981.59	1796.93	2.514	2.652	2.827	5.217	15.548	66.446	5.02	12.37
9	3029.00	3036.80	1823.57	2.497	2.652	2.827	5.858	16.119	63.657	5.02	12.29
10	2932.48	2853.38	1704.35	2.552	2.652	2.827	3.766	14.255	73.583	5.02	12.56
11	2991.11	2998.89	1801.74	2.499	2.652	2.827	5.787	16.056	63.956	5.02	12.30
12	2862.66	2869.81	1722.47	2.495	2.652	2.827	5.919	16.173	63.405	5.02	12.28
13	2905.40	2918.80	1752.67	2.491	2.652	2.827	6.052	16.292	62.851	5.02	12.26
14	2907.00	2914.00	1754.27	2.507	2.652	2.827	5.482	15.784	65.269	5.02	12.34
15	2921.56	2945.37	1764.16	2.473	2.652	2.827	6.736	16.901	60.145	5.02	12.17
16	2882.00	2899.60	1737.78	2.481	2.652	2.827	6.463	16.658	61.201	5.02	12.21
17	3065.20	3071.00	1837.05	2.484	2.652	2.827	6.333	16.542	61.717	5.02	12.23
18	3209.00	3215.10	1930.96	2.499	2.652	2.827	5.771	16.042	64.024	5.02	12.30
19	3110.60	3116.70	1874.19	2.503	2.652	2.827	5.600	15.889	64.755	5.02	12.32
20	2990.60	2922.00	1746.54	2.544	2.652	2.827	4.065	14.522	72.007	5.02	12.52
21	3127.20	3146.10	1883.86	2.478	2.652	2.827	6.580	16.762	60.746	5.02	12.19
22	3366.50	3372.60	2033.88	2.515	2.652	2.827	5.177	15.512	66.628	5.02	12.38
23	3394.90	3400.00	2047.86	2.511	2.652	2.827	5.326	15.645	65.958	5.02	12.36
24	3420.00	3425.00	2062.67	2.510	2.652	2.827	5.339	15.657	65.899	5.02	12.36
25	3581.10	3608.70	2166.84	2.484	2.652	2.827	6.347	16.555	61.659	5.02	12.22
26	3184.20	3196.70	1914.50	2.483	2.652	2.827	6.358	16.564	61.617	5.02	12.22
27	3269.50	3276.60	1985.69	2.533	2.652	2.827	4.498	14.907	69.826	5.02	12.46
28	3247.50	3254.60	1967.92	2.524	2.652	2.827	4.829	15.202	68.235	5.02	12.42
29	3107.40	3113.70	1882.54	2.524	2.652	2.827	4.828	15.201	68.240	5.02	12.42
36	3107.32	3117.94	1874.40	2.499	2.641	2.827	5.385	16.048	66.441	5.02	12.30
37	3136.62	3143.85	1890.20	2.502	2.641	2.827	5.264	15.940	66.978	5.02	12.31
38	3160.43	3166.95	1901.30	2.497	2.641	2.827	5.449	16.104	66.162	5.02	12.29

Sample #	A	B	C	G_{mb}	G_{mm}	G_{sb}	VTM (%)	VMA(%)	VFB(%)	P_b (%)	V_b (%)
40	2950.50	2966.63	1769.12	2.464	2.641	2.827	6.707	17.220	61.051	5.02	12.13
41	3054.50	3062.57	1840.00	2.498	2.641	2.827	5.399	16.059	66.384	5.02	12.30
42	3049.49	3053.35	1846.10	2.526	2.641	2.827	4.355	15.133	71.222	5.02	12.43
43	3064.15	3069.31	1857.70	2.529	2.641	2.827	4.241	15.032	71.786	5.02	12.45
44	3135.18	3140.17	1897.61	2.523	2.641	2.827	4.462	15.228	70.700	5.02	12.42
46	3072.08	3086.91	1841.60	2.467	2.641	2.827	6.591	17.118	61.494	5.02	12.14
47	3195.40	3201.00	1932.00	2.518	2.641	2.827	4.656	15.400	69.769	5.02	12.39
48	3195.54	3201.05	1933.06	2.520	2.641	2.827	4.575	15.329	70.152	5.02	12.40
50	3026.93	3046.80	1818.46	2.464	2.641	2.827	6.693	17.208	61.106	5.02	12.13
51	3080.18	3096.97	1853.06	2.476	2.641	2.827	6.240	16.806	62.871	5.02	12.19
52	3073.20	3079.98	1852.30	2.503	2.641	2.827	5.216	15.897	67.192	5.02	12.32
53	3007.56	3012.56	1816.00	2.514	2.641	2.827	4.828	15.553	68.960	5.02	12.37
54	3191.40	3198.55	1942.90	2.542	2.641	2.827	3.763	14.608	74.243	5.02	12.51
56	3276.12	3285.79	1970.00	2.490	2.641	2.827	5.723	16.347	64.990	5.02	12.25
57	3187.63	3196.03	1920.76	2.500	2.641	2.827	5.355	16.021	66.574	5.02	12.30
58	3140.40	3170.28	1905.90	2.484	2.641	2.827	5.954	16.552	64.028	5.02	12.22
59	3115.71	3124.48	1870.50	2.485	2.641	2.827	5.920	16.522	64.170	5.02	12.23

Table B.2 Volumetrics properties for the various asphalt beams for the AC14 80/100 HMA

Sample #	A	B	C	G_{mb}	G_{mm}	G_{sb}	VTM (%)	VMA(%)	VFB(%)	P_b (%)	V_b (%)
2	2961.75	2979.76	1752.40	2.413	2.595	2.827	7.009	18.926	62.964	5.02	11.88
3	3106.10	3126.93	1840.20	2.414	2.595	2.827	6.977	18.897	63.080	5.02	11.88
4	3045.07	3067.98	1801.92	2.405	2.595	2.827	7.316	19.193	61.883	5.02	11.84
5	2888.16	2926.76	1830.90	2.636	2.595	2.827	NA	NA	NA	5.02	12.97
6	2990.94	3024.34	1777.25	2.398	2.595	2.827	7.579	19.422	60.979	5.02	11.80
8	3237.30	3249.20	1918.44	2.433	2.595	2.827	6.255	18.268	65.758	5.02	11.97
9	3062.55	3077.20	1814.40	2.425	2.595	2.827	6.543	18.519	64.669	5.02	11.94
10	3210.83	3233.00	1894.04	2.398	2.595	2.827	7.591	19.433	60.936	5.02	11.80
11	2948.35	2973.40	1758.08	2.426	2.595	2.827	6.513	18.493	64.781	5.02	11.94
12	3024.73	3031.87	1805.30	2.466	2.595	2.827	4.971	17.148	71.013	5.02	12.14
15	3067.06	3083.87	1830.36	2.447	2.595	2.827	5.712	17.795	67.900	5.02	12.04
16	2587.97	2615.72	1540.95	2.408	2.595	2.827	7.209	19.100	62.257	5.02	11.85
17	3023.32	3036.76	1800.98	2.446	2.595	2.827	5.723	17.804	67.856	5.02	12.04
18	3016.68	3028.84	1803.54	2.462	2.595	2.827	5.126	17.283	70.344	5.02	12.12
19	3065.32	3088.38	1818.32	2.414	2.595	2.827	6.993	18.912	63.021	5.02	11.88
20	2892.30	2918.95	1720.63	2.414	2.595	2.827	6.989	18.908	63.036	5.02	11.88
21	3065.25	3077.13	1823.56	2.445	2.595	2.827	5.772	17.847	67.658	5.02	12.03
22	3222.20	3230.08	1931.85	2.482	2.595	2.827	4.355	16.611	73.785	5.02	12.22
24	3079.04	3086.37	1848.93	2.488	2.595	2.827	4.114	16.402	74.915	5.02	12.25
25	2947.90	2958.79	1752.10	2.443	2.595	2.827	5.859	17.923	67.311	5.02	12.02
26	2882.03	2902.02	1708.60	2.415	2.595	2.827	6.939	18.864	63.217	5.02	11.89
27	3065.88	3072.29	1833.00	2.474	2.595	2.827	4.667	16.883	72.359	5.02	12.18
28	2955.50	2962.00	1775.80	2.492	2.595	2.827	3.986	16.290	75.532	5.02	12.26

Sample #	A	B	C	G_{mb}	G_{mm}	G_{sb}	VTM (%)	VMA(%)	VFB(%)	P_b (%)	V_b (%)
29	3047.69	3054.00	1822.65	2.475	2.595	2.827	4.621	16.844	72.564	5.02	12.18
30	3083.50	3050.00	1837.94	2.544	2.595	2.827	1.965	14.528	86.476	5.02	12.52
31	2898.29	2924.95	1840.37	2.672	2.595	2.827	NA	NA	NA	5.02	13.15
32	3016.27	3024.23	1808.79	2.482	2.595	2.827	4.369	16.624	73.719	5.02	12.21
33	3078.06	3083.02	1833.00	2.462	2.595	2.827	5.109	17.269	70.413	5.02	12.12
34	3206.58	3218.56	1919.26	2.468	2.595	2.827	4.897	17.084	71.337	5.02	12.15
35	2999.36	3020.40	1789.20	2.436	2.595	2.827	6.122	18.152	66.273	5.02	11.99
36	3013.98	3029.96	1800.36	2.451	2.595	2.827	5.542	17.646	68.595	5.02	12.06
37	3109.44	3116.60	1869.80	2.494	2.595	2.827	3.895	16.210	75.975	5.02	12.27
38	3080.94	3088.82	1846.30	2.480	2.595	2.827	4.447	16.692	73.356	5.02	12.20
39	3194.53	3202.51	1909.63	2.471	2.595	2.827	4.784	16.985	71.836	5.02	12.16
40	3053.02	3073.83	1806.87	2.410	2.595	2.827	7.140	19.040	62.500	5.02	11.86
41	2970.00	2998.72	1771.34	2.420	2.595	2.827	6.752	18.701	63.896	5.02	11.91
42	3132.27	3140.53	1878.53	2.482	2.595	2.827	4.355	16.611	73.783	5.02	12.22
43	3186.64	3089.40	1911.60	2.706	2.595	2.827	-4.262	9.099	146.834	5.02	13.32
44	3081.40	3089.91	1840.31	2.466	2.595	2.827	4.975	17.152	70.997	5.02	12.14
45	3087.61	3105.21	1831.00	2.423	2.595	2.827	6.622	18.588	64.375	5.02	11.93
46	2858.83	2896.69	1690.44	2.370	2.595	2.827	8.670	20.374	57.445	5.02	11.66
47	2984.83	2994.38	1767.24	2.432	2.595	2.827	6.268	18.279	65.710	5.02	11.97
48	2976.94	2994.38	1767.24	2.426	2.595	2.827	6.516	18.495	64.771	5.02	11.94
49	3009.60	3021.47	1793.78	2.451	2.595	2.827	5.532	17.638	68.634	5.02	12.06
50	3003.56	3021.60	1775.71	2.411	2.595	2.827	7.099	19.004	62.644	5.02	11.86
51	2950.44	2973.60	1767.10	2.445	2.595	2.827	5.763	17.839	67.695	5.02	12.04
52	3325.47	3229.94	1987.00	2.675	2.595	2.827	NA	NA	NA	5.02	13.17
53	3148.49	3156.50	1890.97	2.488	2.595	2.827	4.128	16.413	74.851	5.02	12.24
54	3141.30	3147.35	1885.20	2.489	2.595	2.827	4.091	16.381	75.028	5.02	12.25

Sample #	A	B	C	G_{mb}	G_{mm}	G_{sb}	VTM (%)	VMA(%)	VFB(%)	P_b (%)	V_b (%)
55	2975.50	2989.84	1765.59	2.430	2.595	2.827	6.340	18.342	65.433	5.02	11.96
56	2833.00	2876.36	1677.46	2.363	2.595	2.827	8.940	20.609	56.620	5.02	11.63
57	3233.87	3255.03	1917.15	2.417	2.595	2.827	6.853	18.790	63.527	5.02	11.90
58	2998.20	3017.40	1785.40	2.434	2.595	2.827	6.220	18.237	65.896	5.02	11.98
59	3222.03	3234.37	1920.46	2.452	2.595	2.827	5.501	17.611	68.763	5.02	12.07
60	2556.21	2565.61	1517.97	2.440	2.595	2.827	5.974	18.023	66.853	5.02	12.01

APPENDIX C – ASPHALT MIX DESIGN

Aggregate and binder quantities for specimen preparation are given below for AC14 80/100 HMA. Based on the job mix formula (JMF) as presented in Section 3.1.4, and reproduced in Table C.1, the mix recipe is calculated by the density method.

Table C.1 Key mix design variables for AC14 80/100

Variable	AC14 80/100
P_b	5.02 %
P_a	94.98 %
VTM	5.00 %
Surface voids	4.25 %
G_{mb}	2.465
G_{mm}	2.565
Mould dimensions	40 x 30.5 x7.5 cm

The amount of aggregate and binder mass is determined with the knowledge of both the asphalt mix density and volume. Density is given by the JMF, and the volume is known by the space of the mould to compact the samples in. The asphalt bulk density is expressed as Equation C–1

$$G_{mb} = \frac{m_t}{V_{slab}} = \frac{m_{agg} + m_{bind}}{V_{slab}} \qquad \textbf{C–1}$$

where:

G_{mb}= asphalt bulk density
m_t = total asphalt mass of the sample (or slab in this case) (grams)
m_{agg}= mass of aggregate in the sample (grams)
m_{bind} = mass of binder in the sample (grams)
V_{slab} = volume of mould (cm^3)

In addition, the density or air voids of the mix is given by Equation C–2

$$VTM(\%) = 100\left(1 - \frac{G_{mb}}{G_{mm}}\right) \qquad \textbf{C–2}$$

where:

$\mathrm{VTM}(\%)$ = total air voids in the asphalt mixture
G_{mb} = asphalt bulk density
G_{mm} = theoretical maximum specific density

Equating these equations together and rearranging for the mass of the asphalt mixture m_t gives Equation C–3.

$$m_t = m_{agg} + m_{bind} = V_{slab} * G_{mm} * \left(1 - \frac{\mathrm{VTM}(\%)}{100}\right) \qquad \textbf{C–3}$$

Now accounting for the effect of surface air voids η, which is given by the correct volume divided by the uncorrected volume. Explicitly the surface voids is the saturated surface dry weight minus the submerged weight in water, all divided by the volume of the specimen. The total mass is thus Equation C–4. The mass quantities required for the AC14 80/100 is also calculated by Equation C–5 and Equation C–6.

$$\begin{aligned} m_t = m_{agg} + m_{bind} &= \eta * V_{slab} * G_{mm} * \left(1 - \frac{\mathrm{VTM}(\%)}{100}\right) \qquad \textbf{C–4} \\ &= 0.9575 * 40.5 \text{ x } 30.5 \text{ x } 7.5 * 2.565 * \left(1 - \frac{5.02\ \%}{100}\right) \\ &= 21{,}344.18 \text{ grams} \end{aligned}$$

The mass of aggregate and binder is determined by their proportion of the mix.

$$\begin{aligned} m_{agg} &= \left(\frac{P_{agg}}{100}\right) m_t \\ &= \left(\frac{94.98}{100}\right) * 21{,}344.18 \text{ grams} \qquad \textbf{C–5} \\ m_{agg} &= 20{,}272.7 \text{ grams} \end{aligned}$$

$$\begin{aligned} m_{agg} &= \left(\frac{P_{agg}}{100}\right) m_t \\ &= \left(\frac{94.98}{100}\right) * 21{,}344.18 \text{ grams} \qquad \textbf{C–6} \\ m_{agg} &= 20{,}272.7 \text{ grams} \end{aligned}$$

APPENDIX D – TABLE OF MODULUS RESULTS

Table D.1 Tables of results for the stiffness modulus of the AC14 60/70

AC14 60/70 Stiffness Modulus (MPa)

Temperature	Frequency	Beam # 9	Beam # 3	Beam #15	Beam # 25	Average	Std. deviation
5°C	0.2 Hz	4492	5012	5119	-	**4766.3**	305.4
		4319	4919	5042	-		
		4385	4874	4932	-		
		4342	4940	4875	-		
		4278	4921	5045	-		
	1 Hz	7291	7062	7686	-	**7265.7**	490.5
		6750	7100	7762	-		
		6651	7244	8191	-		
		6603	7109	7825	-		
		6644	7349	7719	-		
	2 Hz	7865	8247	8626	-	**8221.9**	429.0
		7781	8045	8951	-		
		7886	8022	8692	-		
		7657	8257	8703	-		
		7708	8099	8790	-		
	5 Hz	9172	9637	10128	-	**9659.5**	400.3
		9329	9507	10193	-		
		9248	9628	10215	-		
		9158	9493	9921	-		
		9248	9752	10263	-		
	10 Hz	10310	10711	11472	-	**10880.3**	496.8
		10370	10745	11186	-		
		10484	10809	11765	-		
		10170	10784	11559	-		
		10637	10712	11491	-		
	15 Hz	11476	12055	12873	-	**11947.1**	588.9
		11530	11580	12291	-		
		11632	11847	12639	-		
		11355	11383	13201	-		
		-	11560	11838	-		

AC14 60/70 Stiffness Modulus (MPa)

Temperature	Frequency	Beam # 9	Beam # 3	Beam #15	Beam # 25	Average	Std. deviation
10°C	0.2 Hz	2915	2703	2531	-	**2629.1**	160.9
		2894	2671	2451	-		
		2811	2554	2441	-		
		2711	2479	2441	-		
		2713	2618	2503	-		
	1 Hz	4937	4171	4937	-	**4572.8**	246.2
		4553	4396	4553	-		
		4686	4234	4868	-		
		4674	4215	4674	-		
		4631	4432	4631	-		
	2 Hz	5722	5211	5722	-	**5584.1**	196.9
		5733	5336	5733	-		
		5733	5328	5733	-		
		5727	5290	5727	-		
		5650	5466	5650	-		
	5 Hz	7025	6757	7025	-	**6908.5**	161.5
		7029	6676	7029	-		
		7007	6627	7007	-		
		7042	6694	7047	-		
		6978	6707	6978	-		
	10 Hz	8271	8067	8271	-	**8227.9**	184.3
		8378	7983	8378	-		
		8335	7984	8335	-		
		8357	7876	8357	-		
		8401	8025	8401	-		
	15 Hz	9672	8742	9672	-	**9352.8**	441.5
		9734	8988	8734	-		
		9534	8820	9534	-		
		9805	8973	9805	-		
		9735	8809	9735	-		

AC14 60/70 Stiffness Modulus (MPa)

Temperature	Frequency	Beam # 9	Beam # 3	Beam #15	Beam # 25	Average	Std. deviation
20°C	0.2 Hz	605	659	-	-	**598.0**	122.8
		574	690	-	-		
		598	658	-	-		
		274	692	-	-		
		565	665	-	-		
	1 Hz	1038	-	1252	1162	**1131.5**	130.6
		1004	-	1278	1138		
		1042	-	1328	1140		
		1051	-	-	-		
		1059	-	-	-		
	2 Hz	1318	-	-	-	**1343.0**	25.5
		1373	-	-	-		
		1364	-	-	-		
		1342	-	-	-		
		1318	-	-	-		
	5 Hz	1993	-	2531	2190	**2200.0**	272.6
		1992	-	2552	2139		
		2014	-	2501	2089		
		2040	-	-	-		
		1977	-	-	-		
	10 Hz	2524	-	3085	2652	**2691.3**	270.5
		2521	-	3059	2644		
		2483	-	2885	2653		
		2493	-	-	-		
		2480	-	-	-		
	15 Hz	3161	-	-	-	**2959.2**	115.2
		2879	-	-	-		
		2907	-	-	-		
		2944	-	-	-		
		2905	-	-	-		

AC14 60/70 Stiffness Modulus (MPa)

Temperature	Frequency	Beam # 9	Beam # 3	Beam #15	Beam # 25	Average	Std. deviation
25°C	0.2 Hz	-	-	-	-	-	-
		-	-	-	-		
		-	-	-	-		
		-	-	-	-		
		-	-	-	-		
	1 Hz	667	795	665	506	**688.2**	73.2
		620	792	652	496		
		611	758	634	506		
		-	-	-	-		
		-	-	-	-		
	2 Hz	-	-	-	-	-	-
		-	-	-	-		
		-	-	-	-		
		-	-	-	-		
		-	-	-	-		
	5 Hz	1136	1243	1024	993	**1262.3**	148.4
		1112	1474	1272	948		
		1384	1393	1323	763		
		-	-	-	-		
		-	-	-	-		
	10 Hz	1457	1737	1453	1153	**1542.0**	138.3
		1443	1718	1472	1162		
		1442	1722	1434	1134		
		-	-	-	-		
		-	-	-	-		
	15 Hz	-	-	-	-	-	-
		-	-	-	-		
		-	-	-	-		
		-	-	-	-		
		-	-	-	-		

AC14 60/70 Stiffness Modulus (MPa)

Temperature	Frequency	Beam # 9	Beam # 3	Beam #15	Beam # 25	Average	Std. deviation
30°C	0.2 Hz	-	-	-	-	-	-
		-	-	-	-		
		-	-	-	-		
		-	-	-	-		
		-	-	-	-		
	1 Hz	460	511	436	316	**460.6**	46.0
		436	538	418	319		
		422	506	418	328		
		-	-	-	-		
		-	-	-	-		
	2 Hz	-	-	-	-	-	-
		-	-	-	-		
		-	-	-	-		
		-	-	-	-		
		-	-	-	-		
	5 Hz	601	949	738	597	**757.1**	124.2
		652	952	685	584		
		700	814	723	527		
		-	-	-	-		
		-	-	-	-		
	10 Hz	955	1061	949	726	**974.6**	68.0
		924	1066	947	719		
		894	1058	917	685		
	15 Hz	-	-	-	-	-	-
		-	-	-	-		
		-	-	-	-		
		-	-	-	-		
		-	-	-	-		

Table D.2 Tables of results for the stiffness modulus of the AC14 80/100

AC14 80/100 Stiffness Modulus (MPa)

Temperature	Frequency	Beam # 9	Beam # 3	Beam #15	Beam # 25	Average	Std. deviation
5°C	0.2 Hz	4492	5012	5119	-	**4766.3**	305.4
		4319	4919	5042	-		
		4385	4874	4932	-		
		4342	4940	4875	-		
		4278	4921	5045	-		
	1 Hz	7291	7062	7686	-	**7265.7**	490.5
		6750	7100	7762	-		
		6651	7244	8191	-		
		6603	7109	7825	-		
		6644	7349	7719	-		
	2 Hz	7865	8247	8626	-	**8221.9**	429.0
		7781	8045	8951	-		
		7886	8022	8692	-		
		7657	8257	8703	-		
		7708	8099	8790	-		
	5 Hz	9172	9637	10128	-	**9659.5**	400.3
		9329	9507	10193	-		
		9248	9628	10215	-		
		9158	9493	9921	-		
		9248	9752	10263	-		
	10 Hz	10310	10711	11472	-	**10880.3**	496.8
		10370	10745	11186	-		
		10484	10809	11765	-		
		10170	10784	11559	-		
		10637	10712	11491	-		
	15 Hz	11476	12055	12873	-	**11947.1**	588.9
		11530	11580	12291	-		
		11632	11847	12639	-		
		11355	11383	13201	-		
		-	11560	11838	-		

AC14 80/100 Stiffness Modulus (MPa)							
Temperature	**Frequency**	**Beam # 9**	**Beam # 3**	**Beam #15**	**Beam # 25**	**Average**	**Std. deviation**
10°C	0.2 Hz	2915	2703	2531	-	**2629.1**	160.9
		2894	2671	2451	-		
		2811	2554	2441	-		
		2711	2479	2441	-		
		2713	2618	2503	-		
	1 Hz	4937	4171	4937	-	**4572.8**	246.2
		4553	4396	4553	-		
		4686	4234	4868	-		
		4674	4215	4674	-		
		4631	4432	4631	-		
	2 Hz	5722	5211	5722	-	**5584.1**	196.9
		5733	5336	5733	-		
		5733	5328	5733	-		
		5727	5290	5727	-		
		5650	5466	5650	-		
	5 Hz	7025	6757	7025	-	**6908.5**	161.5
		7029	6676	7029	-		
		7007	6627	7007	-		
		7042	6694	7047	-		
		6978	6707	6978	-		
	10 Hz	8271	8067	8271	-	**8227.9**	184.3
		8378	7983	8378	-		
		8335	7984	8335	-		
		8357	7876	8357	-		
		8401	8025	8401	-		
	15 Hz	9672	8742	9672	-	**9352.8**	441.5
		9734	8988	8734	-		
		9534	8820	9534	-		
		9805	8973	9805	-		
		9735	8809	9735	-		

AC14 80/100 Stiffness Modulus (MPa)

Temperature	Frequency	Beam # 9	Beam # 3	Beam #15	Beam # 25	Average	Std. deviation
20°C	0.2 Hz	605	659	-	-	**598.0**	122.8
		574	690	-	-		
		598	658	-	-		
		274	692	-	-		
		565	665	-	-		
	1 Hz	1038	-	1252	1162	**1131.5**	130.6
		1004	-	1278	1138		
		1042	-	1328	1140		
		1051	-	-	-		
		1059	-	-	-		
	2 Hz	1318	-	-	-	**1343.0**	25.5
		1373	-	-	-		
		1364	-	-	-		
		1342	-	-	-		
		1318	-	-	-		
	5 Hz	1993	-	2531	2190	**2200.0**	272.6
		1992	-	2552	2139		
		2014	-	2501	2089		
		2040	-	-	-		
		1977	-	-	-		
	10 Hz	2524	-	3085	2652	**2691.3**	270.5
		2521	-	3059	2644		
		2483	-	2885	2653		
		2493	-	-	-		
		2480	-	-	-		
	15 Hz	3161	-	-	-	**2959.2**	115.2
		2879	-	-	-		
		2907	-	-	-		
		2944	-	-	-		
		2905	-	-	-		

AC14 80/100 Stiffness Modulus (MPa)

Temperature	Frequency	Beam # 9	Beam # 3	Beam #15	Beam # 25	Average	Std. deviation
25°C	0.2 Hz	-	-	-	-	-	-
		-	-	-	-		
		-	-	-	-		
		-	-	-	-		
		-	-	-	-		
	1 Hz	667	795	665	506	**688.2**	73.2
		620	792	652	496		
		611	758	634	506		
		-	-	-	-		
		-	-	-	-		
	2 Hz	-	-	-	-	-	-
		-	-	-	-		
		-	-	-	-		
		-	-	-	-		
		-	-	-	-		
	5 Hz	1136	1243	1024	993	**1262.3**	148.4
		1112	1474	1272	948		
		1384	1393	1323	763		
		-	-	-	-		
		-	-	-	-		
	10 Hz	1457	1737	1453	1153	**1542.0**	138.3
		1443	1718	1472	1162		
		1442	1722	1434	1134		
		-	-	-	-		
		-	-	-	-		
	15 Hz	-	-	-	-	-	-
		-	-	-	-		
		-	-	-	-		
		-	-	-	-		
		-	-	-	-		

AC14 80/100 Stiffness Modulus (MPa)

Temperature	Frequency	Beam # 9	Beam # 3	Beam #15	Beam # 25	Average	Std. deviation
30°C	0.2 Hz	-	-	-	-	-	-
		-	-	-	-		
		-	-	-	-		
		-	-	-	-		
		-	-	-	-		
	1 Hz	460	511	436	316	**460.6**	46.0
		436	538	418	319		
		422	506	418	328		
		-	-	-	-		
		-	-	-	-		
	2 Hz	-	-	-	-	-	-
		-	-	-	-		
		-	-	-	-		
		-	-	-	-		
		-	-	-	-		
	5 Hz	601	949	738	597	**757.1**	124.2
		652	952	685	584		
		700	814	723	527		
		-	-	-	-		
		-	-	-	-		
	10 Hz	955	1061	949	726	**974.6**	68.0
		924	1066	947	719		
		894	1058	917	685		
		-	-	-	-		
		-	-	-	-		
	15 Hz	-	-	-	-	-	-
		-	-	-	-		
		-	-	-	-		
		-	-	-	-		
		-	-	-	-		

Table C3 Tables of results for the resilient modulus testing of the AC14 60/70

AC14 60/70 Resilient Modulus (MPa)

Temperature	Frequency	Core # 5	Core # 3	Core # 2	Core # 6	Average	Std. deviation
–5°C	1 Hz	25318	18123	20340	26066	**21,372**	5836.8
		25509	17408	25397	26051		
		25234	14836	21330	25899		
		25233	16385	21852	2552		
		25677	16697	22557	24982		
	2 Hz	28248	17460	26037	27648	**26,551**	4356.7
		28378	17633	26574	27852		
		28968	17153	27327	30157		
		29329	-	27685	29059		
		30357	-	28225	29833		
	10 Hz	39122	19050	36743	37051	**34,799**	6612.8
		40385	18421	36482	38358		
		38908	-	36610	33224		
		41013	-	36817	31197		
		39449	-	36481	32270		
	15 Hz	39975	18734	39684	36073	**36,105**	7425.8
		41728	18424	39589	36364		
		43265	-	39773	36612		
		-	-	39640	37642		
		-	-	38527	35547		

AC14 60/70 Resilient Modulus (MPa)

Temperature	Frequency	Core # 5	Core # 3	Core # 2	Core # 6	Average	Std. deviation
1°C	1 Hz	11512	11095	13819	10830	**11,982**	1178.0
		11693	11879	13645	10638		
		11818	11838	13830	10777		
		11864	11675	14015	10922		
		11823	11060	13936	10974		
	2 Hz	13192	12494	15364	12289	**13,565**	1153.8
		13241	12532	15265	12306		
		13309	13693	15240	12375		
		13407	13809	15365	12394		
		13430	13876	15311	12410		
	10 Hz	18773	14050	19419	15738	**18,049**	1716.9
		18879	19186	19284	15944		
		18235	19264	19160	16021		
		18931	19386	19096	15865		
		19057	19506	19255	15939		
	15 Hz	20530	21465	20177	16597	**20,053**	1937.2
		21095	21440	19941	16570		
		20743	21990	20277	17149		
		21513	21778	20335	17385		
		21388	22884	20407	17401		

AC14 60/70 Resilient Modulus (MPa)

Temperature	Frequency	Core # 5	Core # 3	Core # 2	Core # 6	Average	Std. deviation
5°C	1 Hz	9730	9402	8179	10619	**8,655**	1186.9
		7594	9543	7470	-		
		7379	9874	7880	-		
		7534	-	-	-		
		-	-	-	-		
	2 Hz	8310	11486	8630	-	**9,585**	1706.6
		8301	11893	8530	-		
		8439	12155	8517	-		
		-	-	-	-		
		-	-	-	-		
	10 Hz	9825	16063	11535	-	**12,562**	2687.2
		10057	15973	11602	-		
		10329	16061	11612	-		
		-	-	-	-		
		-	-	-	-		
	15 Hz	6134	15621	12325	-	**13,237**	5411.5
		7048	15794	21485	-		
		7078	16214	17437	-		
		-	-	-	-		
		-	-	-	-		

AC14 60/70 Resilient Modulus (MPa)

Temperature	Frequency	Core # 5	Core # 3	Core # 2	Core # 6	Average	Std. deviation
10°C	1 Hz	4914	7118	7879	6693	**6,807**	1346.2
		4804	8507	7939	6828		
		4640	8134	7695	6841		
		4367	8057	7588	7145		
		4687	7806	7091	7398		
	2 Hz	5133	9276	8697	7937	**7,713**	1695.3
		5235	9526	8754	7737		
		5275	9559	8766	7454		
		5189	9707	8682	7607		
		5097	9272	-	7638		
	10 Hz	6991	16406	12837	11061	**11,417**	3201.8
		7032	15595	12788	11074		
		7027	15050	12826	10667		
		7025	14830	12819	10607		
		7029	14683	-	10567		
	15 Hz	7759	16272	-	11707	**12,329**	4001.8
		7709	16528	-	12617		
		7813	16184	-	15276		
		7814	16328	-	-		
		7901	16375	-	-		

AC14 60/70 Resilient Modulus (MPa)

Temperature	Frequency	Core # 5	Core # 3	Core # 2	Core # 6	Average	Std. deviation
20°C	1 Hz	-	-	-	2558	**2,514**	79.4
		-	-	-	2515		
		-	-	-	2543		
		-	-	-	2378		
		-	-	-	2577		
	2 Hz	-	-	-	3023	**2,961**	52.8
		-	-	-	2877		
		-	-	-	2959		
		-	-	-	2974		
		-	-	-	2970		
	10 Hz	-	-	-	4742	**4,733**	102.0
		-	-	-	4740		
		-	-	-	4578		
		-	-	-	4739		
		-	-	-	4865		
	15 Hz	-	-	-	5059	**5,328**	154.7
		-	-	-	5346		
		-	-	-	5378		
		-	-	-	5444		
		-	-	-	5412		

AC14 60/70 Resilient Modulus (MPa)

Temperature	Frequency	Core # 5	Core # 3	Core # 2	Core # 6	Average	Std. deviation
25°C	1 Hz	1362	1709	2245	1948	**1,653**	255.5
		1382	1581	1829	1715		
		1384	1546	1952	1639		
		1407	1482	1909	1601		
		1297	1518	1996	1566		
	2 Hz	2150	1700	2556	1900	**1,922**	241.5
		2176	1821	2112	1787		
		1920	1667	2118	1781		
		1841	1632	2004	1760		
		1870	1596	2244	1796		
	10 Hz	4176	3035	3367	3157	**3,218**	281.6
		3409	2940	3186	3308		
		3390	2988	3193	3200		
		3564	2992	3146	3047		
		3119	2941	3052	3153		
	15 Hz	4217	3282	3306	3332	**3,665**	626.1
		5468	3310	3387	3584		
		4526	3231	3443	3394		
		4656	3234	3275	3303		
		4307	3209	3587	3257		

AC14 60/70 Resilient Modulus (MPa)

Temperature	Frequency	Core # 5	Core # 3	Core # 2	Core # 6	Average	Std. deviation
45°C	1 Hz	151	261	181	-	**198**	45.0
		151	252	177	-		
		158	248	204	-		
		-	-	-	-		
		-	-	-	-		
	2 Hz	182	261	235	-	**219**	29.2
		186	239	222	-		
		184	246	219	-		
		-	-	-	-		
		-	-	-	-		
	10 Hz	224	338	307	-	**302**	45.3
		261	308	349	-		
		261	313	359	-		
		-	-	-	-		
		-	-	-	-		
	15 Hz	-	317	322	261	**303**	29.2
		-	313	307	247		
		-	306	324	331		
		-	-	-	-		
		-	-	-	-		

APPENDIX E – TABLE OF FATIGUE RESULTS

Table E1 Experimental testing programme for the AC14 60/70 – 1st duplicate

Run #	Beam #	Strain (με)	Temperature (°C)	Frequency (Hz)	Initial Stiffness (MPa)	Fatigue Life (cycles)
1	7	300	10	10	16817	147010
2	11	400	10	5	10172	48590
3	4	600	20	10	5027	28700
4	2	300	20	5	4137	1319560
5	15	400	20	5	3716	85290
6	10	500	20	10	4605	18440
7	12	300	30	10	2402	965410
8	8	500	10	10	10605	7920
9	24	500	30	10	2940	326120
10	17	400	30	5	1837	336820
11	1	600	10	5	9434	5360
12	16	400	20	10	4907	133770
13	6	600	30	10	2204	152230
14	23	300	30	5	3478	1093260
15	22	300	20	10	64345	490240
16	5	600	30	5	1113	157730
17	3	600	20	5	3654	25520
18	28	400	10	10	11975	30210
19	13	500	30	5	1392	146600
20	9	500	20	5	4086	52430
21	19	500	10	5	8218	15490
22	18	400	30	10	2245	385380
23	21	600	10	10	10870	3980
24	20	300	10	5	8181	122860
18a	29	400	10	10	12116	45870
6	10	500	20	100	5340	42100

Table E2 Experimental testing programme for the AC14 60/70 – 2st duplicate

Run #	Beam #	Strain (με)	Temperature (°C)	Frequency (Hz)	Initial Stiffness (MPa)	Fatigue Life (cycles)
1	42	600	30	10	1916	174950
2	50	300	30	5	1646	2454120
3	39	300	10	10	11393	392070
4	44	400	20	10	6029	125720
5	49	300	10	5	9130	592090
6	36	600	10	5	9746	19490
7	51	400	10	5	9152	13260
8	46	400	30	5	1281	1410780
9	58	600	20	10	2582	20380
10	57	600	30	5	1284	249180
11	54	300	20	10	6602	842770
12	31	500	20	10	5519	60000
12a	31a	500	20	10	4685	39880
13	40	600	10	10	10040	6700
14	43	500	10	5	10946	11620
15	48	400	20	5	4662	513900
16	47	500	30	10	1833	251240
17	41	300	20	5	4881	1186880
18	37	300	10	5	10312	500900
19	49	400	10	10	11294	47000
20	52	500	10	10	11123	12260
21	53	500	20	5	5989	64410
22	38	300	30	10	1862	810500
23	56	600	20	5		
24	59	400	30	10	2079	457100
25	29	500	30	10	1614	130200

Table E3 Experimental testing programme for the AC14 80/100 – 1st duplicate

Run #	Beam #	Strain (με)	Temperature (°C)	Frequency (Hz)	Initial Stiffness (MPa)	Fatigue Life (cycles)
1	2	500	10	5	5810	43260
2	4	400	10	10	7256	61020
3	10	400	10	5	5047	125180
4	16	300	10	10	5254	450060
5	17	600	10	5	5760	18210
6	18	600	10	10	7126	17500
7	21	300	10	5	5871	398760
8	24	500	10	10		51000
9	1	600	20	5	1844	49370
10	5	300	20	5	2515	504290
11	6	500	20	5	2151	111160
12	8	600	20	10	1379	74060
13	15	300	20	10	3357	824420
14	9	400	20	5	2345	313680
15	20	400	20	10	2495	416510
16	22	500	20	10	3031	189040
17	7	300	30	5	686	160070
18	3	500	30	10		
19	11	600	30	10	890	60900
20	12	400	30	10	1425	181870
21	13	500	30	5	618	186610
22	14	600	30	5	617	201300
23	19	300	30	10	860	197010
24	23	400	30	5	757	62600

Table E4 Experimental testing programme for the AC14 80/100 – 2st duplicate

Run #	Beam #	Strain (με)	Temperature (°C)	Frequency (Hz)	Initial Stiffness (MPa)	Fatigue Life (cycles)
1	32	500	10	5	6900	56660
2	34	400	10	10	8698	49080
3	40	400	10	5	6210	81070
4	41	300	10	10	6967	375580
5	42	600	10	5	6503	20680
6	43	600	10	10	8065	13130
7	37	300	10	5	7825	383910
8	57	500	10	10	6601	27930
9	60	600	20	5	1943	83880
10	38	300	20	5	3249	1349730
11	39	500	20	5	3023	218890
12	58	600	20	10	2374	74000
13	59	300	20	10	2612	434620
14	48	400	20	5	2375	452330
15	53	400	20	10	3561	439690
16	55	500	20	10	2619	263640
17	36	300	30	5	695	134430
18	54	500	30	10	1124	90600
19	49	600	30	10	761	70560
20	50	400	30	10	854	65590
21	51	500	30	5	566	50470
22	47	600	30	5	604	34320
23	52	300	30	10	913	494160
24	56	400	30	5	482	45450